University of Stavanger

Faculty of **Science and Technology**

MASTER'S THESIS

Study program/Specialization: Master of Science in Petroleum Technology / Drilling and Well Technology	Spring semester, 2016 Open
Writer: Jahn Otto Waldeland	…… (Writer's signature)
Faculty supervisor: Kjell Kåre Fjelde	
Thesis title: Inclusion of mass transfer terms in the AUSMV transient flow model	
Credits (ECTS): 30	
Key words: MATLAB Well Control HPHT Well Control Gas solubility in OBM Mass transfer Vaporization AUSMV Scheme Drift flux model	Pages: 79 + enclosure: 39 Stavanger,

Summary

Gas contamination of an oil-based drilling mud while performing drilling operations, having influx of formation gas into the borehole in the form of a gas kick; pose a potential hazard to the personnel, environment and the drilling equipment. This danger grow worse when bottomhole conditions are such that the gas completely dissolves into the oil-based drilling mud and quickly evolves as the gas-cut oil-based drilling mud is circulated up the well. It is therefore crucial to have the ability to understand and model the phenomenon of gas solubility in a flowing well scenario.

The first part of this thesis gives an introduction to well control in general, before going deeper into High-Pressure High-Temperature well control. In addition, gas solubility in oil-based mud is presented, trying to bring into light the various factors affecting gas solubility in oil-based mud and how important it is to understand the behavior of gas contaminated mud. An extensive literature study has been performed to give an overview of the various challenges that may be encountered during drilling operations, and the advancements in well control to diminish these challenges. Since deep water wells with narrow operational windows is currently more common than before, one of the most critical areas for development in well control safety is early kick detection. Being able to model a precise and consistent kick detection system seems to be the common denominator to reduce the High-Pressure High-Temperature issues.

The second part of the thesis is an attempt to introduce the ability to include mass transfer into the AUSMV scheme. The system is modified to fit a water and steam system, looking at the phase transition between water liquid and water vapor. How the conservation variables are updated needed to be modified as we introduce a new source term to the original AUSMV scheme.

First, fixed values for the mass transfer is used to experiment with the AUSMV scheme in a horizontal pipe. The main purpose of this simulation was to see whether the AUSMV scheme could handle the introduction of mass transfer. Simulation showed a significant change to the whole system, as gas is being generated during the simulation. The system is initially stagnant, with no gas present in the well. During the simulation, the temperature increases gradually, eventually leading to boiling of the water liquid and generating gas. The gas is affected by the temperature of the system and will begin to expand, subsequently forcing the system to start flowing towards the outlet of the pipe.

The second simulation is an experimental case using Rohsenows' correlation as a mass transfer equation in a horizontal pipe. Other correlations had to be added in order to solve Rohsenows' correlation: the evaporation energy of water and the interfacial tension between liquid water and water vapor. This makes the mass transfer more complex, and helps to test the ability of the AUSMV scheme to handle mass transfer even further. To make the simulation more realistic, a boiling point criterion has been introduced to the model. This criterion makes the mass transfer equation dependent on both pressure and temperature. When the pressure in the pipe increases due to gas generation, the boiling point temperature of the liquid also increases.

The third simulation is performed in a vertical well with a fixed numerical value for the mass transfer. For this simulation the objective was to see how the AUSMV performed in a vertical case with the inclusion of mass transfer. The simulation was modified to force the liquid to vaporize in the upper sections of the well so that the bottomhole pressure is reduced. When the bottomhole pressure drops it can cause a secondary kick to occur.

The fourth simulation is a comparison of first and second order accuracy method and also comparison of different grid adjustments. The objective of this simulation was to see how the end result changes when using different accuracy methods or by refining the grids in the simulation.

Acknowledgement

First of all I would like to thank my entire family for the support they have given from beginning to end of my master degree at the University in Stavanger.

I would also thank John Emeka Udegbunam for giving me insight into his work in progress which helped me a great deal with my thesis. I wish him all the best in his future endeavors.

And finally I would express a special thanks to Professor Kjell Kåre Fjelde for always being available whenever I needed his help and council. I am very fortunate to have had Professor Kjell Kåre Fjelde as my supervisor, for giving me marvelous feedback and being so helpful.

Jahn Otto Waldeland.

Table of Contents

1 Introduction **1**
1.1 Objective 1
1.2 Contents of the thesis 2
2 Well control in general **4**
2.1 Well Barriers 4
2.2 Well kick and kick detection 8
2.2.1 Causes for kicks 8
2.2.2 Kick detection 11
2.2.3 Flow check 12
2.3 Well control procedures 13
2.3.1 SIDPP and SICP 14
2.3.2 Driller's method 15
2.3.3 Wait & weigth 15
2.3.4 Volumetric method 16
2.3.5 Bullheading 17
2.4 Kick Tolerance 17
3 HPHT well control **18**
3.1 HPHT Challenges 18
3.1.1 Considerations on well control 18
3.1.2 WBM vs. OBM under HPHT conditions 21
3.1.3 Riser gas 26
4 Gas solubility in oil-based mud under HPHT conditions **27**
4.1 Affecting solubility 27
4.1.1 Pressure and temperature 27
4.1.2 Composition of gas influx and base oil 27
4.1.3 Circulation 28
4.2 Consequences of gas dissolution 28
4.2.1 Rheological properties 29
4.2.2 Saturation pressure 29
4.2.3 Density variation 29
4.3 Pressure-volume-temperature models 30

4.3.1 Equations of state method....30
4.3.2 Pressure-volume-temperature correlations....30
5 Advancements in HPHT well control....32
5.1 Hydraulics modeling....32
5.2 Hydraulics modeling....32
5.2.1 Managed pressure drilling as early kick detection....32
5.2.2 Early kick detection through automated monitoring....33
5.3 Cesium formate brines....33
6 Numerical modeling....35
6.1 Introduction....35
6.2 Transient drift flux model....36
6.2.1 Conservation laws....37
6.2.2 Closure laws....40
6.2.3 Source term....41
6.3 AUSMV scheme....42
6.3.1 Conservative variables....42
6.3.2 Discretization....42
6.3.3 Explicit scheme....43
6.3.4 Boundary conditions....45
6.4 Phase transition term....45
6.5 CFL condition....50
6.6 Primitive vs. conservative variables....51
6.7 Second order scheme....52
7 Simulations & Discussion....54
7.1 Mass transfer with a constant numerical value....56
7.2 Horizontal case using the mass transfer equation....60
7.3 Vertical case with a constant numerical value for mass transfer....68
7.4 Comparison of first and second order scheme and grid adjustment....71
7.5 Discussion....74
8 Conclusion and further work....72

List of figures

2.1 Well control equipment 5
2.2 Well barrier schematic 6
2.3 Illustration of the operation window 9
3.1 Density changes of 18 lb/gal OBM 19
3.2 Compared density changes of 18 lb/gal OBM and WBM 22
6.1 Discretization 43
6.2 Discretization of a new timestep 44
6.3 Illustration of pool boiling with water liquid and gas bubbles 46
6.4 Phase transition vs. pressure and temperature for water liquid 49
6.5 Propagation of eigenvalues at the outlet boundary of a cell 51
6.6 Characteristic interpretation of the CFL condition. 51
6.7 Slope limiter concept 53
7.1 Pressure at the start cell vs. time for three different constant numerical values 56
7.2 Liquid massrate out vs. time 57
7.3 Gas massrate out vs. time 57
7.4 Liquid velocity vs. length after 500 seconds 58
7.5 Temperature in the pipe vs. time 58
7.6 a) Liquid velocity vs. length at the end of simulation 59
7.6 b) Gas velocity vs. length at the end of simulation 59
7.7 Gas fraction vs. length at the end of simulation 59
7.8 Pressure at the first cell/start cell vs. time with/without boiling temperature restriction 61
7.9 Temperature in the pipe vs. time 62
7.10 a) Mass transfer vs. length and time without boiling temperature restriction 63
7.10 b) Mass transfer vs. length and time with boiling temperature restriction 63
7.11 a) Pressure vs. length at the end of simulation 63
7.11 b) Boiling temperature vs. length at the end of simulation 63
7.12 Gas fraction vs. length of the pipe at the end of simulation 64
7.13 Liquid massrate out vs. time 65
7.14 a) Gas mass in the pipe vs. time 66
7.14 b) Liquid mass in the pipe vs. time 66
7.15 Liquid mass in the pipe vs. time with zoom 67

7.16 Gas density vs. length at the end of simulation 67
7.17 BHP vs. time 69
7.18 Gas fraction vs. depth at the end of simulation 69
7.19 Pressure at 100 and 1500 seconds vs. depth 70
7.20 Mass transfer at 100 and 1500 seconds vs. depth 70
7.21 Pressure at start cell/first cell vs. time for second and first order accuracy method 71
7.22 Liquid massrate out vs. time 72
7.23 Gas fraction vs. length at the end of simulation 72
7.24 Pressure at start cell/first cell vs. time with 25 and 50 boxes discretization 73
7.25 Liquid massrate out vs. time 73
7.26 Gas fraction vs. length at the end of simulation 74

List of tables

7.1 Properties of water and steam 55
7.2 Simulation data 55

Nomenclature

AUSMV – Advection Upstream Splitting Method

BOP – Blowout Preventer

BHA – Bottom Hole Assembly

BHP – Bottom Hole Pressure

CFL – Courant-Friedrichs-Lewy

ECD – Equivalent Circulation Density

EOS – Equation of State

ESD – Equivalent Static Density

FCP – Final Circulating Pressure

FDS – Flux-Difference Splitting

FVS – Flux-Vector Splitting

GOR – Gas-Oil Ratio

HPHT – High Pressure, High Temperature

ICP – Initial Circulating Pressure

LWD – Logging While Drilling

MPD – Managed Pressure Drilling

MWD – Measurement While Drilling

MFC – Micro Flux Control

NPT – Non-Productive Time

OBM – Oil-Based Mud

OWR – Oil-Water Ratio

PSA – The Petroleum Safety Authority of Norway

PVT – Pressure-Volume-Temperature

ROP – Rate of Penteration

SICP – Shut-In Casing Pressure

SIDPP – Shut-In Drill Pipe Pressure

WBM – Water-Based Mud

WOB – Weight on Bit

List of symbols

A – cross sectional area [m^2]

C_{sf} – surface factor

c – specific heat [J/(kg·K)]

d – diameter [m]

e – internal energy [J/kg]

F - flux

∑F – sum of forces [N]

g – acceleration due to gravity [m/s^2]

G – source term

H – hold up

h – vertical depth [m] or phase enthalpy [J/kg] or heat transfer coefficient [W/K] or evaporation energy [J/kg]

K – distribution coefficient

P – pressure [Pa]

ΔP – pressure loss [Pa]

Pr – Prandtl number of liquid

q – source term or rate of heat addition [W/m^2]

Q – rate of heat loss across the pipeline to the surroundings [W]

R – gas constant

S – drift velocity of gas relative to liquid

t – time [s]

T – temperature [K]

ΔT – difference in temperature [K] or excess temperature [K]

U – heat transfer per unit volume [J/m^3]

v – phase velocity [m/s]

V – pipe section volume [m^3]

W – conservative variables

x – coordinate along the flow direction

z – vertical position of pipeline [m]

α – phase volume fraction

Ψ – rate of mass transfer due to condensation/evaporation [kg/s]

μ - viscosity [Ns/m^3]

σ – surface tension-liquid-gas interface [N/m]

Γ – amount of steam generated [kg/(s·m^2)]

ρ – density [kg/m^3]

Subscripts

B - boiling

c - critical

g – gas or gravity

i – phase, gas/liquid

kick – regarding kick values

l – liquid

mix - mixture

new – new values

old – old values

p – pore

s – sources

spec - specific

0 - reference

1 Introduction

In the aftermath of the 2010 subsea blowout of the Macondo, early kick detection technology became much more prioritized by the regulators and offshore companies to prevent similar events from happening. The National Commission on the BP Deepwater Horizon Oil Spill and Offshore Drilling concluded in their report that the crew did not have sufficient training and lacked the technology to detect that a kick was occurring.

Drilling operations today have been pushed towards new extremes with more complex wells, drilling deeper and longer than before. Even after the accident, there has been limited progress made regarding kick detection. One of the reasons is that kick detection is complicated which involves many sensors and the interpretation of this data.

Early kick detection can, aside from improving safety, represent a large financial opportunity. Detecting kicks, both large and small, can reduce the drilling cost. Even the minor kicks can lead to drilling challenges.

For a realistic kick detection simulator, it is important to include the phase transition of liquid and gas properly. The ability to simulate the gas dissolving into the oil-based mud, and subsequently when the gas goes out of solution at a later stage, is imperative for a sophisticated simulator. This will generate information about whether to expect a secondary kick, where in the well gas will go out of solution and the amount of free gas that appear in the well.

1.1 Objective

One of the objectives of this thesis is to give an overview of well control and High-Pressure, High-Temperature issues that can arise during drilling operations and to express the importance of modeling kick in oil-based mud.

The other objective is to include the mass transfer term in a numerical model called the AUSMV scheme to see if the scheme has the ability to handle such a term. The AUSMV scheme is a simplified model that can be used to simulate the pressure dynamics in a well when considering the flow of water and gas. So far, one has not considered the possibility for including mass transfer between phases.

To achieve this, new functions and modifications have been added to the AUSMV scheme. The mass transfer term is dependent on several variables, such as temperature, pressure,

density, enthalpy and surface tension. Simulations have been performed in order to verify the newly implemented functions are working, and the simulations will be presented in this thesis.

1.2 Contents of the thesis

Well control

Well control is of foremost importance in all the phases of planning, designing and constructing a well. This is particularly important when planning to drill under High Pressure, High Temperature conditions. The concept of well control is to prevent a kick from taking place, and if it occurs, to stop it evolving into a blowout which can harm the external environment. Well control starts when the location of the well has been selected, and not when a kick has occurred.

Gas solubility

When oil-based mud is used as the drilling fluid in the well special precautions needs to be taken, one of them is gas solubility. If a kick occur downhole, the gas influx may contaminate the oil-based mud. Parameters that affect the gas solubility are pressure, temperature and also the composition of the oil-based mud and the gas. Some simulators assume that gas is instantly dissolved into the oil, but this assumption is not correct. There can be free gas at the beginning of the influx, and it is later dissolved by diffusion and convection. The gas solubility may let the kick detection technology to better detect the kick by a volume change if the gas does not dissolve instantly.

Advancements in HPHT well control

As High-Pressure, High-Temperature (HPHT) operation continues to be of international interest, it is important to address the many HPHT challenges effectively in a safe and professional manner. It is therefore important to develop new systems to resolve or reduce the many challenges one can come across during HPHT operations.

Numerical modeling

To simulate the multiphase flow, numerical modeling is used. One has to take advantage a set of conservation equations in order to realistically simulate the flow in a well. The transient drift flux model is such a system which simulates two-phase flow. This model uses three different conservation laws; conservation of mass (gas and liquid) and conservation of momentum. This will result, after combining these three equations, to seven unknown variables. To resolve the problem with the unknown variables, four closure laws are utilized

The AUSMV scheme is an alternative numerical solution for the transient drift flux model. AUSMV is an acronym for Advection Upstream Splitting Method, where the V signifies to a modified velocity splitting function. The AUSMV scheme has potential to be used in well-planning and for education purposes.

Simulation

In this section four different simulation scenarios will be performed. The model used is a simplified water/steam system where the main objective is to demonstrate how mass transfer can be introduced to the AUSMV scheme through simulations.

The first, second and fourth simulation is a horizontal well with no drill pipe present in the wellbore, containing only water liquid. The well starts at atmospheric pressure and temperature, where the temperature gradually increases from 20^{o}C to 110^{o}C. The first simulation uses a constant numerical value for the mass transfer term, to test AUSMVs ability to handle a mass transfer term.

The second simulation introduces a modified AUSMV scheme where a mass transfer equation is implemented. Several additional functions had to be added in order to include a mass transfer equation. The objective is to experiment with the AUSMV scheme even further, making the mass transfer more complex by using several variables that changes throughout the simulation.

The third simulation is performed for a vertical well. As with the first simulation, a constant numerical value is used for the mass transfer. The well has a constant temperature gradient having 40^{o}C at the top and 150^{o}C at the bottom of the well. The initial pressure in the well is induced by the hydrostatic pressure. Since the simulation is using a water-based drilling fluid, it is not able to vaporize the water liquid under these conditions. The mass transfer is therefore forced to activate where the pressure is below 50 bar, making the drilling fluid to act as an oil-based drilling fluid.

The fourth simulation is similar to the second simulation, but instead takes a deeper look into the first and second accuracy method, where the two methods is compared. In addition, the grid adjustment is compared using 25 and 50 discretization boxes.

In the final sections of the thesis, the different results of the three scenarios will be presented and discussed, leading to a conclusion and recommendations for further work.

2 Well control in general

The NORSOK D-010 standard has defined well control as “the collective expression for all measures that can be applied to prevent uncontrolled release of wellbore fluids to the external environment or uncontrolled underground flow”(NORSOK, 2013). The purpose of well control is to avoid a kick from taking place, and if it occurs, to stop it evolving into a blowout.

In the petroleum industry safety is essential to all operations performed, thus well control is one of the main focus areas to which oil companies plan, design and construct wells with well control in mind. Well control does not begin at the occurrence of kick and end when the kick has been killed, but it begins when the location of the well has been selected. By controlling the pressure in the well we are able to maintain the control of the well and can operate the well safely. It is for that reason central to fully comprehend how we can lose control of the well.

The primary well control refers to maintaining a hydrostatic pressure in the wellbore in order to avoid kick situations to take place. It uses drilling or completion fluids and other weight materials to provide sufficient pressure and prevent influx of formation fluid to the wellbore. The purpose is also to prevent fracturing of the rock formation which will cause loss of wellbore fluid to the formation. In some cases, where the operational window is narrow, the primary well control may also be carried out using well control equipment, such as managed pressure drilling (MPD). Secondary well control is performed after the primary well control has failed. For instance, when there are formation fluids entering the wellbore, the BOP is closed to prevent the escape of wellbore fluids from the well. Tertiary well control is used when an underground blowout has occurred and can be controlled by drilling a relief well.

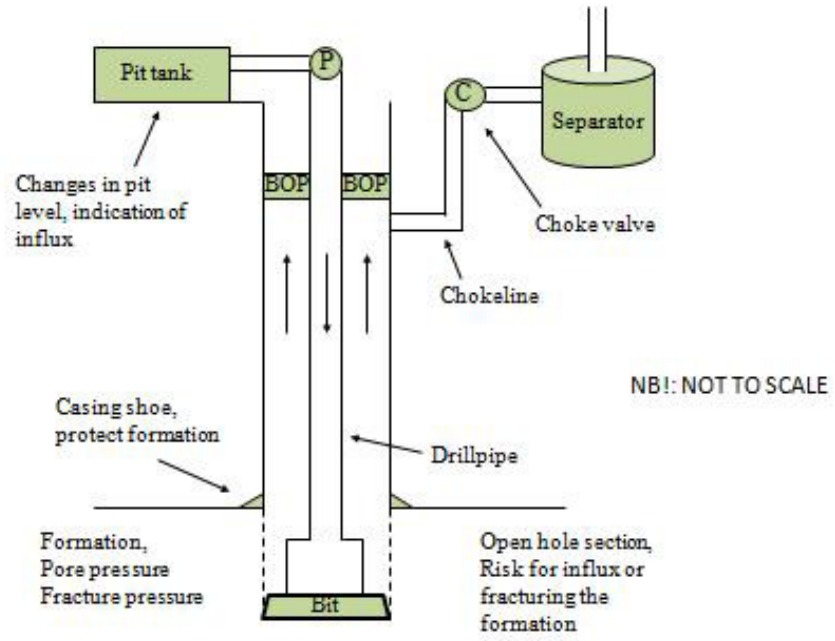

Figure 2.1: Well control equipment

Figure 2.1 is a simple illustration of well control equipment. It shows the most important equipment while drilling:

- The mud is pumped down inside the drillpipe and travels up in the annulus to the pit tank at surface, where pit volume is measured.
- The BOP is used to seal the well in case of a kick situation.
- The chokeline let well fluids to be diverted out of the well when the BOP is closed, while the choke valve is used to control the well pressure.
- The separator segregates the gas from the mud.

2.1 Well Barriers

The significance of having control of the safety in wells cannot be taken too lightly. The Norwegian authorities have, with the Norwegian petroleum industry, developed the NORSOK D-010 standard and this states to follow a 2-barrier philosophy; if the primary barrier fails, the secondary will still maintain the well control. With the NORSOK standard, the schematics give little room for different interpretation from engineer to engineer, and will assure adequate safety since the standard is a reference in the authorities' regulations.

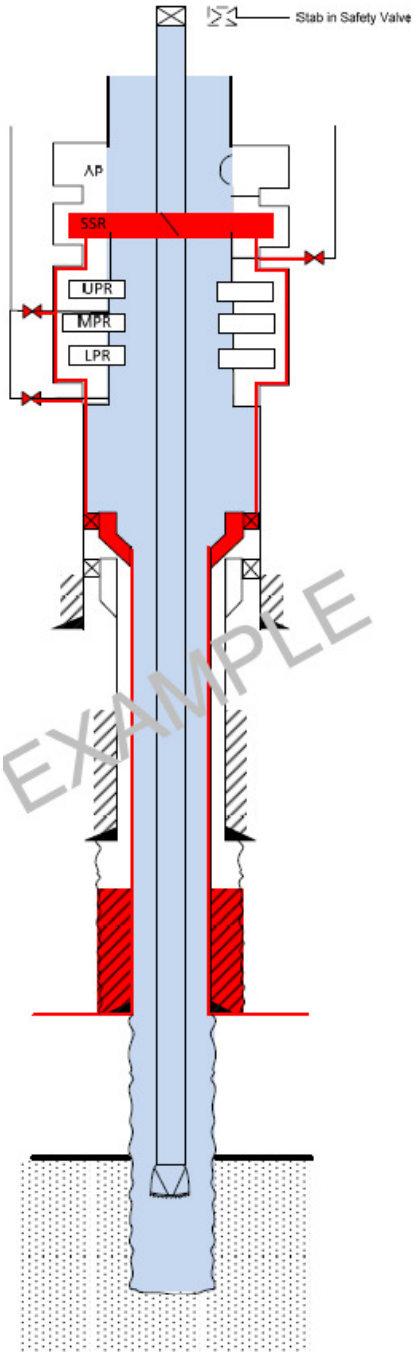

Well barrier elements	EAC table	Verification/monitoring
Primary well barrier		
Fluid column	1	
Secondary well barrier		
In-situ formation	51	
Casing cement	22	
Casing	2	
Wellhead	5	
High pressure riser	26	
Drilling BOP	4	

Figure 2.2: Well barrier schematic (NORSOK, 2013)

The petroleum safety authority (PSA) of Norway is responsible for the regulations regarding the petroleum activity on the Norwegian Continental Shelf. Section 48 in the Facilities regulation addresses how to fulfill the requirements regarding well barriers. The paragraph states the following[1]:

[1] http://www.psa.no/facilities/category405.html#_Toc438216906

Well barriers shall be designed such that well integrity is ensured and the barrier functions are safeguarded during the well's lifetime.

Well barriers shall be designed such that unintended well influx and outflow to the external environment is prevented, and such that they do not hinder well activities.

When a production well is temporarily abandoned without a completion string, at least two qualified and independent barriers shall be present.

When a well is temporarily or permanently abandoned, the barriers shall be designed such that they take into account well integrity for the longest period of time the well is expected to be abandoned.

When plugging wells, it shall be possible to cut the casings without harming the surroundings.

The well barriers shall be designed such that their performance can be verified.

The well barriers need to be verified and this can be achieved through pressure testing, checking ease of access, check reaction times and leakage rates. One vital requirement is that the barriers should be independent.

Requirements regarding well control equipment in case of influx are described in section 49 in the Facilities regulation. More details are given in NORSOK D-001.

NORSOK has defined a well barrier as an “envelope of one or several well barrier elements preventing fluids from flowing unintentionally from the formation into the wellbore, into another formation or to the external environment”(NORSOK, 2013). From the figure we see the primary and secondary well barrier with its well barrier elements while drilling, coring and tripping with shearable string.

The BOP, a secondary barrier element, is the surface well control equipment. The function of the BOP is to supply abilities to shut in and close the wellbore with or without tools/equipment through the BOP. It has different ways of preventing unwanted flow to pass by having numerous closing rams. The first valve that is triggered if a critical situation happens is an annular preventer which is a seal made of rubber that closes around the drill pipe, collars and bottom hole assembly (BHA) preventing any flow to pass through. If the kick is taken when tripping out, it will be possible to strip the drill string back to bottom due to some flexibility in the annular preventer. After the annular preventer has been closed, the pipe rams are activated. These are named lower/middle and the upper pipe ram. These rams

are designed to close around a fixed pipe size. In case the aforementioned valves do not function as wanted, or if all other things fail, a redundancy measure has been implemented. This is the shear and seal ram which cuts the drill string, closes up the entire annulus and prevent any leakage.

2.2 Well kick and kick detection

A kick is when there is influx of formation fluid into the wellbore during drilling; this is an unwanted situation where the well control is compromised. The primary fluid barrier is in a degraded condition – the mud is not adequate to balance the pore pressure by its own. In general this suggests using the BOP to shut in the well and then take out the influx using a choke line to maintain enough back pressure to stop further entry of fluid (Adams & Kuhlman, 1994).

There are three conditions vital for a kick to arise in the well:

1. The exposed formation pressure must exceed the pressure in the wellbore.
2. The permeability of the formation must be sufficient enough to allow flow into the wellbore.
3. The formation fluid needs to have low enough viscosity so that it can flow.

2.2.1 Causes for kick

Loss of the primary well control is typically caused by one of the following causes (Grace, 2003) :

- Insufficient density of the drilling fluid (Insufficient bottomhole pressure (BHP))
- Improper hole fill up on trips
- Swabbing effects
- Lost circulation
- Gas cut mud
- Barite sag

Insufficient density of the drilling fluid

If the hydrostatic pressure of the well fluid column is lower than the formation pressure there will be an influx of formation fluid and a kick will take place. For that reason, it is important

to have an adequate mud weight such that the formation pressure is balanced when being static and such that the fracture pressure is not exceeded during circulation. The difference between pore pressure and fracture pressure is the operating window and this is illustrated in figure 2.3. Although the hydrostatic pressure is satisfactory, a kick can still be induced due to unexpected high pore pressures; the pressure prognosis is incorrect. The mud weight can be inaccurate due to the temperature and pressure effects and other causes that will affect the density of the mud, which will be discussed later.

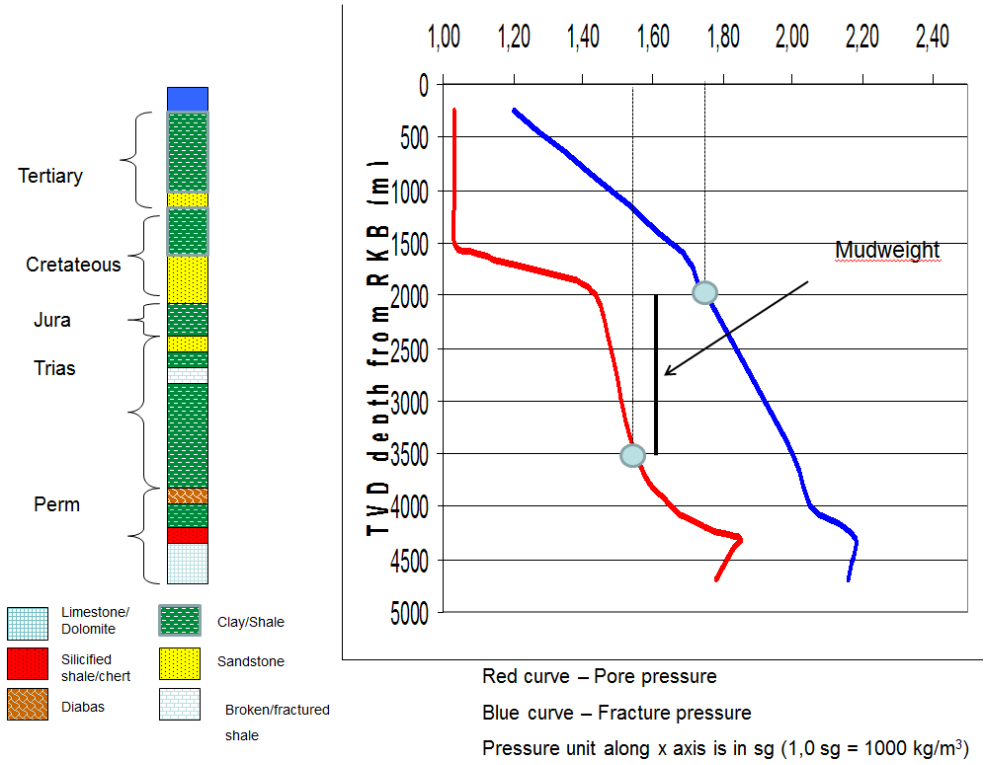

Figure 2.3: Illustration of the operating window(Kjell Kåre Fjelde, 2011).

Improper hole fill up on trips

When tripping out of the well, the mud level in the well should reduce by the same amount of volume equivalent to the removed steel. If this mud volume is not replaced, there will be an improper hole fill up. This can be regarded as an operational problem. Failure to keep the hole full will cause the hydrostatic pressure in the well to drop and a kick may arise. In order to avoid reducing the hydrostatic pressure, the trip tank can be used to fill up the hole.

Swabbing effects

Swab pressures are induced by tripping out of the borehole. The swab effect is negative and decreases the effective hydrostatic pressure. A kick may develop if the negative pressure

effect of swabbing reduces the hydrostatic pressure below the formation pressure. Some variables that controls the swabbing effect are mud properties, hole configuration, pipe pulling speed and the effect of "balled" equipment (Adams & Kuhlman, 1994).

One particular problem by swabbing while using oil-based mud (OBM) is that a kick may go unnoticed while swabbing, since the indicators that warns about a kick is less pronounced in an oil-based mud system.

The industry takes great precautions while tripping in or out of the wellbore under HPHT conditions with a narrow operational window. The procedure is based on a pre-calculation principle. If a kick is suspected to have been taken, the BOP is closed and the returns are circulated across the choke. This is done in all situations where a kick have occurred. This causes the procedure of tripping to increase the non productive time (NPT) (Transocean, 2009)

Balled equipment is when formation rock like clay, sandstone etc. fastens to the pipe or equipment and makes a larger outer diameter which will increase the swabbing effect. One remedy to avoid the swab effect is to keep pumping while pulling pipe out of the hole, called "pumping out of hole". Also the heave effects of an offshore installation has to be considered which can lead to swab effect, this is why an active heave compensator is used.

Lost circulation

Lost circulation is when rapidly mud loss can result in loss of the primary control, which is the hydrostatic pressure. The loss can be the outcome of natural or induced sources. The natural causes include fractured, cavernous, anomalous pressured or depleted formations. Induced loss can be the product of mechanical fracturing resulting from (Caenn, Darley, & Gray, 2011):

1. Too high mud density
2. Excessive annular back pressure
3. Surge effect associated with pipe movement
4. Breaking circulation or pack-off in the annulus.

When experiencing a loss of fluids in the well, the fluid level will drop and a reduction of hydrostatic pressure will take place. If this were to happen then it could lead to a kick situation. When a kick occurs from lost circulation, the well control operations will become more complex since a large volume of formation fluid may enter the wellbore before the

rising mud level is observed at the surface. One of the cures is pumping down lost circulation materials into the fractures.

Gas cut mud

Kicks are occasionally induced by gas contaminated mud, but this is rather uncommon. If a formation filled with gas is drilled, then this will travel up the wellbore during circulation. When the gas reaches close to the surface, it will expand and reduce the overall hydrostatic pressure and can allow a kick to occur.

Barite sag

Barite sag is the unwanted variation in mud density that happens due to the downhole settling of the weighting agent in the mud. The bed of weight material will be deposited on the low side of an inclined well. There are two forms of barite sagging; dynamic and static sagging (Bern et al., 1988).

If the weight material sag out of the drilling fluid when circulation rate is low enough for the flow to become laminar and if there is no or slow rotation of the drill string there will be a dynamic sagging. Even though most current drilling fluids do not sag at static conditions, gas influx from formation may still trigger sagging (Rolv Rommetveit et al., 2003).

A greater loss of weight material from the mud may cause severe well-control difficulties, especially in long horizontal sections, when the lighter mud gets to sections with small inclination where a stronger carrying capacity of the cuttings is needed.

2.2.2 Kick detection

Warning signs and potential kick indicators can be observed at the surface. It is critical to the secondary well control to detect a kick early and limiting its volume by shutting in the well so that the kick can be managed without loss of control. The most important warning indicators are as follows below. If a kick is taken in OBM it can be difficult to detect on the surface, but this will be discussed later in chapter 4.

Flow rate increase

In normal circulation, the flow in and the flow out is in steady state condition; what enters the well must come out. If a kick occurs this balance will be obsolete and the return flow from the well will increase.

Pit volume increase

If there is a pit increase, and this is not the result of surface controlled actions, a kick is in progress. Fluids that go into the wellbore displaces the same volume of mud at the flow line and results in a pit increase. A gain in pit volume combined with a flow rate increase is a confirmation of a kick situation.

Drilling break

An unexpected increase in rate of penetration (ROP), which is called a drilling break, is a warning indicator of a potential kick. This is due to the decrease in the overbalance in the well which will cause a reduction in the chip hold-down effect. The reason that the overbalance is reduced can be a rising pore pressure. Since the overbalance is reduced, it does not push the formation downwards with the same amount of force, and the formation will therefore be easier to drill (Rehm, 2002). The ROP will not be consistent when drilling different formations. For instance, a rock with high permeability and porosity, like sandstone, has a higher ROP due to lower resistance (Grace, 2003).

Improper hole fill up on trips

Usually when tripping operations is performed a trip sheet is recorded with volume of displaced mud while tripping in and volume of pumped mud when tripping out. This trip sheet must be calculated and be ready before well entry, so that any large variations from the calculated volume can signify that there is an influx of formations fluid or a loss of drilling fluids to the formation.

Flowing well with pumps off

When the rig pumps are not circulating the mud and there still is a continued flow from the well, a kick might be in progress. Even though there is a flowing well with the pumps off, it does not necessarily mean that a kick has occurred. This can be the result of temperature effects and/or density difference between inside and outside of the drill string. The temperature effect can cause a fluid volume expansion, which in turn result in an increase return volume at surface.

2.2.3 Flow check

"Anytime the driller, or the person performing the driller's function, has any concerns regarding the wells status, a flow check must be performed." (Transocean, 2009).

A flow check will be initiated if there are any indications that a kick is about to occur. To perform a flow check the mud pumps are shut down and the returns are going through the trip tank. The mud from the trip tank is pumped back with a fill up line into the top of the riser. In the case of a stable well, the mud level in the trip tank will not change. Flow from the well when the pumps are off is anomalous behavior. A flow check normally lasts for 10-15 minutes. In HPHT wells, flow checks must have a minimum duration of 15 minutes and is performed on all connections (Transocean, 2009).

The reason of returning the flow to the trip tank is that the precision of the volume measurements are better at the trip tank than for the mud pits. Since the cross sectional area of the trip tank is smaller, an incremental increase in volume will result in a rather large increase in liquid height in the trip tank.

When performing a flow check there are numerous effects to be aware of. Even if the well is not flowing, it is not unusual that there is a gain immediately after initiating a flow check. A volume change of 100-200 bbls (volume gain and volume loss) may take place during drilling due to ballooning, which is discussed later, and it can be of the same order of volume as a kick that potentially can lead to a blowout (Aadnøy, 2002). Also temperature effects can result in a gain due to net heating of the mud volume in the well during connection.

2.3 Well control procedures

An appropriate kill procedure is initiated after a kick is taken and the well is shut in by closing the BOP. After the BOP is closed, the shut-in casing pressure (SICP) and shut-in drill pipe pressure (SIDPP) can be read. To kill a well is to remove the fluid which has entered the wellbore, and also to re-establish the mud column as the primary barrier. NORSOK has listed four potential kill methods (NORSOK, 2012):

- Driller's method
- Wait & weight
- Volumetric method
- Bullheading

The first two are the most commonly used methods, while the latter two are situational.

2.3.1 SIDPP and SICP

After the BOP has been closed, pressure will begin to increase right after a kick is taken. The wellbore pressure increases due to the formation forces fluids into the well. This influx will continue until the BHP equal the formation pressure and at this point SICP and SIDPP are measured. With the well shut-in and using WBM, invading gas will rise up in the annulus by itself and lead to an increase in SICP and SIDPP. In OBM however, the pressure will increase until it equals the formation pressure. This is due to the dissolved gas in the OBM and there will be no migration unless there is circulation (Rolv Rommetveit et al., 2003). After the well is stabilized, the shut-in pressures can be read. The SIDPP is read at the standpipe manifold, whereas the SICP is read below the choke valve. These values will be used as references when calculating the new mud weight and also when circulating the kick out.

The SIDPP is used to calculate the formation pressure upon taking a kick. This is done by assuming that the bottomhole pressure is equal to the pore pressure.

$$P_p = SIDPP + \rho_{old} g h$$

Where:

P_p – pore pressure

SIDPP – shut-in drill pipe pressure

ρ_{old} – density of current drilling fluid at standard conditions

g – acceleration due to gravity

h – true vertical depth

With this assumption the kill mud density that is used equalize the well can be calculated through a number of equations that will not be mentioned here. One can also calculate the kick influx density by using the SICP and SIDPP with the following equation.

$$\rho_{kick} = \frac{SIDPP - SICP}{g h_{kick}} + \rho_{old}$$

Where:

ρ_{kick} – average influx density at shut-in

h_{kick} – vertical height of influx at shut-in

The first term in the above equation is always negative, so that SICP>SIDPP, and the density of the influx is, as expected, lower than the density of the mud.

2.3.2 Driller's method

This method can be used if the bit is at the bottom of the well. If it is not, stripping to bottom will be required. The invading fluid should in this procedure be circulated out before increasing the drilling fluid density. To complete the driller's method, two rounds of circulation will be necessary. The kick is first circulated out by using the old mud which is already in the wellbore. When performing the second round of circulation, the well is displaced by the kill mud, a heavier mud, which makes the wellbore unable to develop another kick and the primary well barrier is re-established. Throughout the whole process, it is important to maintain constant bottomhole pressure and keep it somewhat higher than the formation pressure.

After the first round of circulation, the invading fluid will be entirely circulated from the wellbore. In order to confirm the kick has been circulated out, the pump is shut down and the well is closed synchronously, while having constant bottomhole pressure. The drillpipe and casing pressures should be the same and almost equal the initial drillpipe pressure after the first circulation.

When performing the second round of circulation, a drilling fluid with a kill mud density is used. This is executed to restore primary well control and prevent a new kick. The new kill mud is calculated based on the initial SIDPP reading; the mud is then used to balance the formation pressure with a safety margin so it is overbalanced. After the second circulation is finished and the well is displaced to kill mud, the shut-in pressures must be reduced to the atmospheric pressure.

(American Petroleum Institute, 2006)

2.3.3 Wait & weight

The wait & weight method is quite similar to the driller's method. Instead of using two circulations as the driller's method, wait & weight only uses one circulation to remove the invading fluid and re-establish the primary well barrier. The wait & weight element of this method is that the kill mud is calculated, the mud is weighed up, and circulation starts immediately.

The pump speed is increased slowly up to a kill rate while also adjusting the choke valve so that the pressure at the kill line is held constant. When initiating the process, the drillpipe pressure must be roughly the same as the calculated initial circulating pressure (ICP). If this is not the case then the reason should be examined. ICP is calculated by the following equation.

$$ICP = SIDPP + \Delta P_{SCR,Riser}$$

Where:

$\Delta P_{SCR,Riser}$ – dynamic pressure loss through the riser.

As circulation continues, the drillpipe pressure is controlled by the choke valve to decrease linearly as calculated in the kill sheet. A kill sheet shows how the pump pressure should be to maintain constant bottomhole pressure. The pump pressure is plotted against pumped mud volume. After the whole drillstring is displaced to kill mud, the drillpipe pressure should have reached the intended final circulating pressure (FCP). Until the circulation is completed, the drillpipe pressure should stay the same at FCP.

$$FCP = \frac{\Delta P_{SCR,Riser}}{\rho_{old}} \rho_{new}$$

Where:

ρ_{new} – kill mud density

2.3.4 Volumetric method

If, for some reason, circulation through the drillstring is impossible the volumetric method can be used. It can also be used in combination with the two aforementioned methods. This is especially applicable when gas migration is causing extreme pressure build up before the desired kill method is initiated (Litlehamar, 2011).

The approach of this method is to keep the BHP constant plus a safety margin while the kick travels upwards in the annulus. Through gradually bleeding off mud through the chokeline, while controlling the backpressure with the choke, this can be achieved. During this bleed off, the choke backpressure is regulated with the drillpipe pressure as reference. This process should proceed until the drillpipe pressure arises to the prerecorded shut-in pressure plus a safety margin (usually 100 psi (American Petroleum Institute, 2006)). This will guarantee that the BHP stays within a designed interval, and no more fluid will invade the wellbore.

2.3.5 Bullheading

Bullheading uses a constant pump rate to force the influx back into the formation without any return to the surface. While circulating, the injection pressure should not lead to a well pressure exceeding the fracture pressure. If this limit is broken then an underground blowout, crossflow from influx zone to the fractured formation, may occur and this will instead make this problem even more complex.

The area of application of bullheading is when H_2S is anticipated to be mixed in the invading fluids, or when the margin of the fracture pressure is too low for a conventional kill to be executed (wait & weight or driller's method). It can also be used even though the drillstring is out of the hole; then mud is pumped down through the bit and choke lines. Bullheading works best if the open hole section is fairly short (American Petroleum Institute, 2006).

2.4 Kick tolerance

Kick tolerance is an important and essential issue to consider when designing the well and when deciding where the different casing shoes should be set. It is an evaluation of how large kicks a well section can handle. It is economically feasible to set the casings as deep as possible. Moreover, if a kick occurs while drilling long open hole sections, there is a risk for breaking down the casing shoe. Therefore it is important to carefully consider kick tolerance while designing a well.

Contradictory to the importance of kick tolerance in the drilling industry, there is no standard of the definition used by any of the operators, drilling contractors or even training institutions. This means there are several definitions on what kick tolerance really is (Santos, Catak, & Valluri, 2011).

One definition is that kick tolerance can be defined as the maximum volume of gas that the open hole section can tolerate and circulated out of the well without fracturing occurring at the weakest point. It can also be defined as the maximum allowable pore pressure, represented as the equivalent circulation density (ECD), such that if a kick with a particular volume occurs the well could be shut in and the kick can be circulated out safely. Kick tolerance relies on the kick size, fracture gradient at the recent casing shoe, formation pressure in the well section and the mud weight that is used (Aadnøy, 2009)

3 HPHT well control

A high pressure high temperature well (HPHT well) is according to NORSOK D-010 a "well with expected shut-in pressure exceeding 690 bar, (10,000 psi), and a static bottom hole temperature higher than 150 °C.

3.1 HPHT challenges

When developing HPHT prospects, some formidable drilling challenges have to be overcome. Rigs used for HPHT drilling are larger due to the requirements for hook load, mud pumps, drill pipe and surface mud capacity to mention a few. Because of these requirements, these rigs are way more expensive. But as far as drilling is concerned, there are a number of key challenges which are faced in HPHT wells regarding the drilling mud, the primary barrier, in particular.

- The operational window between pore and fracture pressure becomes drastically narrower. Loss and kick situations can occur with a minor error. ECD management is important and the use of MPD is an alternative to be able to drill HPHT wells.
- The mud has to be stable under the extremely high pressures and temperatures since unstable mud systems might lead to barite sag, mud gelation and other problems.
- The influx of gas/oil/condensate are above the critical point conditions and will therefore be infinite soluble with OBM which increases the kick severity.
- Effects of temperature and pressure on mud weight and on the ECD cannot be overlooked due to the possible impact on well control, in contrast to conventional drilling.
- Drilling mud rheology must be optimized to minimize ECD and also prevent to create barite sag.
- Ballooning effects and temperature effects which makes it more difficult to differentiate a "false kick" from a "real kick".
- Gas diffusion from formation to wellbore can occur in overbalanced condition, while the well is left uninterrupted for a while and mix with OBM which might trigger well control problems.

3.1.1 Considerations on well control

In HPHT wells, the operational window between pore pressure and fracture pressure is small. The mud weight is adjusted so that the hydrostatic pressure is within the drilling margin and the well is under control, but there are effects which can cause a kick or fracturing in the well.

Temperature and pressure effects

The hydrostatic pressure of the mud column in a well depends on the density of the mud in the wellbore, which diverge from the surface density because of the increases in temperature and pressure in a HPHT well. As with other liquids, the mud, especially OBM, will expand when heat is applied and also compress by pressure (McMordie, Bland, & Hauser, 1982). If the well is temperature dominated there will be net heating of the total mud volume in the well during connections. This will lead to mud volume expansion. It is possible to interpret this expansion of mud as a kick.

If the well is temperature dominated, the density of the drilling fluid will decrease vs. depth and the net effective hydrostatic pressure in the well will be reduced compared to calculation performed using surface measurements of the mud. This may provoke an unsafe situation during drilling operations since the mud weight is lower in the wellbore than on the surface and a kick can occur. When the pump is shut off, no circulation, then a general increase in mud temperature will arise, since there will be more heating in the lower part of the well than cooling in the upper part. This leads to a decrease in the hydrostatic pressure (Skalle, 2013).

The variation of hydrostatic pressure in the wellbore will increase in a HPHT well due to the extreme conditions. The high pressure in the well will compress the mud and cause the density of the fluid to increase, working in the opposite direction as the temperature. The net effect will be determined by whether the well is temperature or pressure dominated. Usually, the surface density cannot be regarded as the density of the mud throughout the wellbore. The ECD in the well is due to friction. This depends on the rheology which is also depending on pressure and temperature conditions (Rolv Rommetveit et al., 2003).

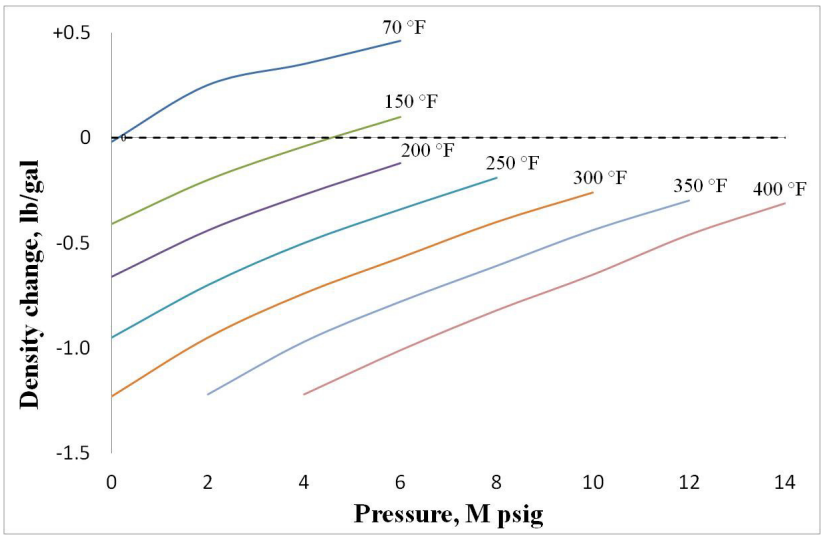

Figure 3.1: Density changes of 18 lb/gal OBM. Figure based on experimental results by McMordie 1982 (McMordie et al., 1982).

Ballooning effect

Since HPHT wells have high temperature and pressure, there is a special phenomenon known as "ballooning effect" that can occur. The expression "ballooning effect" is used since the well's activities is similar to that of a balloon which inflate when the pumps are circulating, and shrink when the well goes back into the stationary situation with the resulting return of the fluids. This can provoke a reverse flow in the well with the pumps shut off; create a "false kick", which may lead to the driller unnecessarily shutting in the well. It is for that reason vital to separate the false kick or lost circulation from the ballooning effect (Aadnøy, 2002).

Drilling mud rheology

In conventional drilling, the rheological properties of the drilling mud are often approximated to be independent of pressure and temperature. The high pressure and high temperature conditions found in deep wells create a considerable challenge to sustain the optimum rheology of the drilling fluid, thus it can no longer be independent of pressure and temperature. The changes in the rheology will cause changes in the ECD while drilling. These alterations in ECD can lead to fracture of the formation when operating in a narrow operational window (R. Rommetveit & Bjorkevoll, 1997).

Gas diffusion

When drilling a HPHT well with OBM and this is left uninterrupted for a period of time, e.g., when logging or tripping, methane will diffuse from the formation through the mud filter cake and the mud invaded zone into the wellbore. This can happen even for an overbalanced well. The rate of methane diffusion is dependent on the temperature, pressure, the reservoir and OBM characteristics, and the near well region conditions (Petersen & Carlsen, 2016). For longer periods of time this can accumulate to be substantial quantities and this will happen even if the well is overbalanced. The result of gas diffusion can be the loss of well control when circulation starts up again or pipe is tripped back into the well or degradation of mud properties including barite sag (discussed earlier in subchapter 2.2) (Rolv Rommetveit et al., 2003).

A high amount of gas dissolved in the mud may weaken the carrying capacity of the mud, causing precipitation of cuttings and weighting material, and even of viscosifying agents such as clays. This may develop two layers of mud with a low density-low viscosity layer on the high side and a high density-high viscosity on the low side. When resuming circulation, the low density layer may flow while the high density stays behind and well control problems may occur (Bradley, Low, Aas, Rommetveit, & Larsen, 2002).

Gas diffusion in water based mud is not really an issue.

3.1.2 WBM vs. OBM under HPHT conditions

The most common drilling fluids that are used today are the water-based mud (WBM) and oil-based mud (OBM), and both have several characteristics that meet the requirements for HPHT purposes. The most common problem affecting the mud in a HPHT environment is the possible damage of the mud properties under high pressures and temperatures.

Effect on hydrostatic and frictional pressure

For fluids of equal density at the surface, in the figure below it is 18 lb/gal, the density of OBM will be greater than that of a WBM at HPHT. This means that the negative density change of the OBM will be less compared to WBM. When trying to keep the hydrostatic pressure within the narrow operational window, changes in the density can be significant enough to induce a kick. Oil mud is considerably more temperature stable than water based mud (McMordie et al., 1982).

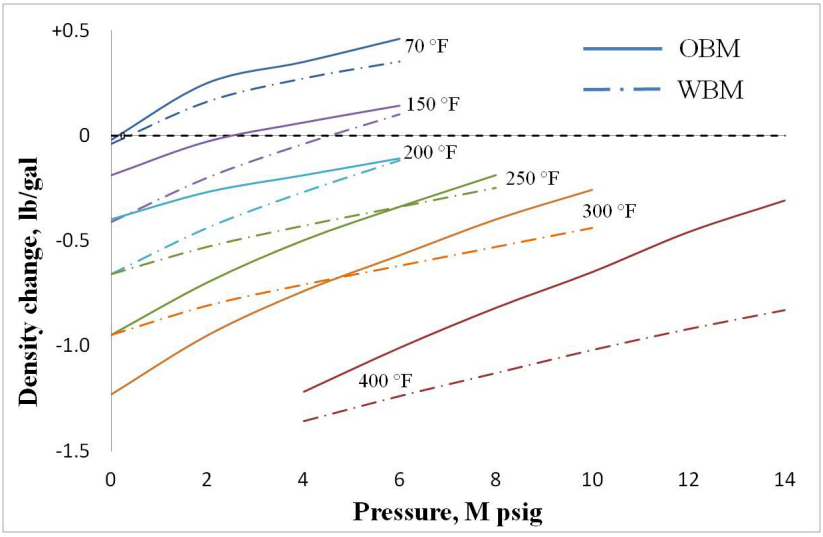

Figure 3.2: Compared density changes of 18 lb/gal OBM and WBM. Figure based on experimental results by McMordie 1982 (McMordie et al., 1982).

WBM can have its properties destroyed by the high temperature and this can lead to loss of viscosity and fluid loss control. With its reduced properties, it cannot longer provide the necessary function of transporting cuttings and may change the frictional pressure drop and subsequently lead to loss of well control. OBM can be formulated to endure elevated temperatures over extensive periods of time. Through a comparative study of OBM vs. WBM, Amani et al shows that OBM is more tolerant to HPHT conditions. They also show that the failure temperature, where the mud loses its mechanical and rheological properties, is significantly higher for OBM than for WBM. It is concluded that OBM is a proper choice for most of the HPHT application, as long as there is no violation of environmental regulations (M. Amani, Al-Jubouri, & Arash, 2012).

Kick detection & solubility

Increase in pit gain and return flow rate is one of the primary kick indicators. Gas solubility has been the reason for problems of early kick detection when using OBM. Studies done by O'Brien, Thomas et al, O'Bryan and O'Bryan and Bourgoyne have revealed through their work that there will be no to little increase in pit level as the gas dissolves in the OBM over time and the detection of kicks is certainly more of a difficult issue than in WBM (O'Brien, 1982; P. L. O'Bryan, 1985; P. L. O'Bryan & Bourgoyne, 1987; Thomas, Lea, & Turek, 1984). Also, Cockburn stated that "OBM with gas in solution, reduce the time the driller has to react to this potentially dangerous situation."(Cockburn, 1987)

Kick detection can become more difficult when using OBM due to the solubility of gas in the OBM's base fluid. As the temperature and pressure increases, the solubility of gas in oil-based drilling fluids increases (Patrick L. O'Bryan, Bourgoyne, Monger, & Kopcso, 1988). The solubility of gas into the OBM increases with pressure and under HPHT conditions. It is considered that a dry gas is infinitely soluble in the OBM. Hence, quite large influx volumes can be taken without being properly noticed.

When there is a gas influx in WBM, the gas will occupy a small volume in the well under HPHT conditions. As the gas ascends up the well it will depressurize and increase in volume. This will delay the detection of the gas, but it is not as serious as with OBM, due to the infinite solubility of gas in OBM under HPHT conditions (Bland, Mullen, Gonzalez, Harvey, & Pless, 2006).

As the dissolved gas in OBM is circulated up in the well, the decrease in pressure along the well will at some point lead to that the base oil can no longer keep the dissolved gas. Free gas will boil out rapidly, leading to sudden increase in pit gain. Rapid well control response is required and the BOP must be shut in. It is important to avoid that the kick enters riser and it is vital to know where the influx is anticipated to boil out. If the gas travels above the BOP and into the riser, the gas will boil out inside the riser. This will result in an overboard diversion of oil based fluids, or in the worst case scenario unloading the riser. The rapid expansion of free gas in possible combination with unloading the riser will lead to a quick reduction in bottomhole pressure. This can make it possible to induce a secondary kick. Hence, when using OBM it is very common to close BOP and circulate across choke in all situations where a kick possibly can have been introduced. This is done to avoid taking undetected kicks unnoticed to surface. This is why early kick detection is crucial, and the faster it is detected on the surface, the smaller influx will occur resulting in a less risky situation with an easier well control.

Gas migration

Free gas migrates and travels up the wellbore faster than liquid while gas in solution in mud does not migrate (Thomas et al., 1984). Due to the invading gas being infinite soluble in OBM, (Bland et al., 2006), the kick will not migrate up the wellbore without any circulation. Whereas using WBM the free gas will migrate quickly. If the local fraction of the gas void exceeds 10% the flow will be dominated by large bubbles and migrate upwards at a high velocity (Johnson, Rezmer-Cooper, Bailey, & McCann, 1995). Additionally to this, very

small bubbles, typically smaller than 2 mm in diameter, will stay still relative to the fluid and is held suspended by the liquid phase (Johnson et al., 1995).

This gas fraction of small bubbles, which remain suspended, will have two different effects during a well control operation. Firstly, as the gas travels upwards in the well it will leave behind a trail of gas, reducing the volume of gas migrating. Secondly, this gas left in suspension will begin to increase the compressibility of the mud in the well and consequently decrease how fast the shut-in surface pressure will rise. This may result in the misinterpretation that the gas is migrating slowly when it is actually not.

Thomas et al. concluded that large concentrations of gas may travel fast up in the well and can enter the riser which may unload the entire riser (Thomas et al., 1984). This will be discussed later in subchapter 3.1.3 Riser gas.

Kick tolerances & well pressure development during kill circulation

One of the more positive effects of using OBM is that the maximum casing shoe pressure is lower than for WBM. Especially when circulating the well, the gas influx will be dissolved in the oil phase of the mud. This leads to a larger density between true depth and casing shoe and consequently a lower casing shoe pressure when circulating the kick at a constant bottomhole pressure.

In WBM, the gas bubble will migrate even when the well is shut-in. For this reason, the gas bubble will result in a continuous pressure build-up until the kick is just below the BOP. On the other hand, in OBM the gas influx is dissolved in the mud. The consequence of having a dissolved gas kick in the mud is that there will be no gas migration when there is no circulation (Rolv Rommetveit et al., 2003).

One important aspect to consider for the well pressure development is the thermal expansion of the fluid while operating under HPHT conditions. The pressure increase in a shut-in well due to the thermal expansion can have a great impact on the well's kick tolerance and should accounted for (Mosti, Anfinsen, & Flatebø, 2008).

Reservoir compatibility

Formation damage is of great concern, especially when it comes to horizontal wells due to the larger area of formation that are drilled and exposed to the mud. Even shallow damage in such a well can lead to greatly reduced production rates (Longeron, Alfenore, Salehi, & Saintpère, 2000)

Since oil-based drilling fluids usually has very low fluid loss to the formation, resulting in a thin filter cake, permeability tests performed always indicate less damage to the formation than WBM (Soliman, 1995)

The results presented by Longeron et al shows that OBM is to be preferred when it comes to reservoir compatibility (Longeron et al., 2000). The flow initiation pressures on the cores used in the laboratory tests damaged with the OBM are lower than the cores damaged by WBM. Therefore the well will produce more easily while using an OBM.

Environmental impact

Release of OBM to the environment has far more serious environment and biological consequences than WBM. Hence, it is prohibited to release cuttings with OBM. OBM cuttings may have some toxic components, like aromatic hydrocarbons, which cause harm to the biological life at sea. WBM is less harmful to the environment, which makes it the preferred choice when approaching the environmental aspect (M. Amani et al., 2012).

One of the problems with OBM offshore is how to deal with the returns. It can either be shipped back to land and treated there, called skip and ship, re-injected into a re-injection well or dumped directly into the sea. All of these solutions have their challenges, but a new drilling waste management method called the TCC® technology treats the OBM so that the base oil can be re-used. It is developed by Termtech and uses thermal energy to separate and recover the components of the cuttings while maintaining the original quality of the components prior to treatment. This will make the OBM more environmental friendly in the long run (Kleppe, Michelsen, Handgraaf, Albriktsen, & Haugen, 2009).

Differential sticking

The differential sticking mechanism is as follows: A section of the drill string rests at the low side of a deviated hole. During rotation the pipe is lubricated by a film of mud, and the pressure on all sides of the pipe is equal. If the rotation is stopped, i.e. during a connection, the pipe in contact with the filter cake is not in contact with the mud column, and the differential pressure between the two sides of the pipe causes drag when trying to pull the pipe. If this drag is greater than the pulling power of the rig, the pipe is stuck. Therefore, drag increase when pulling the pipe is an indication of differential sticking.

Oil-based muds are much better for avoiding differential sticking. This is due to a much lower coefficient of friction than WBM, but also because they produce very thin filter cakes. This

was confirmed by Adams, N. who did a comprehensive study of 310 cases of stuck pipe where only one occurred when OBM was in the hole (Adams, 1997).

3.1.3 Riser gas

If any free formation gas enters the riser prior to BOP closure, the gas will continue to ascend with volumetric expansion, normally in accordance with Boyle's law. In deep water, with a long riser, the expansion is rather dramatic. Theoretically, a gas bubble of 15 bbl at the bottom of a 900 m long riser, have the capability to displace all of the fluids within the riser as it expands to atmospheric pressure (Hall, Roche, & Boulet, 1986). When the gas travels upwards, the mud is pushed out the diverter at the top of the riser. When using OBM, the unloading scenario will also be affected by the bubble point of the composition of drilling fluid and dissolved gas. This will affect the unloading process (Kozicz, 2012). Therefore, the circumstances result in a hazardous free-flowing riser blowout with mud and gas being expelled over the side of the rig. The mud column in the riser will be evacuated and subject the riser pipe to seawater collapse pressure.

One example of a solution for riser gas handling is developed by Managed Pressure Operations International Ltd[2]. It uses a flow spool to divert the riser returns, after having activated the special annular BOP, to a pressure control manifold. The annular BOP is supposed to be on active standby during all rig operations. The pressure control manifold will apply backpressure to make the well overbalanced and control multiphase return flow from the riser. If you apply back pressure you will also move the bubble point, i.e. change the location of where gas is released. In this case, a less impending unloading process will be the result. While using this system, the risk of diverting OBM overboard is reduced if a riser gas situation happens (Yeo, Macgregor, Pinkstone, & Piccolo, 2015).

[2] http://www.managed-pressure.com/

4 Gas solubility in oil-based mud under HPHT conditions

Oil-based mud is the preferred drilling fluid for HPHT wells and is frequently used, as discussed earlier in the well control chapter. In order to perform safe and efficient well operations, it is important to understand how the gas influx behaves in drilling fluids. The oil-based mud (OBM) may be contaminated by the gas during drilling, and this can lead to potential danger to the drilling equipment, environment and the personnel. The greatest threat is when the gas completely dissolves into the drilling fluid, which is the case for HPHT wells, and rapidly goes out of solution when the drilling fluid is circulated up in the well (P. L. O'Bryan, 1985).

4.1 Affecting solubility

There are several factors that have an impact on the solubility of gas in an oil-based mud. Some of these elements are presented below.

4.1.1 Pressure and temperature

O'Bryan et al. conducted experiments regarding how the gas solubility is affected by the pressure and temperature. Their result showed that gas solubility increased with higher pressure, and decreased at higher temperature (P. L. O'Bryan, 1985). However, Thomas et al. proved that the solubility actually increases with increasing temperature, at high pressures, which contradicts the observations of O'Bryan (Thomas et al., 1984). This inconsistency of results is due to the characteristics of solubility of a low volatility component in a supercritical solvent. This means that for high pressures the solubility increases with temperature, and at low pressures solubility in fact decreases with temperature (Brunner, 1994).

4.1.2 Composition of gas influx and base oil

Most of experiments performed, with gas solubility as its scope, have used methane gas since the major part of reservoir fluids is mainly composed of methane (Bureau, de Hemptinne, Audibert, & Herzhaft, 2002).

The specific gravity of the gas has an effect on the solubility of formation gas in OBM; the higher specific gravity, the greater gas solubility. This is the case for low to intermediate pressures (P. L. O'Bryan, 1985). This also applies when methane is mixed with other compounds like toluene, which represents the aromatic particles of oil. The specific gravity

will go up, and with smaller fractions of methane, the gas solubility increases (Bureau et al., 2002).

When it comes to the composition of the base oil, it has negligible effects on the solubility at low pressures. However, at HPHT conditions, the gas solubility in base-oil differs when using different base-oil composition. For instance, the change of oil-water ratio (OWR) in the mud will affect the solubility; the higher the OWR, the higher the gas solubility (P. L. O'Bryan, 1985). The chemical structure similarity of the base-oil and the methane has to be taken into account, as simpler base-oil composition can absorb more methane gas than complex structured base-oils (Flatabø et al., 2015).

4.1.3 Circulation

Slow circulation rates, with resulting laminar flow in the annulus, may cause the gas to be "strung out" up the annulus. This means the gas-oil ratio (GOR) profile of the annulus will be stretched thin and cover a longer part of the annulus. Over time the gas-in-oil solution could cover the whole wellbore (Hornung, 1990).

When the pump rate is at normal drilling rate, the flow regime around the drill collar section will be turbulent. This significantly increases the rate of gas dissolution, due to the mixing of the flow (R. Rommetveit & Olsen, 1989).

While having drilling fluid containing invading gas, the gas bubbles will be dispersed due to convection and molecular diffusion. The main mechanism, however, is believed to be convection as long as the well is being circulated. This convective process increases the solubility of the gas into the oil-based mud (P. L. O'Bryan & Bourgoyne, 1989).

4.2 Consequences of gas dissolution

The effect of gas solubility changes the properties of the drilling fluid when the gas is mixed into the mud, which can lead to well control issues. The fact that the formation volume factor of gas, relative volume of gas at reservoir conditions to the volume of gas at standard conditions, is different when gas is dissolved into mud could be a sign of that small changes of composition of the gas and liquid are taking place (Silva et al., 2004).

4.2.1 Rheological properties

It is important to understand the alteration to the rheological properties of the OBM when gas mixes with the mud, due to the well control issues that can arise (Mahmood Amani, 2012).

When gas is dissolved into the OBM, the shear stress is heavily reduced, and similarly the viscosity is reduced. Results presented by Torsvik et al shows that OBM, based on linear paraffin, mixed with methane gives an effect of reducing the shear stress by about 40% (Torsvik, Skogestad, & Linga, 2016).

4.2.2 Saturation pressure

With dissolved gas mixed into the OBM, the well run the risk of having gas boiling rapidly out of solution followed by a large volume expansion. This occurs when the wellbore pressure at a point is below the saturation pressure of the mixture. The consequences of flashed gas can be severe and may lead to a blowout at the surface or unloading of the riser (Rolv Rommetveit et al., 2003). The bottomhole pressure will be reduced and secondary kicks can be taken.

The saturation pressure, the pressure where vapor and liquid are in equilibrium, initially increases rapidly with increasing GOR, but levels off with further increase in GOR. Therefore, for high concentration of dissolved gas, the gas will boil out of the mud-gas mixture deeper down in the wellbore than for low concentration of gas. However, the saturation pressure decreases for very high concentration of dissolved gas (Flatabø et al., 2015). In terms of the OBM density, the saturation pressure remains the same with increasing GOR, so the GOR will still give the same effect independent of the density (Silva et al., 2004).

4.2.3 Density variation

While drilling HPHT wells with invading gas it is essential to correctly calculate the gas-mud mixture density. These kinds of wells are usually long, and minor inaccuracies in densities can have a considerable impact on the volume balance calculations throughout the well (Torsvik et al., 2016).

The density of oil-based drilling fluid is dependent of the pressure and temperature in the well (McMordie et al., 1982). The gas solubility, as mentioned earlier, also relies on the pressure and temperature. Gas mixed into the mud also has an effect on the density. O'Bryan et al presents results showing that when gas dissolves into the OBM, the density of the mud decreases (P. L. O'Bryan & Bourgoyne, 1987).

4.3 Pressure-volume-temperature models

Pressure-volume-temperature (PVT) properties such as saturation pressure, GOR, formation volume factors, mixed density, are necessary to predict the characteristics and behavior of drilling fluids at HPHT conditions. Therefore, one can either use an equation of state or PVT correlations to complete the missing data related to the properties of the mixed fluid.

4.3.1 Equations of state method

With the intention of understanding the process of dissolution of gases in drilling mud, especially while operating in the borehole with higher pressures and temperatures, mathematical models using the equations of state have been developed. These models are used to simulate the mixture behavior under given conditions of gas concentration and pressure, where the pressure-volume-temperature equipment is limited and cannot give viable experimental data (Atolini & Ribeiro, 2007). However, modeling with high pressures and temperatures may prove difficult for the simulators that extrapolate the results of experimental data, when approaching the critical region of the mixture. Marteau et al. examined these risks and compared the different equations of state with experimental data and questioned if these models could be relied upon (Marteau, Obriot, Barreau, & Behar, 1997). For instance, Torsvik et al. showed that for density prediction of OBM, the two standard models, based on Peng-Robinson and Soave-Redlich-Kwong equations of state (Peng & Robinson, 1976; Soave, 1972), deviates from the experimental results regarding density differences under HPHT conditions. However, their work shows that by tuning the PVT models with a series of density measurements, the EOS's shows promising potential (Torsvik et al., 2016).

One example of a PVT simulator is PVTsim which is developed by Calsep[3]. This simulator uses equation of state to calculate phase behavior of petroleum fluids.

4.3.2 Pressure-volume-temperature correlations

One of the earlier PVT correlations that model the dissolution of gas into oil was developed by Standing. However, Standing's work, which his PVT correlation is based on, is developed for California oils and does not make corrections for other oil types or non-hydrocarbon content. The correlation assumes that the saturation pressure is a function of dissolved GOR, density of fluids, and temperature (Standing, 1947). It is common that PVT correlations are only developed for fluid properties in a certain geographical area. It is known that one

[3] http://www.calsep.com/

correlation predicts one or more properties, like density or viscosity, better than other correlations. Therefore, a different correlation has to be used for different properties to achieve better results (Wu & Rosenegger, 2000).

5 Advancements in HPHT well control

The high temperatures and pressures encountered in HPHT wells can constrain the variety and utility of down-hole tools and fluid selection. These constrains can be so severe that LWD/MWD tools become ineffective, resulting in down-hole annular pressure measurements used for pressure management, unavailable. It may be the case that the only way to gather information on the down-hole pressure, is through temperature/hydraulics models and the drilling mud (Bland et al., 2006).

5.1 Hydraulics modeling

Hydraulics models have been developed to give information other than pump pressure and bit hydraulics. They can be used for planning, but in some cases they can also provide real-time information about the pressure in the well and can give real-time ECD and equivalent static density (ESD) during drilling. This is crucial when the temperature in HPHT wells exceeds the tolerable temperature of the tools run downhole.

Drillbench[4] is such planning software which is owned by Schlumberger, and developed by former SPT Group. It has several modules where one of them is the dynamic hydraulics model, which helps to understand the transient behavior of the well and to help to plan the drilling of the well.

5.2 Early kick detection

One of the most critical areas for development in well control safety, as mentioned before, is early kick detection. The urgent need for earlier, more precise, more consistent kick detection in an extensive range of drilling operations has turned out to be increasingly important as drilling in deep water wells with narrow operational windows is currently more common.

5.2.1 Managed pressure drilling (MPD) as early kick detection

Usually MPD systems use complex, high precision flow metering, typically a Coriolis meter, which is put on the return line to monitor for an influx downhole. This system will do a comparison with inflow, usually determined by a stroke counter, to the measured outflow from the Coriolis meter. This will give a far more swift warning of an influx than looking at the pit gain. The MPD system offshore will be using a rotating control device to divert the flow to the return system. Thus, the circulating volume in the riser will be stable, and the rig

[4] https://www.software.slb.com/products/drillbench?tab=Overview

heave will not affect the volume in the riser. By using the Coriolis meter on the return line, the resolution of the kick detection will be significantly increased and can detect gas influx in OBM (Wood Group Kenny, 2015). A new type of kick detection system, called Microflux Control (MFC) which contains a Coriolis meter, has shown that this system work nearly as well with OBM as with WBM when detecting kicks. Since the gas does not instantly react with the OBM, and the MFC detection is in real-time, the MFC can distinguish a kick of a very small volume; this is how MFC overcome the gas solubility kick masking mechanism (Santos, Catak, Kinder, & Sonnemann, 2007).

An automated response to a kick can be initiated if the system has a fully automated choke in combination with a kick detection algorithm. One of the great advantages with MPD is that if it automatically detects a kick, it can counter it by increasing the surface backpressure.

5.2.2 Early kick detection through automated monitoring

Numerous parameters are currently monitored automatically, but most of the time they are displayed in simple logs which can be difficult to interpret. Information about ROP, WOB, flow rate etc. can be used to help detecting a kick. By processing these parameters, an automatic kick detector can be developed so that an alarm will be triggered in the case of a kick. These types of kick detection systems are software based and have the great advantage of being relatively easy and inexpensive to be installed on existing rigs.

5.3 Cesium formate brines

Under some conditions while drilling a HPHT well, problems can be encountered even when using OBM that cannot be solved. Saasen, A. et al mentions barite sag and well geometry as significant problems while drilling the Huldra field in Norway with OBM. It was necessary to have as little contribution to the ECD as possible (Saasen et al., 2002). The main benefits of using cesium formate brines compared to OBM are as follows, mentioned in the same paper:

- There is no barite sag potential, since the density is given from the clear brine itself
- Low ECD
- Low gas solubility and enhanced kick detection
- The same environmental impact as WBM.
- Quick thermal stabilization during flow checks.

The main issue with cesium formate brines as drilling fluid is the very high cost compared to standard drilling fluid systems. This implies a need to avoid losses of the brine and also contamination.

6 Numerical modeling

6.1 Introduction

Multiphase flow simulators are at this time widely used in the design and operation of facilities offshore. Some examples where the multiphase flows simulators are used are blowouts, flow assurance and underbalanced drilling operations. The models are separated into two categories: Steady-state models; the flow is assumed to be steady in time, and transient models; the flow is dependent of time. These models can describe two-phase flow with a two-fluid model composed of conservation equations for each of the phases concerning mass, momentum and energy (Danielson, Brown, & Bansal, 2000):

Steady-state model:

$$(AH_i\rho_i v_i)_{in} = (AH_i\rho_i v_i)_{out} + \psi$$

$$(AH_i\rho_i v_i^2)_{in} = (AH_i\rho_i v_i^2)_{out} + \sum F$$

$$\left(A\rho_g v_g\left(h_g + \frac{v_g^2}{2} + gz\right)\right)_{in} + \left(A\rho_l v_l\left(h_l + \frac{v_l^2}{2} + gz\right)\right)_{in} =$$

$$\left(A\rho_g v_g\left(h_g + \frac{v_g^2}{2} + gz\right)\right)_{out} + \left(A\rho_l v_l\left(h_l + \frac{v_l^2}{2} + gz\right)\right)_{out} + Q$$

Transient model:

$$\frac{d}{dt}(VH_i\rho_i) = (AH_i\rho_i v_i)_{in} - (AH_i\rho_i v_i)_{out} + \psi$$

$$\frac{d}{dt}(VH_i\rho_i v_i) = (AH_i\rho_i v_i^2)_{in} - \left(AH_i\rho_i v_i^2\right)_{out} + \sum F$$

$$\frac{d}{dt}\left[V\rho_g\left(e_g + \frac{v_g^2}{2} + gz\right) + V\rho_l\left(e_l + \frac{v_l^2}{2} + gz\right)\right] =$$

$$\left(A\rho_g v_g\left(h_g + \frac{v_g^2}{2} + gz\right)\right)_{in} + \left(A\rho_l v_l\left(h_l + \frac{v_l^2}{2} + gz\right)\right)_{in} -$$

$$\left(A\rho_g v_g\left(h_g + \frac{v_g^2}{2} + gz\right)\right)_{out} - \left(A\rho_l v_l\left(h_l + \frac{v_l^2}{2} + gz\right)\right)_{out} - Q$$

Where:

i – phase, gas/liquid

A – pipe cross-sectional area [m^2]

H_i – hold up of phase i

ρ_i – density of phase i [kg/m^3]

v_i – velocity of phase i [m/s]

Ψ – rate of mass transfer due to condensation/evaporation [kg/s]

$\sum F$ – sum of forces on phase i (pressure, gravitational and friction) [N]

V – pipe section volume [m^3]

h_i – enthalpy of phase i [J/kg]

g – acceleration due to gravity [m/s^2]

z – vertical position of pipeline [m]

Q – rate of heat loss across the pipeline wall to the surroundings [W]

e_i – internal energy of i [J/kg]

In order to solve the parameters $\sum F$, Q and Ψ, and also simulate the flow conditions the models use closure laws. The closure laws will be explained in section 6.2.2. By using a combination of conservation equations and closure laws the model can be solved. The conservation laws form a system of partial differential equations which are complex to solve analytically. Instead the models are solved numerically and often implemented in a software tool.

6.2 Transient drift flux model

As discussed in the previous section, the conservation equations are rather complex, so the models are often simplified. Rather than using a momentum conservation equation for each phase a mixture momentum equation is used. The energy equation is often neglected due to the assumption of a constant temperature gradient which is a function of the geothermal gradient. This condenses down to a model which is comprised of two mass conservation laws, one momentum conservation law and four closure laws which are shown in section 6.2.1 and 6.2.2.

The theory behind the drift flux model is based on references (Udegbunam, Fjelde, Evje, & Nygaard, 2015) and (Evje & Fjelde, 2002).

The drift flux model has a generic form, and is expressed as:

$$\partial_t W + \partial_x F(x, W) = G(x, w)$$

Where:

W – conservative variables

F – flux

G – source term

x – coordinate along the flow direction

t – time

6.2.1 Conservation laws

A conservation law expresses that a particular quantifiable property of an isolated physical system, like mass or momentum, does not vary as the system progress over time. A conservation law can be expresses mathematically as a continuity equation, which is a partial differential equation that gives a relation between the amount of the quantity and the transport of that quantity. The drift flux model uses three conservation laws; conservation of gas and liquid mass, and the conservation of momentum. Given that the model is based on two-phase flow, two different mass conservation equations are needed; one equation for the conservation of gas and one for the conservation of liquid.

Conservation of mass

The law of conservation of mass states that for a closed system, the mass is preserved while the system evolves through time. This implies that mass cannot be created nor destroyed – i.e. processes that alter the chemical or physical properties of matters in an isolated system will result in no change of mass. The most basic assumption is described below; we assume flow area is uniform:

$$Mass_{inn} = Mass_{out}$$

The following equations are the conservation laws for gas and liquid respectively:

$$\frac{\partial}{\partial t}(\rho_g \alpha_g) + \frac{\partial}{\partial z}(\rho_g v_g) = \Gamma_g$$

$$\frac{\partial}{\partial t}(\rho_l \alpha_l) + \frac{\partial}{\partial z}(\rho_l v_l) = \Gamma_l$$

Conservation of momentum

The law of conservation of momentum express that the quantity of momentum remains constant; momentum cannot be created nor destroyed but can only be changed through forces as explained by Newton's laws of motion. The equation is defined as a mixture momentum equation:

$$\frac{\partial}{\partial t}\Big(\big(\rho_l \alpha_l v_l + \rho_g \alpha_g v_g\big)\Big) + \frac{\partial}{\partial z}\Big(\big(\rho_l \alpha_l v_l^2 + \rho_g \alpha_g v_g^2\big)\Big) + \frac{\partial}{\partial z} P = -(\rho_{mix} g) + \frac{\Delta\, P_{fric}}{\Delta\, z}$$

Conservation of energy

Along with conservation of mass and conservation of momentum, the conservation of energy is a fundamental concept of physics. As energy is neither created nor destroyed, it can be converted from one form to another. It can be converted from potential energy to kinetic energy, but the total energy within the domain remains unchanged. The mixed energy conservation equation is stated below:

$$\frac{\partial}{\partial t}\left(\rho_g \alpha_g \left(e_g + \frac{v_g^2}{2} + gx\right) + \rho_l \alpha_l \left(e_l + \frac{v_l^2}{2} + gx\right)\right) + \frac{\partial}{\partial x}\left(\rho_g \alpha_g v_g \left(h_g + \frac{v_g^2}{2} + gx\right) + \rho_l \alpha_l v_l \left(h_l + \frac{v_l^2}{2} + gx\right)\right) = h_s + U$$

Where:

$\rho_{g/l}$ – density gas/liquid [kg/m^3]

$\alpha_{g/l}$ – volume fraction gas/liquid

$v_{g/l}$ – velocity gas/liquid [m/s]

$e_{g/l}$ – internal energy gas/liquid [J/kg]

g – gravitational constant [m/s^2]

x – position of pipeline [m]

$h_{g/l}$ – enthalpy gas/liquid [J/kg]

h_s – enthalpy of mass sources [J/kg]

U – Heat transfer per unit volume [J/m^3]

To solve the energy equation becomes rather complex when representative thermodynamic models needs to be implemented in order to model the phase transition terms. A scheme which uses a six-equation model is an extension of AUSM+ by Paillére and García-Cascales.

The scheme is rather complex since it uses six-equations representing the conservation laws. It also uses advanced algorithms to calculate the pressure and enthalpy (García-Cascales & Paillère, 2006).

However, another alternative is to bypass the energy equation and this is for instance being investigated by John Emeka Udegbunam at the University of Stavanger. This model is developed for its simplicity and clarity. The following theory is a short summary of what he is working on, and which may be implemented into the AUSMV scheme. Additionally, this formulation may ease the modeling of phase transition, since phase transition is heavily dependent on the heat transfer of the system. With this model, however, one does not need to formulate complex energy equations.

The basic equation for convective heat transfer is:

$$Q = hA\Delta T$$

Where:

Q – heat transferred per unit time [W]

h – heat transfer coefficient [W/K]

ΔT – difference in temperature between the surroundings and the fluid [K]

What the model wants to achieve is the temperature profile in the well, for each segment in the AUSMV scheme. The equations used to find the temperature distribution is developed by L.R. Raymond (Raymond, 1969). John Emeka Udegbunam is discretizing these equations to make a transient temperature distribution model. The model predict the heat transfer between the formation, annulus and drillpipe, which subsequently can be used to model the heat flux from cell to cell, which in turn can be used to calculate the mass transfer between the phases.

6.2.2 Closure laws

The closure laws are used to condense the number of unknown variables in a system. In order to express the unknown variables, simplified equations are used with known quantities. In the transient drift flux model there are four closure laws used:

1. Phase-volume fraction
2. Liquid density
3. Gas density
4. Gas slippage

Phase-volume fraction

The phase-volume fraction defines the distribution of volume between gas and liquid. Since this a two-phase model, the sum of gas and liquid fractions will always be equal to one, as expressed in the following equation equation.

$$\alpha_l + \alpha_g = 1$$

Liquid density

The liquid density is affected by the temperature and pressure. However, since the effect is minimal, a linearized equation can be used. The liquid density model is based on the equation of state (EOS) for the liquid density. An EOS is a well-designed relationship between a complete set of state variables. For this equation (Stamnes, 2011) the state variables are, like for most EOS, pressure, temperature and volume[5].

$$\rho_l = \rho_{l,0} + \frac{\rho_{l,0}}{\beta}(P - P_0) - \rho_{l,0}\alpha(T - T_0)$$

Where $\rho_{l,0}$, P_0 and T_0 is the reference density, pressure and temperature, respectively. β represents the bulk modulus and is affected by pressure: $2.2 \cdot 10^9$ $[Pa]$. Whereas α is the volumetric thermal expansion coefficient: 0.000207 $[K^{-1}]$

[5] https://www.e-education.psu.edu/png520/m7_p3.html

Gas density

The gas density is also affected by pressure and temperature. The equation below is developed from the ideal gas law but uses instead a specific gas constant, R_{spec}, to be implemented into the AUSMV scheme.

$$\rho_g = \frac{P}{R_{spec}T}$$

The specific gas constant is in this case the specific gas constant of steam: $461.5\ [\frac{J}{kg \cdot K}]$

Gas slippage

To solve the unknown variables of velocities, the following equation has been introduced:

$$v_g = Kv_{mix} + S$$

Where v_{mix} is the mixture velocity of the fluid, v_g is the gas velocity and K and S are flow dependant parameters. K is the distribution coefficient and S is the drift velocity of gas relative to liquid. These parameters have values depending on the flow regimes present. The values used here were $K = 1.2\ ,\ S = 0.5$

6.2.3 Source term

The source term, q, can be split into two components as

$$q = F_g + F_w$$

Where F_g represents the gravity term. It can be expressed by the following equation:

$$F_g = g(\alpha_l \rho_l + \alpha_g \rho_g) cos\theta$$

Where g is the acceleration due to gravity, and θ is wellbore inclination.

The component F_w represents the loss of pressure due to friction, and can be calculated by the following equation.

$$F_w = \frac{2f\rho_{mix}v_{mix}|v_{mix}|}{d_o - d_i}$$

The friction factor f is dependent on the type of flow, whether it is laminar or turbulent. The type of flow needs to be determined using the Reynolds number which again depends on geometry, fluid viscosities, mixture density and mixture velocity.

6.3 AUSMV Scheme

The advection upstream splitting method (AUSMV) is a simple and robust transient model which can handle dynamic flow systems. The AUSMV is a hybrid scheme that combines flux-vector splitting (FVS) and flux-difference-splitting (FDS) scheme to get an efficient and accurate scheme. In order to avoid the numerical dissipation, which can be experienced when using the FVS scheme, the velocity-splitting function is modified. One can find a more detailed description in a paper by Evje and Fjelde (Evje & Fjelde, 2002).

6.3.1 Conservative variables

The three conservation equations regarding mass of liquid, mass of gas and momentum can be written on a conservative vector form:

$$\partial_t \begin{bmatrix} \alpha_l \rho_l \\ \alpha_g \rho_g \\ \alpha_l \rho_l v_l + \alpha_g \rho_g v_g \end{bmatrix} + \partial_x \begin{bmatrix} \alpha_l \rho_l v_l \\ \alpha_g \rho_g v_g \\ \alpha_l \rho_l v_l^2 + \alpha_g \rho_g v_g^2 + P \end{bmatrix} = \begin{bmatrix} \Gamma_l \\ \Gamma_g \\ -q \end{bmatrix}$$

One can also write the previous equation as:

$$\partial_t \begin{bmatrix} w_1 \\ w_2 \\ w_3 \end{bmatrix} + \partial_x \begin{bmatrix} v_l w_1 \\ v_g w_2 \\ v_l^2 w_1 + v_g^2 w_2 + P(w_1, w_2) \end{bmatrix} = \begin{bmatrix} \Gamma_l \\ \Gamma_g \\ -q \end{bmatrix}$$

Where $(w_1,\ w_2,\ w_3)^T = \left(\alpha_l \rho_l,\ \alpha_g \rho_g,\ \alpha_l \rho_l v_l + \alpha_g \rho_g v_g\right)^T$ are the conservative variables.

The unknowns in this set of equations are ρ_l, ρ_g – the liquid and gas densities; α_l, α_g – the phase-volume fractions; v_l, v_g – the velocities of liquid and gas; and P – common pressure for gas and liquid. The q variable corresponds to the source term.

Earlier versions of the AUSMV scheme have assumed that there is no mass exchange between the liquid and the gas phases, so that: $\Gamma_l = \Gamma_g = 0$. However, in this thesis, the mass exchange terms have been included. How the mass exchange terms is defined and implemented in the code will be explained in chapter 6.4.

6.3.2 Discretization

To sequentially apply the conservation and the closure laws described in the previous chapter, the well first needs to be divided into a certain number of segments. The length of the well is divided into boxes of equal sizing. The equations are then solved for each box. The flow variables in each box are considered as constant. With an increase of boxes, the discretization

will be more refined; the solution will be more accurate, but require more computing power and lead to an increase in computational time.

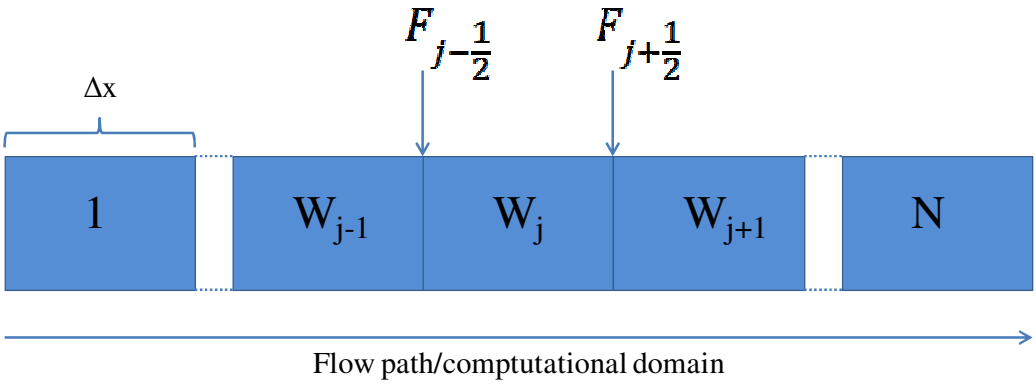

Figure 6.1: Discretization

6.3.3 Explicit scheme

Numerical discretization is regularly divided into two categories: explicit or implicit. The explicit model base its calculations on known values from the previous time level when processing the solution in time, whereas the implicit model calculates the unknown variables based on matrices and iterations. The implicit approach is more complicated to implement, but it is more computationally efficient since one can simulate with larger time steps. The AUSMV scheme treats the fluxes explicit in time, meaning that the values are derived from "old" values when calculating the conservative variables at a new time level.

Calculating new values

First, the well is discretized into N cells, where each cell has a length Δx. The flow variables are initialized by, for instance, assuming static conditions. The numerical flux F^{AUSMV} is calculated using the formulas presented in a paper by Evje & Fjelde (Evje & Fjelde, 2003). Figure 6.2 visualize the updating process.

$$w_{i,j}^{n+1} = w_{i,j}^{n} - \frac{\Delta t}{\Delta x}\left(F_{j+\frac{1}{2}}^{AUSMV} - F_{j-\frac{1}{2}}^{AUSMV}\right) - \Delta t q_i^n$$

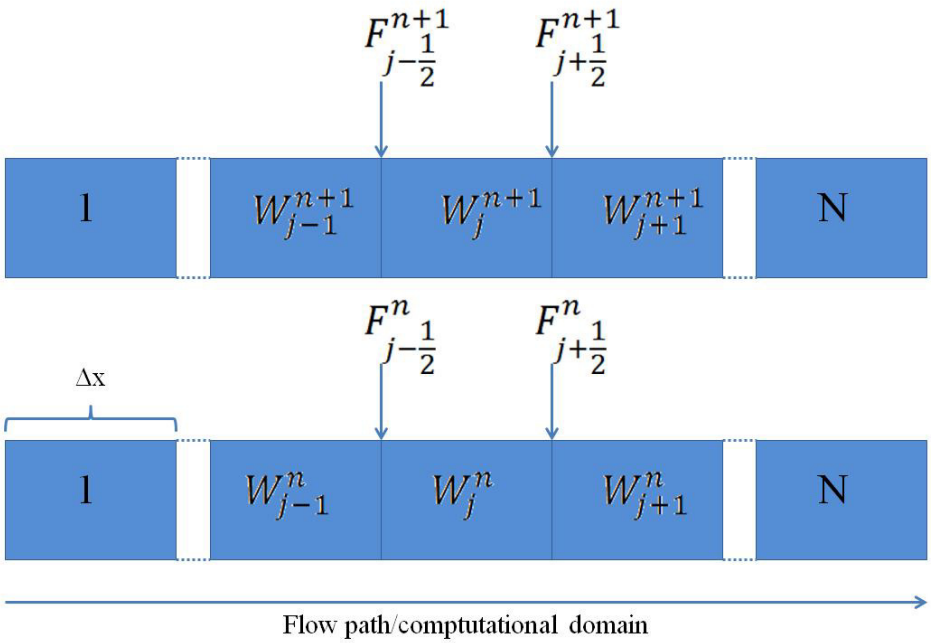

Figure 6.2: Discretization of a new timestep

The indices i and j stand for conservative variables and cells, respectively. The F^{AUSMV} term represent mass and momentum fluxes. The time step Δt is limited by the CFL condition and this will be defined later in this chapter.

When the AUSMV fluxes at the cell interfaces has been found, the conservative variables at the new time level (n+1) are calculated using the "old" values from time level (n). All the cells at the new time level will then be updated.

Numerical flux

In finite-volume codes for the Navier-Stokes and Euler equations an important role is taken by the numerical scheme that takes into account the inviscid interaction of adjacent fluid cells at their interface, for example the fluid cell W_j with the two flux terms in figure 6.2. Such a scheme merges two separate sets of state quantities, quantities on both sides of the interface, into one set of fluxes normal to the interface (van Leer, Thomas, Roe, & Newsome, 1987).

How the numerical flux $F_{j\pm\frac{1}{2}}$ is defined is usually the difference between the various numerical schemes. In the formulation of AUSM type schemes, the flux is divided into a convective part F^c and a pressure part F^p. For detail, one can look in a paper by Evje and Fjelde (Evje & Fjelde, 2003).

6.3.4 Boundary conditions

The numerical fluxes at the inlet and the outlet boundaries have to be specified rather than using the formulas detailed by the AUSMV scheme. The scheme uses the variables that are physically determined by the simulation and use an extrapolation method to find the values for the unknown variables.

How the boundary is treated depends on the status of the well. The well can be divided into two states; open or closed well.

Open well

At the inlet boundary, the mass flow rates of gas and liquid are known; hence, both mass and convective fluxes can be determined directly. The inlet pressure or pressure flux needs to be calculated. The formula that can be used for this is:

$$P_{inlet} = P(1) + \frac{\Delta x}{2}\rho_{mix} g cos\theta + \frac{\Delta x}{2} F_w$$

The mass and convective momentum fluxes are extrapolated using the midvalues in the boundary cell at the outlet boundary, whereas the outlet-pressure flux is set to atmospheric pressure. If a well kill or an MPD operation is in progress, the outlet-pressure would be set equal to the choke pressure.

Closed well

During a closed well state, the inlet mass and convective momentum fluxes are set to zero. The same is true for the outlet mass and convective fluxes. The inlet pressure flux is found by the equation above. Whereas the outlet pressure flux is determined by the following equation:

$$P_{outlet} = P(N) - \frac{\Delta x}{2}\rho_{mix} g cos\theta - \frac{\Delta x}{2} F_w$$

6.4 Phase transition term

In this thesis, the focus is on boiling of water and the phase transition from liquid to gas (steam). Boiling can be classified as flow boiling and pool boiling. A stationary or non-flowing fluid that exceeds the saturation temperature, a superheated fluid, is known as pool boiling. Saturation temperature is the temperature for a related saturation pressure at which a liquid boils into its vapor phase.

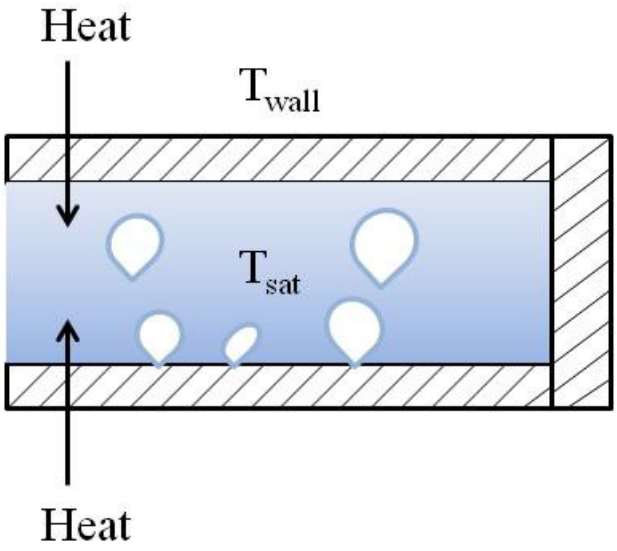

Figure 6.3: Illustration of pool boiling with water liquid and gas bubbles.

Boiling of a fluid during flow through a tube with wall heat flux is called flow boiling. Due to the simplicity of pool boiling, this has been introduced in the code in this work. The physical phenomenon of pool boiling can be categorized into four different regimes, based on the excess temperature ($\Delta T = (T_{wall} - T_{sat})$ where T_{wall} is the wall temperature and T_{sat} is the liquid saturation temperature). The temperature of the liquid is assumed to be equal to the wall temperature. The regimes are:

1. Purely convective boiling $\Delta T < 5^oC$
2. Nucleate boiling $5^oC < \Delta T < 50^oC$
3. Unstable (nucleate ↔ film) boiling $50^oC < \Delta T < 200^oC$
4. Stable film boiling $\Delta T > 200^oC$

Nucleate boiling (2) is what has been utilized in the work of this thesis since the temperature range applied in this thesis is more related to the nucleate boiling. Also, according to Kothandaraman (Kothandaraman, 2005), the nucleate boiling process is the most useful process when designing equipment and the convective boiling is to slow to be practical in this model.

Because there are many variables influencing this process, a direct correlation for this process is hard to obtain. However, Rohsenow made a correlation (Rohsenow, 1951):

$$q = \left[\frac{c_l \Delta T}{h_{fg} Pr^n C_{sf}}\right]^3 \mu_l h_{fg} \left[\frac{g(\rho_l - \rho_g)}{g_o \sigma}\right]^{0.5}$$

Where:

q – rate of heat addition [W/m^2]

c_l – specific heat of liquid [J/(kg·K)]

ΔT – excess temperature [K]

h_{fg} – evaporation energy [J/kg]

Pr – Prandtl number of liquid

n – constant, 1 for water and 1.7 for other fluids

C_{sf} – surface factor, assumed as 0.013

μ_l – dynamic viscosity of the liquid [Ns/m^2]

ρ_l – density of the liquid [kg/m^3]

ρ_g – density of the gas [kg/m^3]

σ – surface tension-liquid-gas interface [N/m]

g – gravitational acceleration [m/s^2]

g_0 – force conversion factor = 1 in SI units [kgm/Ns^2]

In order to calculate the amount of steam generated through evaporation, the definition of evaporation energy is used, so that:

$$\Gamma_g = \frac{q}{h_{fg}}$$

Where:

Γ_g – amount of steam generated [kg/(s·m^2)]

It is assumed that the steam has its source from the liquid phase, which gives:

$$\Gamma_g = -\Gamma_l$$

The evaporation energy, h_{fg}, depends on the temperature. For simulation purposes, a simple correlation equation has been purposed by Popiel and Wojtkowiak (Popiel & Wojtkowiak, 1998):

$$h_{fg} = a + bT + cT^{1.5} + dT^{2.5} + eT^{3}$$

Here a, b, c, d and e are constants and T is temperature in Kelvin. In the temperature range where this equation is applicable, from 5-370°C, the maximum error is roughly 0.12% (Affandi, Mamat, Kanafiah, & Khalid, 2013)

The interfacial tension between water-vapor also needs to be correlated since this depends on the temperature. The following equation is presented by Vargaftik et al. (Vargaftik, Volkov, & Voljak, 1983).

$$\sigma = B\left[\frac{T_c - T}{T_c}\right]^{\mu}\left[1 + b\left(\frac{T_c - T}{T_c}\right)\right]$$

Here B, b and μ are constants. T and T_c are temperature of fluid and critical temperature of fluid, respectively. The critical temperature of a substance is the temperature above which a gas cannot be liquefied, no matter how much pressure is applied.

In addition, a boiling point restriction has been experimented with. The boiling point is the temperature at which the vapor pressure of the liquid is equal to the surrounding pressure. In other words, the surrounding pressure that works on the liquid is less or equal to the vapor pressure at a given temperature, leading to evaporation of liquid. Hence, the boiling temperature relies on the pressure of the system. If the pressure in the system increases, the required temperature to start boiling the liquid also increases. An illustration of various pressures and temperatures where evaporation is taking place is shown in the following figure.

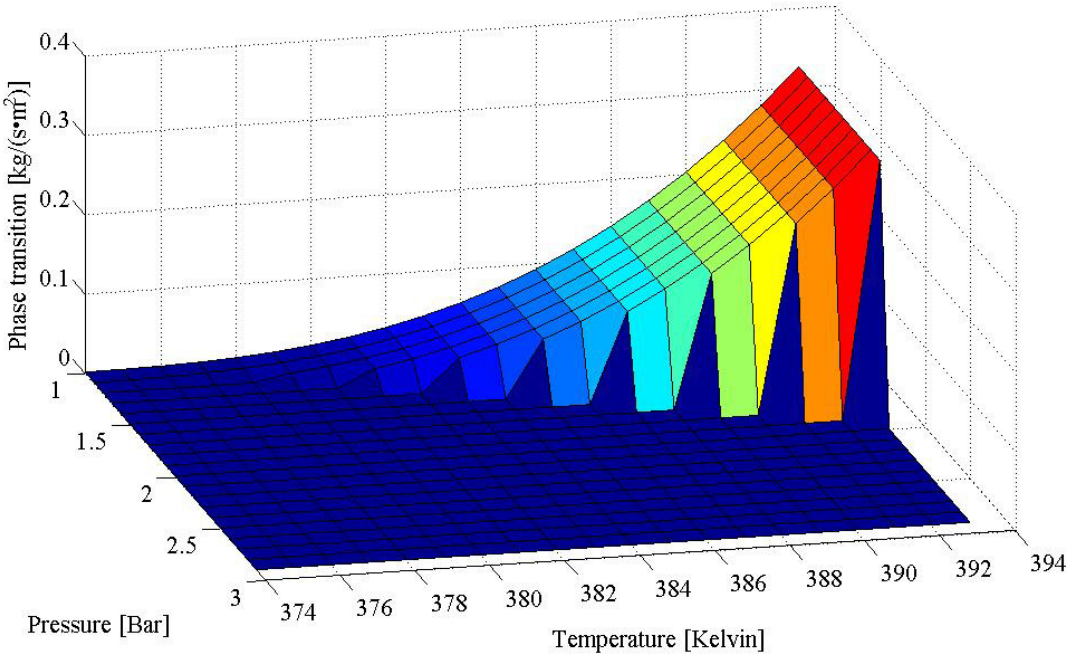

Figure 6.4: Phase transition vs pressure and temperature for water liquid.

Figure 6.4 illustrates how the increase in pressure affects the phase transition, in terms of the boiling point restriction. If the pressure is increased, the temperature also needs to be increased in order to have mass transfer. The figure also illustrates how the phase transition increases with temperature.

The boiling point can be calculated using the Clausius-Clapeyron equation:

$$T_B = \left(\frac{1}{T_0} - \frac{R ln\left(\frac{P}{P_0}\right)}{0.018 h_{fg,0}} \right)^{-1}$$

Where:

T_B – boiling point at current surrounding pressure [K]

R – ideal gas constant, 8.314 [J/(K·mol)]

P – surrounding pressure [kPa]

P_0 – reference pressure where the corresponding T_0 is known [kPa]

h_{fg} – evaporation energy of the liquid at P_0 [J/kg]

T_0 – reference boiling temperature [K]

After the equations have been defined, the numerical scheme, where the conservation variables are updated, needs to be modified to implement the phase transfer term. The new modified scheme is described as:

$$w_{1,j}^{n+1} = w_{1,j}^{n} - \frac{\Delta t}{\Delta x}\left(F_{j+\frac{1}{2}}^{AUSMV} - F_{j-\frac{1}{2}}^{AUSMV}\right) + \frac{\Delta t}{\Delta x}\Gamma_l$$

$$w_{2,j}^{n+1} = w_{2,j}^{n} - \frac{\Delta t}{\Delta x}\left(F_{j+\frac{1}{2}}^{AUSMV} - F_{j-\frac{1}{2}}^{AUSMV}\right) + \frac{\Delta t}{\Delta x}\Gamma_g$$

6.5 CFL condition

While simulating hyperbolic partial differential equation, stability usually tends to be a problem. To reduce the instability issue, a time restriction condition named after Courant, Friedrichs and Lewy (CFL) is used. The condition controls how the simulation will request information (Hirsch, 2007). The condition is implemented in the scheme using the following equation, limiting the timestep length.

$$\Delta t = CFL\frac{\Delta x}{\max(|\lambda_1|, |\lambda_2|, |\lambda_3|)}$$

Where λ_1, λ_2 and λ_3 represents the eigenvalues of the scheme. These eigenvalues are important since from these values one extract the wave speeds in order to determine the CFL condition.

The system have three eigenvalues; the first and third eigenvalue refer to sonic wave propagation, upward and downward respectively, whereas the second eigenvalue represent the speed of gas volume travelling downstream. The eigenvalues can be defined as:

$$\lambda_1 = v_l - \omega,\ \lambda_2 = v_g, \lambda_3 = v_l + \omega$$

If the condition $\alpha_g\rho_g << \alpha_l\rho_l$ is met and the liquid is assumed as incompressible, then an approximate sound velocity can be derived (Benzoni-Gavage, 1991):

$$\omega = \sqrt{\frac{P}{\alpha_g\rho_l(1 - K\alpha_g)}}$$

Figure 6.5 illustrates the eigenvalue propagation at the outlet boundary. In the figure the first wave propagates inwards, while the other two propagates outwards. The direction of the eigenvalues is defined by its sign. Positive eigenvalues propagates forward, while the negative eigenvalue propagate backwards.

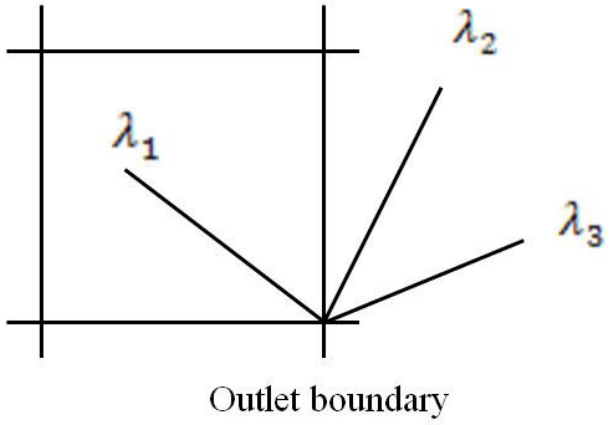

Figure 6.5: Propagation of eigenvalues at the outlet boundary of a cell

Figure 6.6 is an illustration of how the information propagates in a simulation. Figure 6.6 a) is a stable CFL case and figure 6.6 b) is an unstable case. The stable case shows that the information only propagates within the schemes numerical domain. The unstable case show the situation when the time step is too large and physical information is propagated from a domain exceeding the numerical domain of the scheme (Hirsch, 2007).

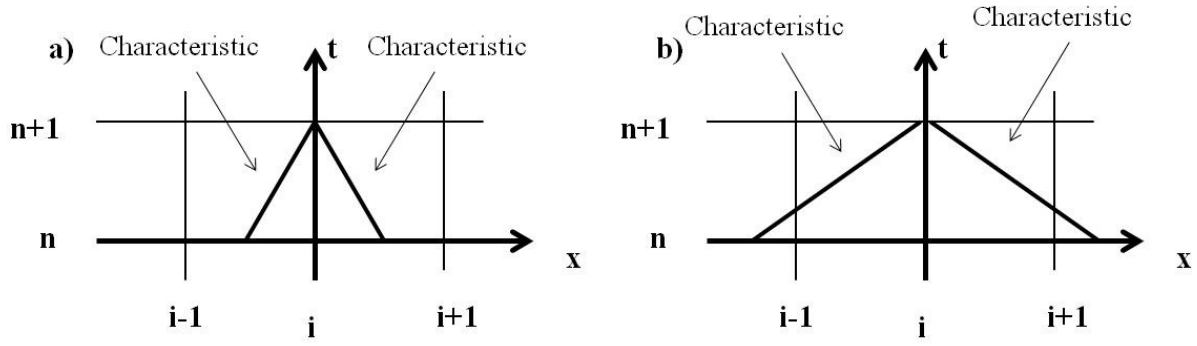

Figure 6.6: Characteristic interpretation of the CFL condition. a) stable condition and b) unstable condition.(Hirsch, 2007)

6.6 Primitive vs. conservative variables

The primitive variables that need to be calculated are phase-fractions, phase velocities and pressure. In order to determine the primitive variables at the new time level, the mass-conservative variables $w_{1,j}$ and $w_{2,j}$ is used. However, the mass-conservative variables need to be divided by the average area, and then multiplied by the same parameter after the primitive variables has been calculated. This is the case if area changes is included in the model.

There is a need for converting the conservative variables $w_{1,j}$,$w_{2,j}$ and $w_{3,j}$ to physical variables like pressure, temperature etc. How this is done is shown in Appendix A and is written by

John Emeka Udegbunam. As an example, the phase volume fractions are determined by the following equations:

$$\alpha_{g,i}^{n+1} = \frac{w_{2,i}^{n+1}}{\rho_{g,i}^{n+1}}$$

$$\alpha_{l,i}^{n+1} = 1 - \alpha_{g,i}^{n+1}$$

6.7 Second order scheme

The basic AUSMV scheme uses a first order accuracy method. This means, however, that there will be numerical diffusion that will smear out sharp transition zones. For instance, an interface between a one-phase region and a two-phase flow region will not be sharp. A way to reduce this problem is by increasing the number of cells but this increase the computational time. A more effective way of dealing with this problem is to extend the scheme into a second order scheme by introducing slope limiters (K. K. Fjelde, Frøyen, & Ghauri, 2016).

Slope limiter

In the case of using slope limiters, the cell variables are no longer considered constant. As an alternative, a slope limiter is used to determine the boundary values in each of the cells which in turn are used to determine the numerical fluxes. In the second order AUSMV scheme, the minmod limiter has been used to generate the slopes (LeVeque & Yee, 1990).

The minmod function of two arguments is express as:

$$minmod(a,b) = \begin{cases} a & if\ |a| < |b|\ and\ ab > 0 \\ b & if\ |b| < |a|\ and\ ab > 0 \\ 0 & if\ ab \leq 0 \end{cases}$$

If a and b has the same sign, then the minmod function selects the smaller in modulus, else it returns zero.

Instead of defining the slope on the *i*-th cell by always looking at the downwind difference or by always looking at the upwind difference, the minmod method evaluates the two slopes and decides to use the one that is smaller in magnitude. The following figure shows the concept.

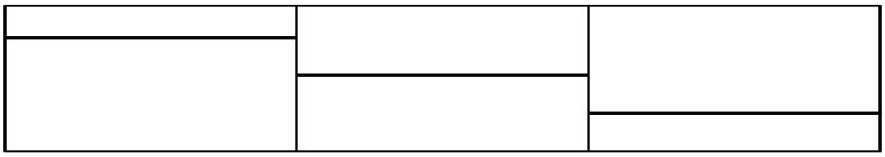

First order method: The flow variables are considered as constant

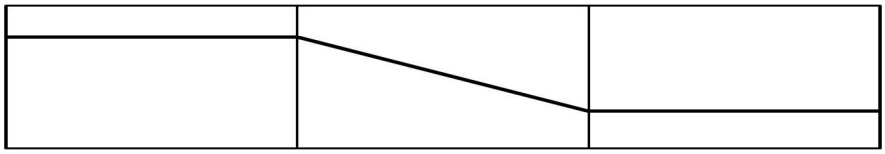

Second order method/Slope limiter concept: The method gives a better resolution of gas distribution in the well

Figure 6.7 Slope limiter concept

7 Simulations & Discussion

In this chapter there is three different simulation cases regarding the mass transfer term implemented in the AUSMV scheme:

1. Mass transfer with a constant numerical value for mass transfer
2. Horizontal case using the mass transfer equation
3. Vertical case with a constant numerical value for mass transfer
4. Comparison of first and second order scheme and grid adjustment.

All the four cases use the same dimension of the pipe/wellbore when it comes to length and diameter. There is no drillpipe inside the wellbore, so the simulations only consider pipe geometry. An "artificial" horizontal geometry is assumed for better studying the effect of including the mass transfer term in the AUSMV scheme. Mass transfer between water and steam will be considered. The temperature in the pipe increases uniformly for the horizontal cases, to simplify the simulation, from 20^{o}C to 110^{o}C. This simplification is implemented since the scope of this thesis is to introduce the mass term, and to activate the mass transfer term during the simulation. Since the simulation is using water as the drilling fluid, the mass transfer term gets activated at the boiling temperature of water at atmospheric pressure which is at 100^{o}C. In the horizontal case with the mass transfer equation, a boiling temperature restriction has been introduced to test the AUSMV scheme even further. The boiling temperature restriction makes some sections of the pipe unable to generate gas. The pressure in the pipe geometry increases when gas is introduced to the system, which leads to a higher boiling point of the liquid to produce vapor. More detail about the boiling temperature restriction can be found in subchapter 6.4.

There will be no influx of fluid into the pipe/wellbore as the simulation is looking at vaporization of the water already present in the pipe. The pipe initially only contains water and there is no gas present in the pipe.

All the simulations will be performed in MATLAB, which is a great tool to handle complex models and input functions while visualizing the results in form of graphs. The code can be found in appendix B and C.

The specification of the experimental properties is as follows:

Depth

For the first two and fourth case we assume a 2000 meter horizontal pipe with atmospheric conditions, whereas the vertical well has a well depth of 2000 meter.

Diameter

The pipe has a diameter of 0.2159 m (8.5”). This geometry is uniform and there is no discontinuities in the cross sectional area. This is a simplification of the pipeline geometry and is not realistic with any actual wellbore configuration when considering the vertical case. The AUSMV scheme can handle flow area discontinuities, but will not be considered in this thesis.

Fluid properties

Water has been selected as the fluid, and water steam is the resultant vaporization product. The following table gives the fluid properties at atmospheric conditions.

Table 7.1: Properties of water and steam

Fluid	Density	Viscosity	R	Sound velocity
Water	1000 kg/m^3	0.001 Pa-s	-	1500 m/s
Steam	0.59 kg/m^3	0.000012 Pa-s	461.5 J/(kg-K)	477.5 m/s

These properties are at atmospheric conditions and the density and viscosity vary with temperature, whereas the sound velocity of steam is only valid for temperatures above 100 degrees.

Simulation data

The first three simulations are run using a second order accuracy scheme, whereas the third simulation compares first and second order accuracy scheme.

Table 7.2: Simulation data

Simulation	First/Second order	Number of boxes	Timestep	CFL number
First (Chapter 7.1)	Second	25	0.01 s	0.1875
Second (Chapter 7.2)	Second	25	0.01 s	0.1875
Third (Chapter 7.3)	Second	25	0.01 s	0.1875
Fourth (Chapter 7.4)	First and second	25 and 50	0.01s and 0.005s	0.1875

7.1 Mass transfer with a constant numerical value

The temperature increases linearly from 20°C to 110°C over the course of the simulation, lasting 2000 seconds; this is shown in figure 7.5. The scheme uses second order accuracy method. The mass transfer term is activated once the temperature hits 100°C. The mass transfer term is implemented using interpolation between the temperatures from 100°C to 110°C to make the mass transfer stable. By using an interpolated constant numerical value as the mass transfer rate there might occur oscillations due to a stiff source term. Stiff source terms, such as mass transfer of phases, is when the term is reacting on a short timescale (LeVeque & Yee, 1990). The mass transfer term act as a stiff source term since it suddenly gets activated when the temperature in the borehole reaches 100°C. However, when stiff source terms are experienced, a more refined time integration procedure which involves small time steps is necessary to prevent the oscillations.

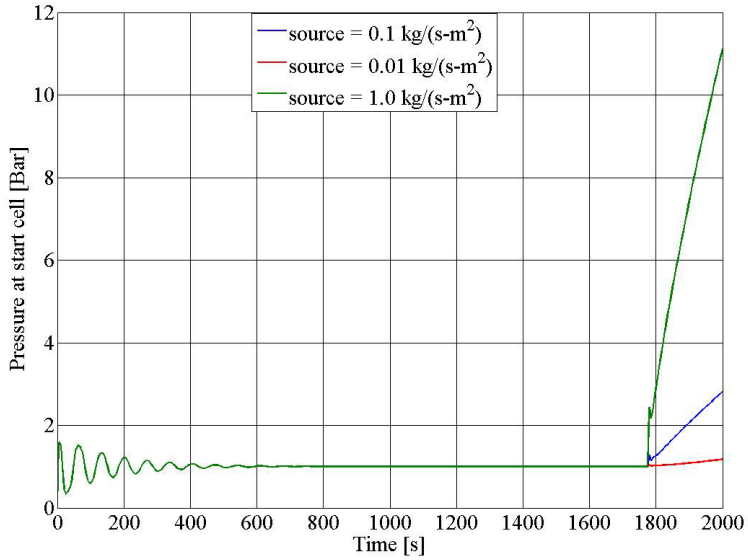

Figure 7.1: Pressure at the start cell vs. time for three different constant numerical values.

Initially, when simulation starts, the pipe is at atmospheric conditions (1 bar and 20°C). Then we start to increase the temperature. This leads to a constant small out flow of the liquid due to thermal expansion. This can be seen in figure 7.2 and 7.4, where the liquid massrate out is slightly above zero until the mass transfer term is activated. The liquid massrate out of the pipe increases rapidly after the mass transfer term is activated. When the numerical value of the mass transfer is 1.0 kg/(s·m^2), the liquid mass rate out will evidently decrease, since there is less liquid and there is a large amount of gas present in the pipe, as seen in figure 7.7. Whereas the gas massrate out will continue to increase rapidly throughout the simulation, since gas is produced continuously, presented in figure 7.3.

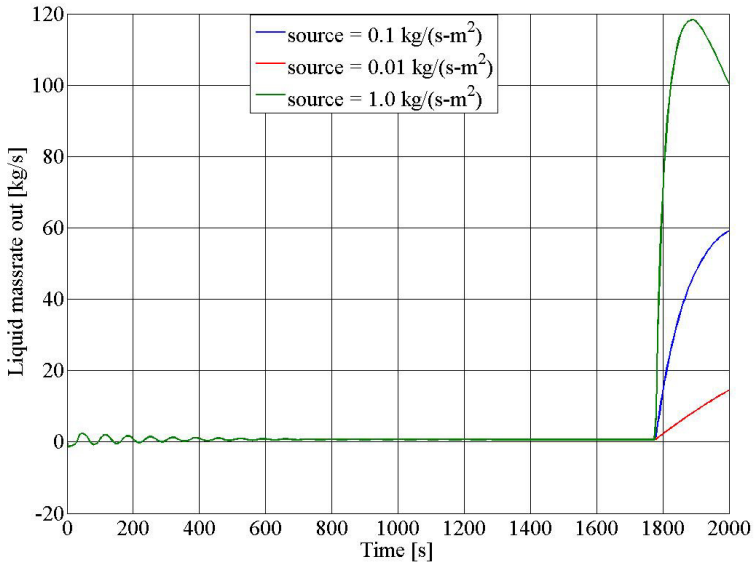

Figure 7.2: Liquid massrate out vs. time.

The oscillations seen in the inlet pressure is caused by acceleration effects. Initially, the system is stagnant, but as soon as we start to increase temperature, the water will start to move as seen in figure 7.4, causing an acceleration effect making the system to move due to thermal expansion. Figure 7.4 supports the claim that the pressure pulses is induced by the initiated fluid flow as the temperature increases. These pressure pulses will be damped by friction over time as seen from figure 7.1.

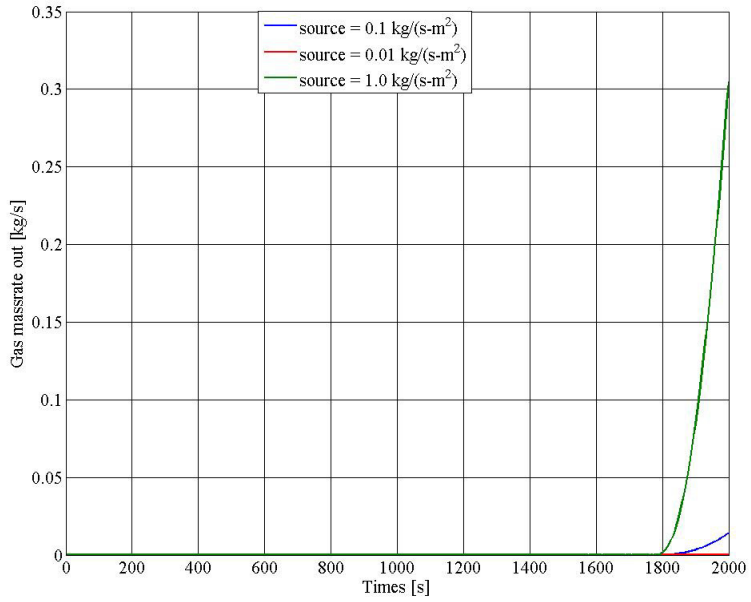

Figure 7.3: Gas massrate out vs. time.

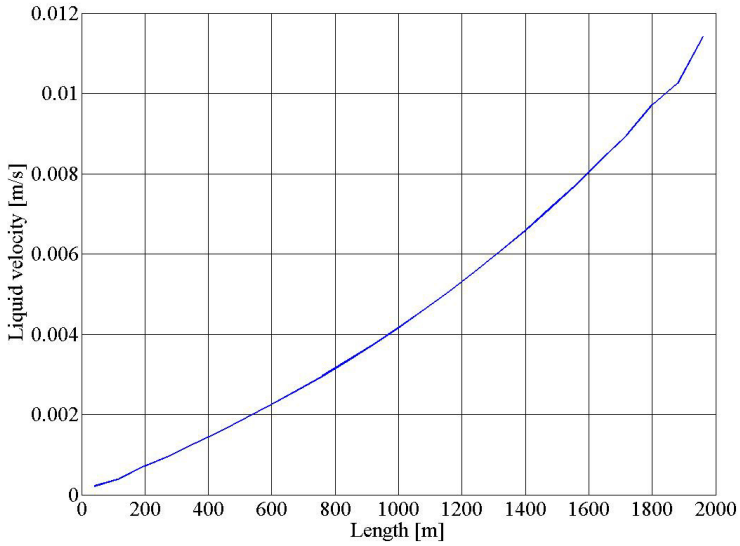

Figure 7.4: Liquid velocity vs. length after 500 seconds.

The magnitude of the numerical mass transfer constant used in the scheme has a great effect on the result of the scheme, as illustrated in figure 7.1. Having a too large numerical value causes the mass transfer term to be the dominant source term in the scheme. As seen from simulation, when temperature reaches 100°C (see figure 7.1), the inlet pressure suddenly increases. When steam starts to form, the fluid flow will increase due to gas expansion. This causes rapid increase in the inlet pressure due to frictional forces. When the numerical value of the mass transfer is 1.0 kg/(s·m^2), the pressure increase is much larger than for the other values.

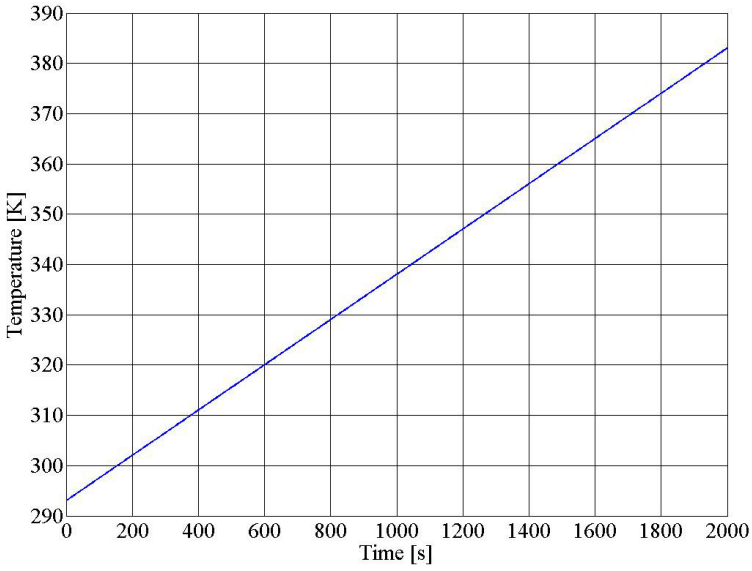

Figure 7.5: Temperature in the pipe vs. time.

The temperature increases linearly, as seen in figure 7.5. The temperature distribution is uniform throughout the entire pipe.

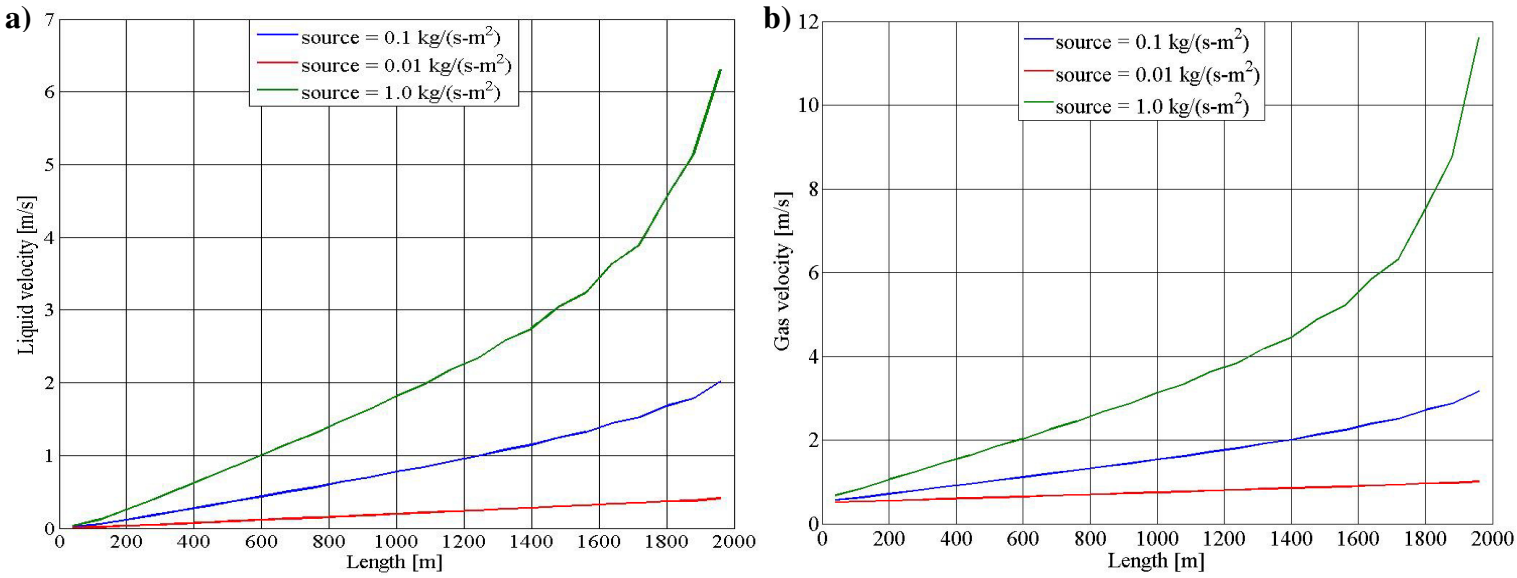

Figure 7.6: a) Liquid velocity vs. length at the end of simulation. b) Gas velocity vs. length at the end of simulation.

After the simulation has run its course, there are some significant changes applied to the system. A system that was initially stagnant and containing no gas, is now a flowing system of both liquid and gas, illustrated in figure 7.6 a) and b). However, with a numerical value of the mass transfer of 1.0 kg/(s·m^2), the liquid and gas velocities seems rather large, which support the claim of having a dominant source term in the form of mass transfer.

How the mass transfer term impact the gas fraction is illustrated in the following figure.

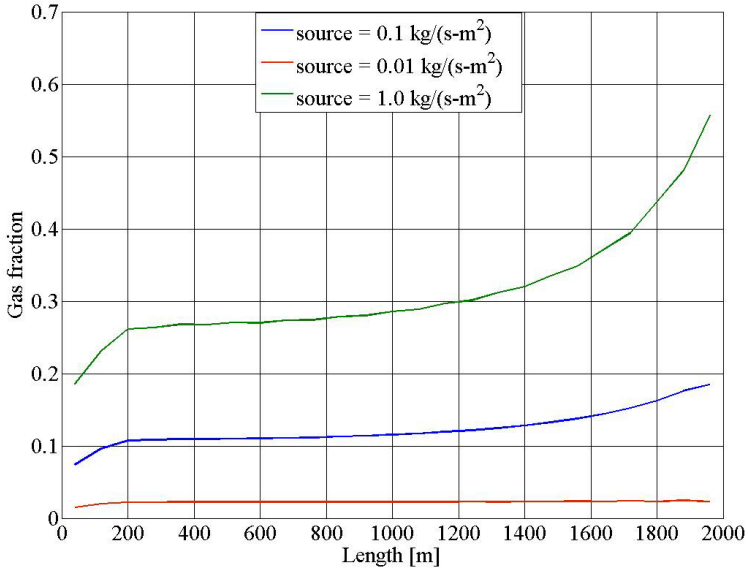

Figure 7.7: Gas fraction vs. length at the end of simulation.

Figure 7.7 shows how the mass transfer term heavily impacts the gas fraction of the pipe with 1.0 kg/(s·m^2) mass transfer, to almost no impact with 0.01 kg/(s·m^2). The mass transfer constant is the same for all the sections of the pipeline, and contributes to a pressure increase and initiated fluid flow.

The AUSMV scheme seems to still handle the transition well when the mass transfer term is included. Once the mass transfer term is activated, the model seems to contain a stiff source term where oscillations are created. There is a "jump" in pressure (see figure7.1) as soon as the mass transfer term is activated, even with the interpolation of the mass transfer. The time integration is already refined, having a CFL condition well below the required value (see table 7.2), causing the oscillations to be rather small.

7.2 Horizontal case using the mass transfer equation

For the horizontal case the mass transfer equation mentioned in section 6.4 is used to calculate the phase transition of the water phase to the gas/steam phase along the pipe. The model uses second order accuracy method. Table 7.2 shows the simulation data used in this case. The mass transfer equation activates at 100^{o}C and increases gradually with temperature, since the equation is heavily dependent on the temperature. However, the mass transfer equation is also dependent on the fluid densities, which again is dependent on pressure.

Initially there is no fluid flow, since there is no influx of fluid into the pipe. The water inside the pipe will be heated gradually for each time step and will reach the saturation temperature of 100^{o}C and start boiling. The temperature in the pipe increases linearly, shown in figure 7.9, from 20^{o}C to 110^{o}C during the simulation, which lasts for 3500 seconds. The liquid phase will start to transfer into the gas phase. This will also make the fluids inside the pipe to start flowing towards the open end of the pipe due to increase of gas volume. The mass transfer term increases rapidly after it gets activated since the temperature keeps increasing, as seen in figure 7.10.

The results in this horizontal case will include two variants of the mass transfer term; one without the boiling temperature restriction and one with the boiling temperature restriction. The boiling point is dependent on the pressure of the system. If the pressure in the system increases, the required temperature to start boiling the liquid also increases. Hence, some sections of the pipe will be unable to generate gas, illustrated in figure 7.10 b). A more detailed description of the boiling point restriction is found in subchapter 6.4.

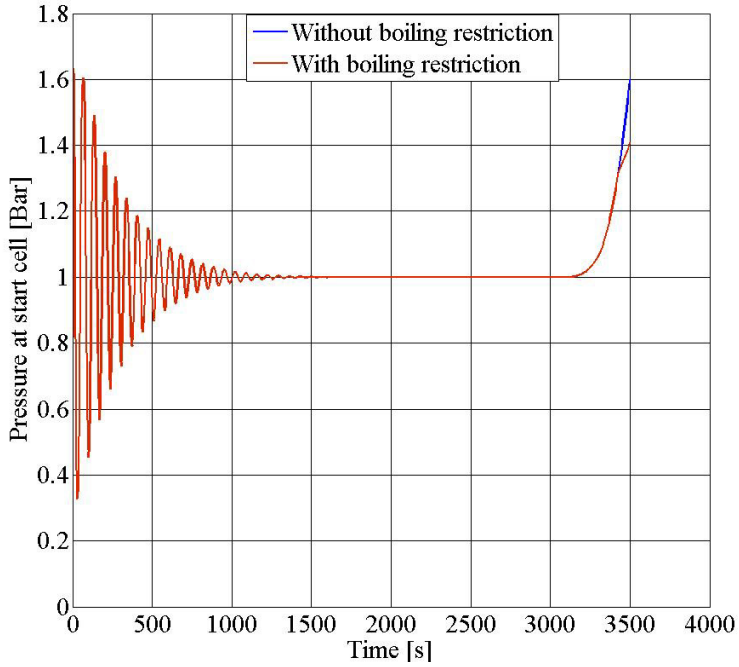

Figure 7.8: Pressure at the first cell/start cell vs. time with/without boiling temperature restriction.

The simulation runs for 3500 seconds and it reaches the saturation temperature of water at 3120 seconds. The oscillations at the start of the simulation are due to the thermal expansion of fluid, causing fluid to move. When the system starts to flow it creates pressure pulses that eventually will be dampened by friction. The pressure will then increase due to the expansion of gas as the temperature increases and the friction caused by the rapid increase in fluid flow. The inlet pressure increases smoothly after the mass transfer term is turned on and there is no sudden increase of pressure. The mass transfer equation makes the vaporization of liquid increase gradually which is expected. Hence, it was not necessary to introduce an interpolation to smooth the model.

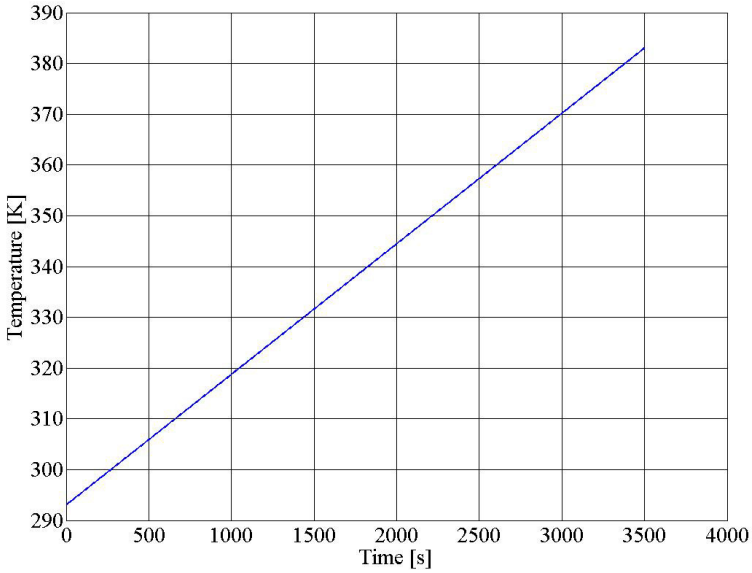

Figure 7.9: Temperature in the pipe vs. time.

For the blue curve in figure 7.8, the boiling point restriction is not included. All the numerical cells will contribute to the mass transfer of water to steam. That causes the pressure to increase rapidly when the temperature reaches 100^{o}C and boiling starts. There is a pressure increase in this scenario, reaching pressures around 1.6 bar in the start cell. Since this scenario has no boiling point restriction, the pressure continues to increase rapidly.

For the red curve in figure 7.8, the boiling point restriction makes its impact on the model. The initial pressure increase is similar to that of the blue curve. However, as the temperature increases further, the boiling point restriction in some parts of the pipe is triggered. This is due to the pressure increase, and as the pressure increases, so does the boiling point of the liquid (see figure 7.10 b)). This result in no mass transition for several of the numerical cells, illustrated by the empty “holes” in figure 7.10 b). Due to the dynamics of the system it seems that some sections are “turned” off and on again. The pressure increase then stagnates and increases at a slower rate shown in figure 7.8.

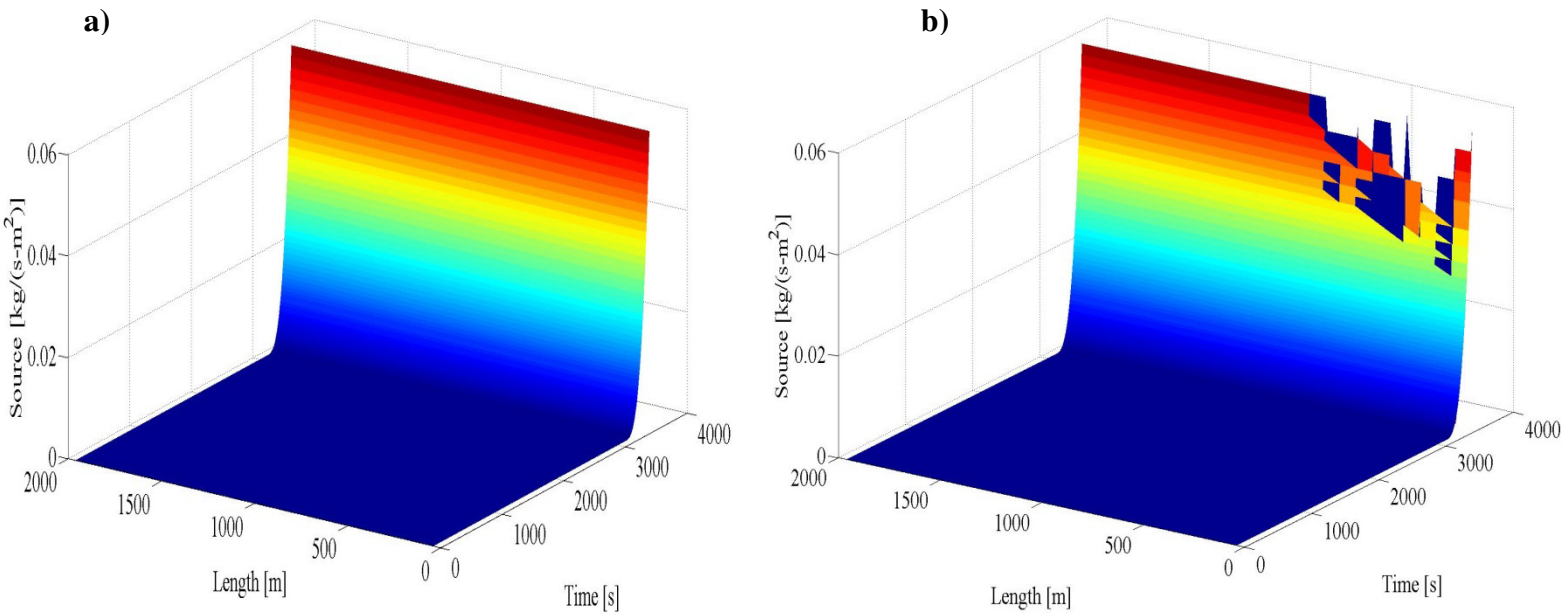

Figure 7.10: a) Mass transfer vs. length and time without boiling temperature restriction. b) Mass transfer vs. length and time with boiling temperature restriction

Figure 7.12 illustrates the gas fraction vs. length of the pipe at the end of the simulation. The simulation starts with a gas fraction of zero, making the pipe only filled with water. Throughout the simulation the gas fraction increases, resulting in around 11 % gas at the outlet cell at 3500 seconds.

The blue curve in figure 7.12 has a smoother curve, having a more even distribution of gas in the pipe. Since the mass transfer term is active throughout the entire simulation, steam is generated at all locations.

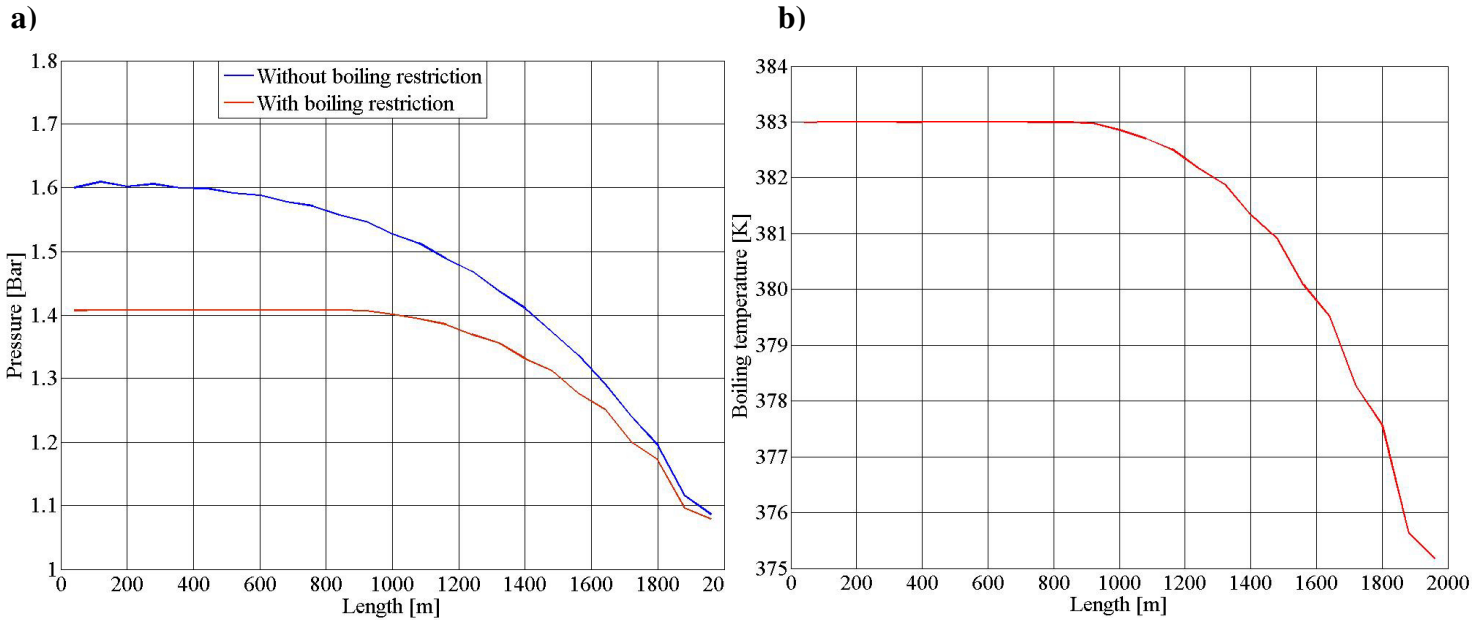

Figure 7.11: a) Pressure vs. length at the end of simulation. b) Boiling temperature vs. length at the end of simulation.

The red curve in figure 7.12 shows that the gas fraction at the outlet of the pipe geometry is much higher compared to the inlet section of the pipe geometry. This can be seen in combination with the boiling temperature plot in figure 7.11 b). The end temperature of the simulation is 383 K (110^{o}C). For the first section of the pipe, the pressures will be larger due to friction, seen in figure 7.11 a). This decreases the amount of damp being generated here. In the outlet section of the pipe, the pressure is lower, generating more damp. One can look at the red curve in the pressure plot (figure 7.11 a)) in combination with the boiling temperature plot (figure 7.11 b)) to see how the pressure affects the mass transfer. When the pressure decreases, so does the required temperature to generate gas.

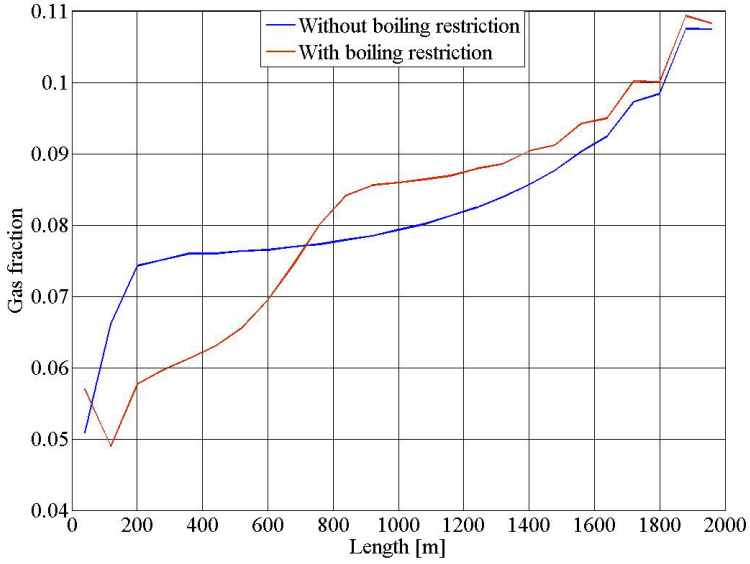

Figure 7.12: Gas fraction vs. length of the pipe at the end of simulation.

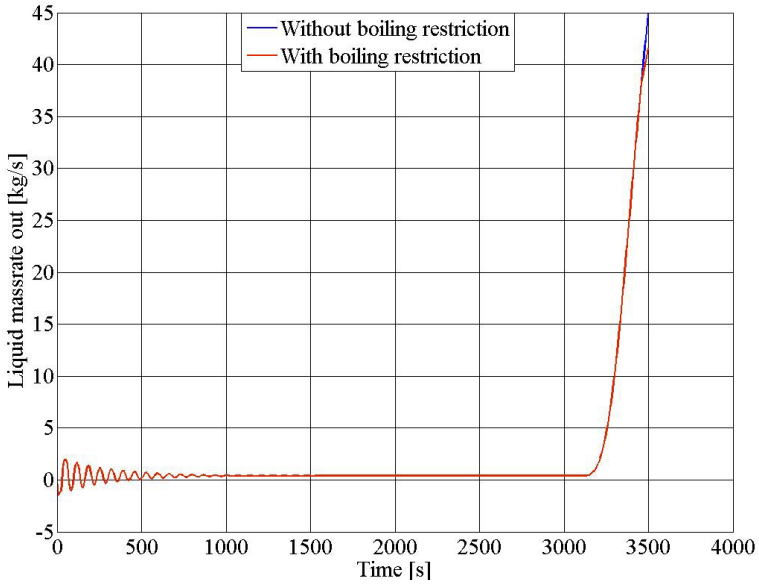

Figure 7.13: Liquid massrate out vs. time.

The simulation starts with no flow, so that the initial liquid massrate out is equal to zero and continues to be close to zero until the mass transfer term is activated. There will be some liquid exiting the pipeline due to the thermal expansion of liquid. Once the phase transition starts, a substantial liquid flow is initiated. The fluid flow is initiated by the generation and expansion of gas as the volume of gas is increasing with every time step. There are oscillations at the beginning of the simulation, which is caused by the same reason as for the pressure plot in figure 7.8.

When there is no restriction to the boiling point of the system, as illustrated by the blue curve in figure 7.13 the liquid massrate out keeps increasing as the temperature continues to rise after 3120 seconds where the mass transfer term is active.

With the boiling point restriction in the red curve, the liquid massrate out is also increasing vs. time. However, towards the end of the simulation, there is a slight decline of the growth rate of the curve. This is caused by the boiling point restriction. As the simulation runs, there will be fewer sections of the pipe that contribute to the vaporization of liquid (see figure 7.10 b)), resulting in less gas development and the liquid massrate out increase will be reduced.

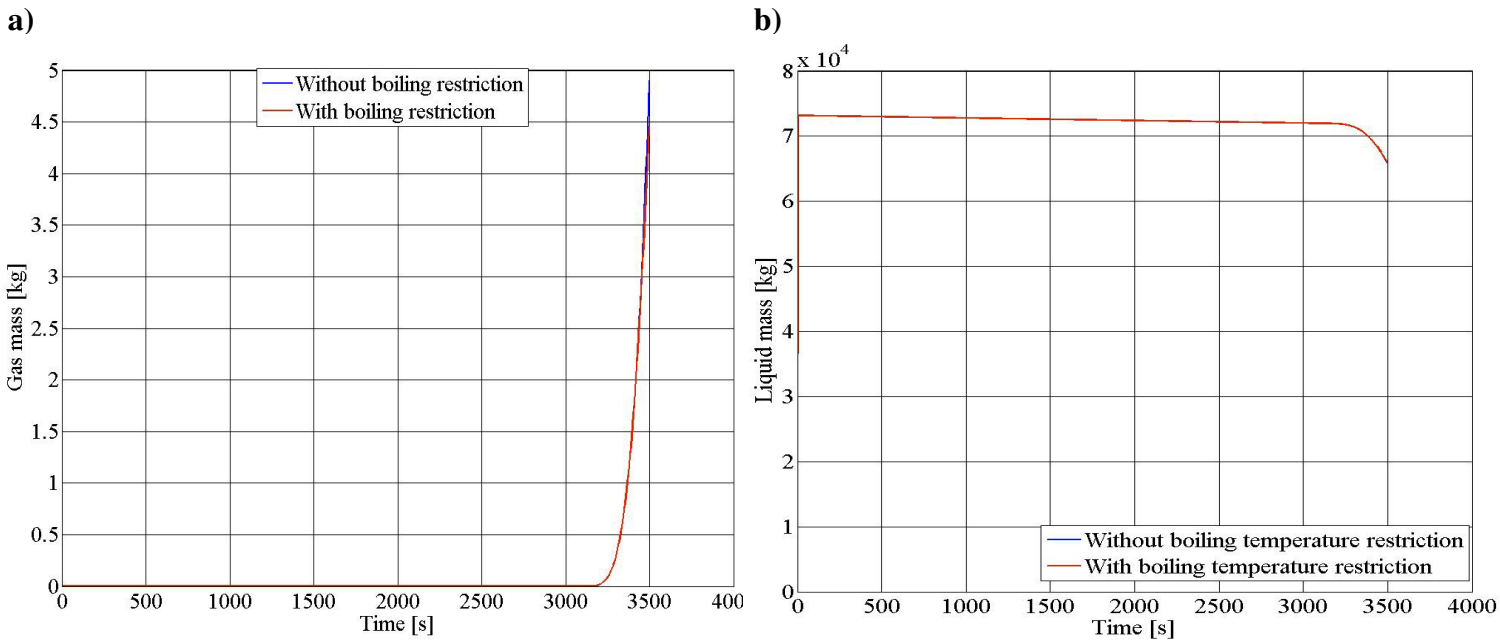

Figure 7.14: a) Gas mass in the pipe vs. time. b) Liquid mass in the pipe vs. time.

There is no gas present in the pipe at the start of the simulation. The pipeline is filled with liquid water. Some liquid is still exiting the pipe, even when the mass transfer term is not activated. This is due to the thermal expansion of the liquid.

The gas is not generated until the mass transfer term is active. This is illustrated in figure 7.14 a) where the gas mass in the system increases rapidly when the mass transition starts. The blue curve has a slightly larger increase in gas mass than the red curve, since it has no boiling point restriction.

Figure 7.14 b) shows the liquid mass in the pipe vs. time. The liquid mass is reduced by two sources when the mass transfer term is activated: the mass transfer from liquid to gas and liquid exiting the pipeline. We also observe a gradual small decrease in the liquid mass from start of simulation until boiling starts. This is caused by the thermal expansion of water. However, the loss of liquid mass is accelerated when boiling starts. More mass is lost for the case without including boiling temperature restriction (blue curve) vs. the case with that (red curve). Although, the difference of the two curves is not substantial due to the great amount of liquid present in the pipeline, as seen in figure 7.15.

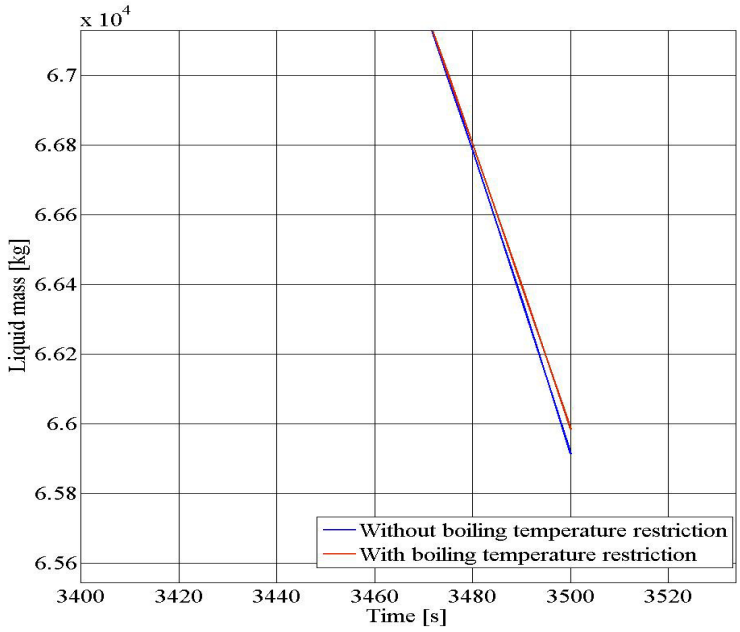

Figure 7.15: Liquid mass in the pipe vs. time with zoom.

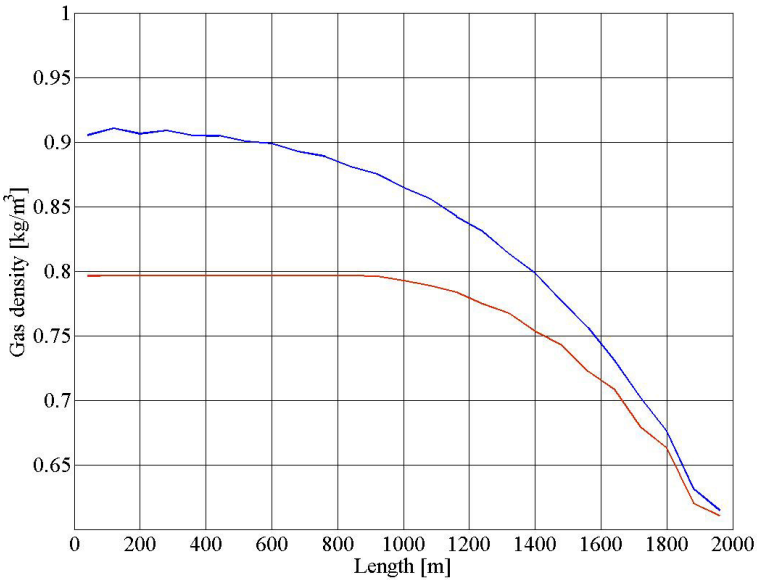

Figure 7.16: Gas density vs. length at the end of simulation.

How the temperature affects the densities of the fluids has not been the focus of this thesis. However, it is interesting to see how the AUSMV scheme handles the newly formed gas from vaporization in the pipe. The gas density is dependent on the temperature and the pressure in the pipe, where pressure compresses the gas and temperature expands it. The pressure will be higher than the atmospheric pressure at the end of the simulation, compressing the gas, resulting in a higher gas density. The atmospheric steam density is 0.59 kg/m^3, but at these pressures it is higher even with the increased temperature.

The temperature profile is the same throughout the simulation for both models, which means that the density difference is induced by the pressure difference of the two models. One can see the resemblance in the two figures, figure 7.16 and figure 7.11 a), where the pressure profile and the gas density are quite similar.

7.3 Vertical case with a constant numerical value for mass transfer

For the vertical case, the mass transfer equation will not function in the same sense as for the horizontal case shown earlier. The drilling fluid used in the simulation is water. The scheme uses second order accuracy method. Due to the hydrostatic pressure of the water column in the annulus, the boiling point of the drilling fluid exceeds the temperature in the well resulting in no mass transfer between the phases. This is the case if we use the model with boiling temperature restriction. The temperature in each segment is increasing with depth, having 40^{o}C at the top of the well and 150^{o}C at the bottom. The simulation runs for 2000 seconds. The well is 2000 meter and we have for simplicity used pipe geometry with 0.2159 meter in outer diameter.

However, one could have considered models for vaporization of oil, but that would require a much more complex modeling effort. It is easier to use water based mud in the simulation, since there are many reliable correlations which is used in combination with the mass transfer equation.

Without the boiling temperature restriction of the mass transfer, the high pressures and the high borehole temperature gradient in the well causes a large fraction of the well to vaporize, as there are no terms in the scheme to limit the generation of gas.

The mass transfer is therefore instead considered as a constant numerical value for the sections of the well that has a pressure below 50 bar. Simulation data for this case is shown in table 7.2. The mass transfer, as in the horizontal case with a constant numerical value is interpolated, but instead by interpolating the pressure in the borehole. What we are trying to accomplish, is to see the effect this has on the bottom hole pressure of the well. The water based mud then acts as an oil based mud, where the boiling happens at low pressure, low temperature.

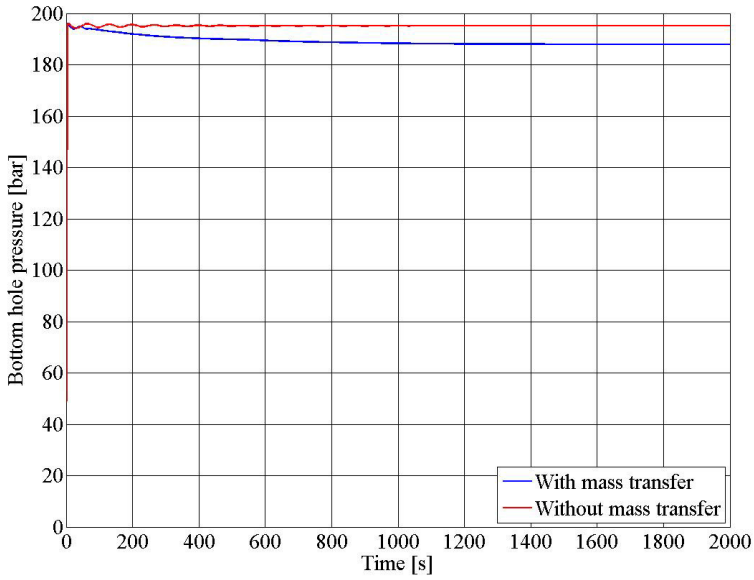

Figure 7.17: BHP vs. time.

The mass transfer term is active from the start of the simulation. The blue curve in figure 7.17 shows the decrease in BHP as a result of mass transfer over time. As the gas fraction in the upper section of the well increases, the mixed density will decrease, resulting in a lower BHP. The pressure stabilizes after some iteration due to the development of gas decreases. The mass transition decreases over time since there is less and less liquid that can be vaporized in the sections with lower than 50 bar pressure. One of the problems when considering a well with a drop in BHP is that a secondary kick can occur.

The red curve show the simulation without a mass transfer term, so the pressure is not experiencing any change, but is added to compare the two models.

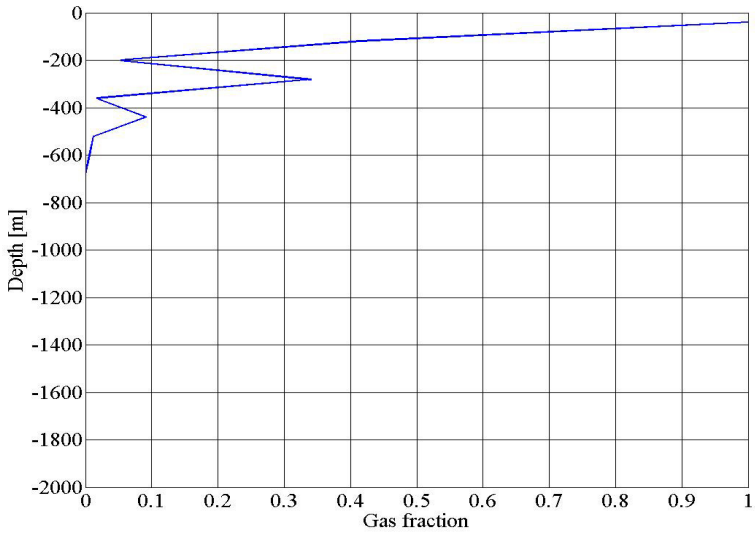

Figure 7.18: Gas fraction vs. depth at the end of simulation.

The gas fraction plot for the simulation, seen in figure 7.18, is plotted against depth and gives a good description of where the gas is present in the well. The gas fraction profile has an uneven curve due where the gas generation is taking place, and the movement of the gas and liquid. Gas is generated in sections of the well where the pressure is lower than 50 bar. As the phase transition occurs and generates gas, the hydrostatic pressure will decrease due to the reduced mixed density in the upper cells (see figure 7.19). This will result in even more sections of the well contributing to the phase transition between liquid and steam, as seen in figure 7.20.

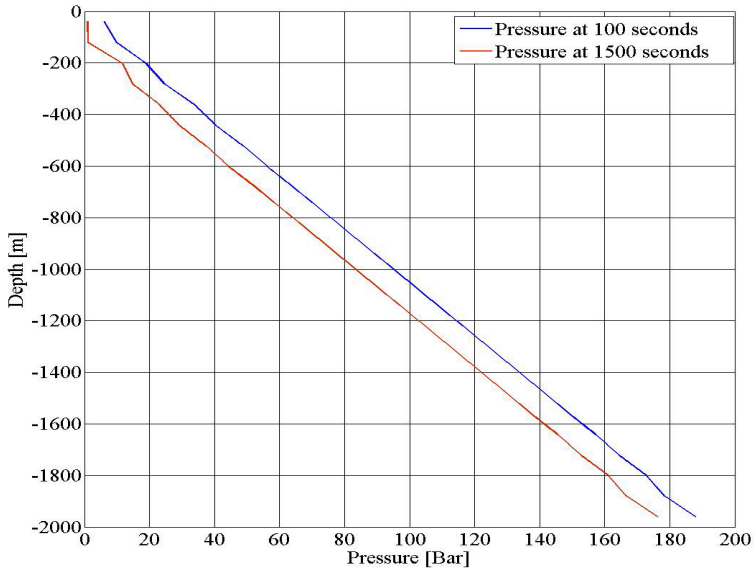

Figure 7.19: Pressure at 100 and 1500 seconds vs. depth.

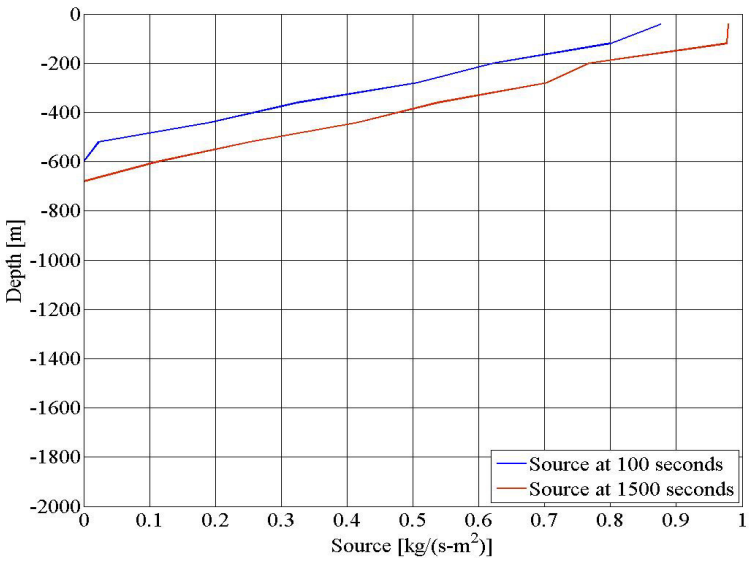

Figure 7.20: Mass transfer at 100 and 1500 seconds vs. depth.

7.4 Comparison of first and second order scheme and grid adjustment

This case is similar to that of subchapter 7.2, having a horizontal pipe using mass transfer equation for the transition between the phases. The boiling point temperature restriction is also included in this case. Like before, the temperature increases gradually from 20°C to 110°C seen in figure 7.9. The mass transfer equation is activated when the temperature in the pipe is 100°C. Three different simulations is run and compared. The first comparison is between the first and second order accuracy method. Here, the same grid adjustment is used where the 2000 meter long pipe is divided into 25 boxes. The second comparison uses second order accuracy method where the pipe is divided into 25 and 50 boxes.

Comparison of first and second order scheme

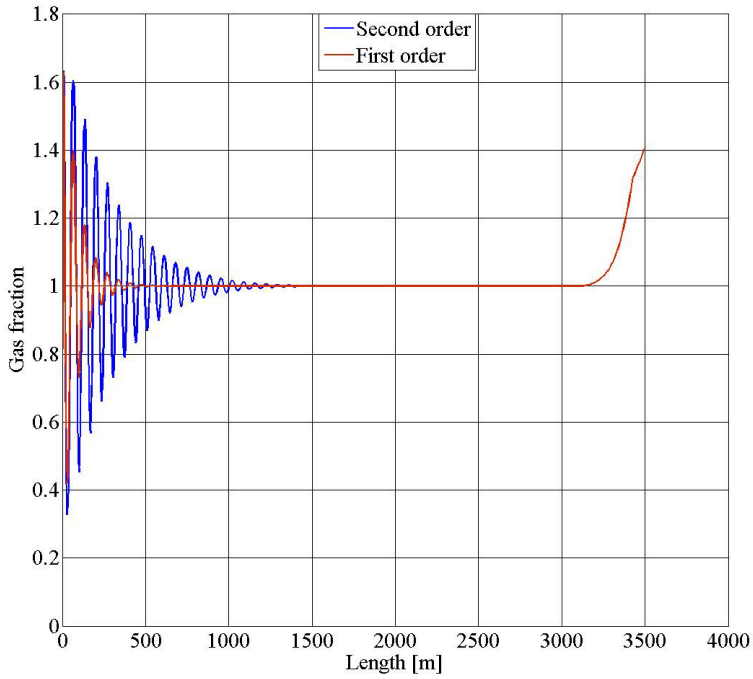

Figure 7.21: Pressure at start cell/first cell vs. time for second and first order accuracy method.

When using a slope limiter, which is the case for a second order scheme, the cell variables are no longer considered constant. A slope limiter is used to determine the boundary values in each of the cells which in turn are used to determine the numerical fluxes. Using a slope limiter will give larger pressure pulses when the frictional forces are as low as it is in this case. It is the pressure pulses seen in figure 7.21 that is different in the plot. This is due to how the numerical fluxes are calculated, when the cell variables are not considered constant. The

end result of the blue and red curve in figure 7.21 does not deviate much, only in the order of a few Pascal.

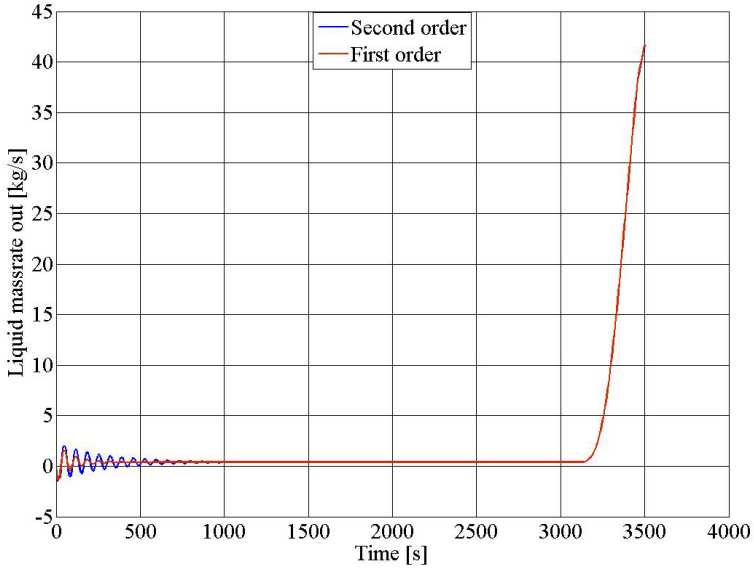

Figure 7.22: Liquid massrate out vs. time.

The same applies to the liquid massrate out when comparing second and first order accuracy method as for the pressure at the start cell (figure 7.21). The main difference is the oscillations displayed in figure 7.21 and 7.22. In fact, the first order scheme (red curve) has an incremental higher liquid massrate out than the second order (blue curve), dampening the pressure pulses in figure 7.21 faster.

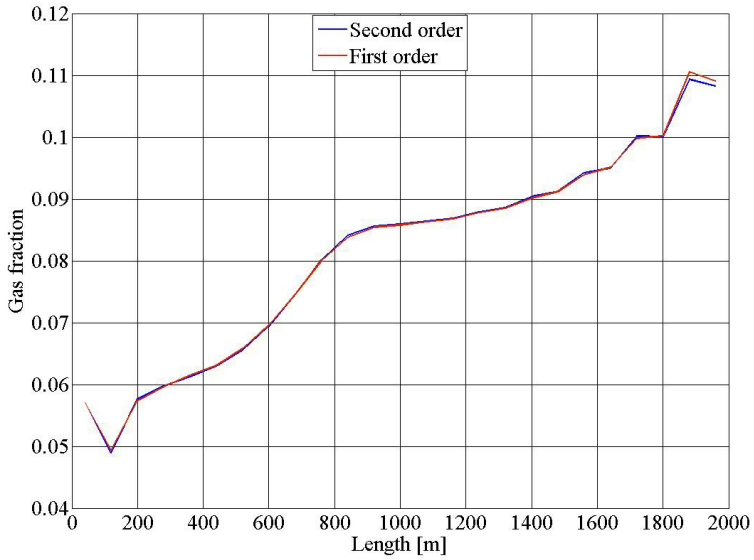

Figure 7.23: Gas fraction vs. length at the end of simulation.

Figure 7.23 shows the gas fraction vs. length of the second and first order accuracy scheme. In this figure it was expected to see the difference between the two methods, since using second

order accuracy method will make it easier to see transition zones. In figure 7.23 the blue and red curve are quite similar, but there is still some deviation.

Comparison of grid adjustment

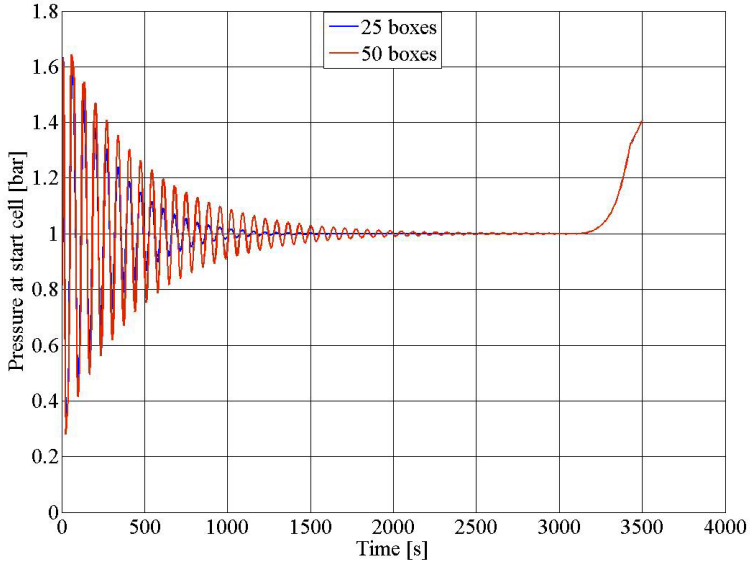

Figure 7.24: Pressure at start cell/first cell vs. time with 25 and 50 boxes discretization.

When the number of cells is increased the time step is also more refined, to keep the CFL number the same. This increases the computational time, but gives a better resolution of the results. With the increased number of cells, the pressure pulses are more visible and continuous for a longer period of time, illustrated by the red curve, than for the blue curve in figure 7.24.

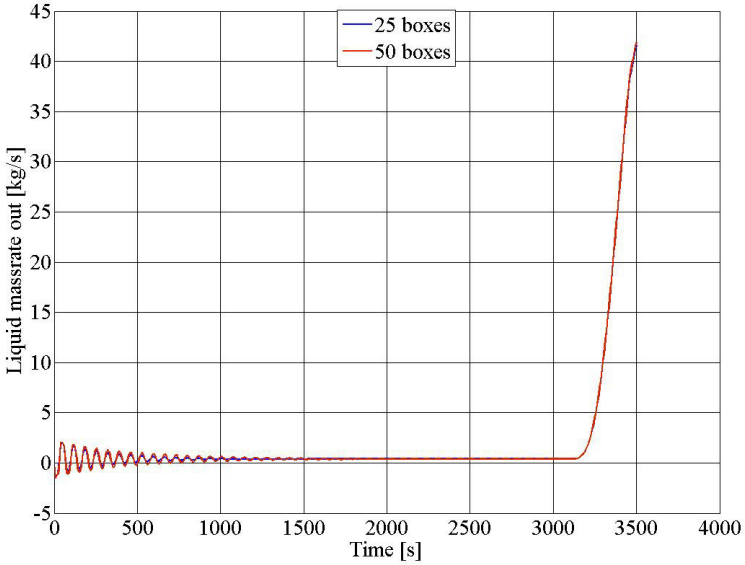

Figure 7.25: Liquid massrate out vs. time.

The red and blue curves in figure 7.25 are very similar. Other than the oscillations at the start of the simulation is a bit more intense for the red curve than for the blue curve. For the red curve, the oscillations do not seem to be completely diminished until shortly before the mass transfer is activated.

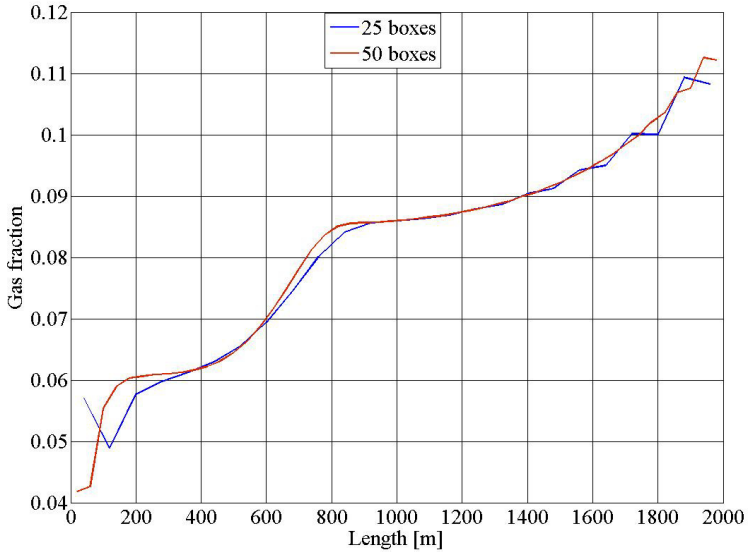

Figure 7.26: Gas fraction vs. length at the end of simulation.

The blue curve in figure 7.26 has some sharp edges compared to the red curve where it is smoother. The abrupt changes that occur when introducing mass transfer between the phases benefits from having more boxes to adjust to these changes. This gives a more smooth gas fraction curve. The values for gas fraction are, however, quite similar.

7.5 Discussion

The main objective of this thesis is to see if the AUSMV scheme has the ability to handle a mass transfer term and to confirm that mass transfer has an impact on the condition of the pipe/well.

By looking at the graphs of the three different cases one can see some notable results produced by the AUSMV scheme when including mass transfer that should be discussed.

- **Pressure**

When considering the pressure at the inlet cell for the horizontal cases, one can observe the pressure increase as the mass transfer term is activated. The original model without the mass transfer term will not have any significant change in pressure, and will remain close to constant throughout the simulation as there is no initial or forced fluid flow in the system. However, for both the horizontal cases with a constant numerical value for mass transfer or

using the mass transfer equation, there is a pressure increase at the first numerical cell in the whole pipe, but mostly at the inlet, as seen in figure 7.1 and 7.8. The pressure increase is mainly due to the frictional pressure caused by the fluid flow introduced by the mass transfer term. It was uncertain if the AUSMV scheme would be able to handle this phase transition, but as seen in the plots it produces good results. For the mass transfer term, we considered a model both with and without restriction on the boiling temperature. When including the restriction model, the mass transfer mechanism also became dependent on the pressure in the pipeline. This leads to lower steam volumes leading to a different flow behavior with less gas expansion and reduced pressures in the pipeline.

For the vertical case the bottom hole pressure decreases. Here only the upper part of the well, where the pressure is under 50 bar, contribute to the vaporization of liquid. This is, however, not a realistic case since the water based drilling fluid now is forced to act in a similar way as oil based drilling fluid. When gas normally boils out of the mud and lowers the hydrostatic pressure in the fluid column. This can lead to a secondary kick. This simulation is performed to experiment and study the AUSMV scheme to see if it could handle the mass transfer in a vertical borehole. This forced boiling of the liquid in the upper part of the well leads to a lower hydrostatic pressure, which again leads to a lower bottom hole pressure, as seen in figure 7.17.

When comparing both second order and first order accuracy method and the grid adjustment from 25 to 50 boxes, the end result of pressure at the start cell looks similar (figure 7.21 and 7.24). The pressure pulses do, however, deviate in both cases.

- **Gas fraction**

The gas fraction graphs are presented in figure 7.7, 7.12, 7.18, 7.23 and 7.26. The gas fraction, with the mass transfer term in the scheme, will increase over time as long as the criteria for mass transfer are fulfilled, since the temperature increases over time. The mass transfer equation in subchapter 6.4 is used to calculate the amount of gas generated throughout the simulation. The gas will be generated gradually and not have a sudden “jump” in gas fraction volume. This model is also applicable for other fluids than water. With the addition of boiling point criterion, the mass transfer is dependent on both pressure and temperature, the mass transfer process becomes more realistic. This makes sections of the pipeline unable to generate gas.

When comparing the second and first order accuracy method the gas fraction curves (figure 7.23) are quite similar. One use the slope limiter to reduce numerical diffusion that will smear out sharp transition zones, but it does not appear any sharp transition zones in this case. Thus, the values for gas fraction are similar.

Increasing the amount of boxes in the scheme seems to be beneficial to make the gas fraction curve smoother, seen in figure 7.26. There are more cells to handle the changes when mass transfer between the phases is introduced.

It is also possible to observe the gas fraction in the form of gas mass in figure 7.14 a). Here the sudden increase of gas mass is a result of the vaporization of liquid.

- **Fluid velocity**

All of the cases have no initial fluid flow or forced fluid flow. Once the simulation starts, there will be fluid moving towards the open end of the well/pipe due to the expansion of the liquid since the temperature is gradually increased. The liquid will decrease in density, but increase in volume, to force liquid to exit the well. This is observed in the 0-3120 second interval in figure 7.14 b) where the liquid mass decreases by a small amount over time. When the mass transition starts it will generate gas, which expands to a greater extent than liquid, making the fluid to flow even faster. As more and more gas is developed, the velocity keeps increasing gradually. This is presented in figure 7.13.

The oscillations seen in the inlet pressure (see figure 7.8) is caused by acceleration effects. Initially, the system is stagnant, but as soon as we start to increase temperature, the water will start to move as seen in figure 7.4, causing an acceleration effect making the system to move due to thermal expansion. Figure 7.4 supports the claim that the pressure pulses are induced by the initiated fluid flow as the temperature increases. These pressure pulses will be damped by friction over time as seen from figure 7.1 and 7.8. It takes a while until the pressure pulses is dampened, since the friction force that dampens the pulses is quite low.

8 Conclusion and further work

The first part of this thesis deal with well control, where the focus has been on how important it is to model mass transfer in order to simulate kick in oil-based mud. AUSMV is a transient model for multi-phase fluid flow which can be used for this purpose. The second part of this thesis is the first attempt to see how we can implement the mass transfer into the AUSMV scheme.

The original AUSMV scheme assumes the mass transfer to be equal to zero, but has been modified to include the mass transfer term to simulate the phase transition from liquid to gas. Here, water and steam has been considered. The AUSMV scheme has been experimented with to test its ability to handle mass transfer, and the scheme seems to successfully simulate the three cases with mass transfer without any numerical instability. The scheme proves to be an adaptable tool for different scenarios when introducing mass transfer. For the first three simulations, second order accuracy method is used. The fourth simulation compares first and second order accuracy method and also grid adjustment.

- The literature study of well control in HPHT wells shows that one of the most crucial areas for development in well control safety is early kick detection. There is an urgent need for earlier, more precise and more consistent kick detection as it has become more important as drilling in deep water wells with narrow operational windows is currently more common.
- A mass transfer term has successfully been implemented into the AUSMV scheme and the scheme seems to handle it nicely. First, we experimented with fixed values for the phase transfer, and then we used Rohsenows' correlation as a mass transfer equation. In order to be able to implement the mass transfer equation into the scheme, several correlations for the different variables in the equation had to be added to the scheme. The correlations for latent heat of evaporation and interfacial tension are added to the scheme. The constants used in calculation of the gas variables were also changed to function for water vapor. With the new addition of phase transition, how we update conservation variables in the scheme also had to be modified.
- A boiling point criterion has been experimented with to make the model more realistic, as the criterion is dependent on both pressure and temperature. When the pressure in the pipe increases as gas is generated, the boiling point temperature of the liquid increases. Sections fulfilling this criterion activate the mass transfer equation. When

the boiling point criterion is excluded in the scheme, all the numerical cells contribute to the mass transfer.

- The increase in gas fraction is a direct result of the vaporization of liquid made possible by the mass transfer, as there is no other source to increase the amount of gas in the well.
- The pressure variation after the mass transfer term is activated shows the ability of the scheme to handle the newly formed gas, and give realistic representation of the processes occurring in a well when gas is boiling out of the liquid.
- When gas starts to form, it will expand and force fluids rapidly out of the system. This is to be expected as the well cannot contain the increase in gas volume, making the fluids to exit the well.
- Changing from second to first order accuracy method seems not to significantly change the end result of the simulation. The second order accuracy method helps to diminish numerical diffusion that smear out sharp transition zones. However, there is no sharp transition zones detected in the horizontal case, making the improvement by using second order accuracy method not visible.
- Increasing the amount of boxes to handle the changes of mass transfer gives smoother plots, especially for the gas fraction. The grid adjustment gives a longer simulation run time, but also gives more refined results.
- Stiff source terms could be expected when introducing a mass transfer term that suddenly gets activated; however, the simulation runs smoothly without much sign of a stiff source term.

Further work

The AUSMV scheme has proven to be adaptable for multiphase flow scenarios with the implemented mass transfer term. However, there are some extensions to be made that will further advance the model to make it more realistic and take advantage of the potential this scheme possesses.

This thesis work focus on the ability of the AUSMV scheme to handle mass transfer of the phases. It contains only models for water-based drilling fluid, and its resultant water vapor. It would be beneficial to implement models for hydrocarbon gas solubility in the oil-based mud

and the vaporization of the gas in the upper parts of the well. Then the scheme would be able to simulate what can be experienced during kick scenarios using OBM. A dissolved gas kick can flash rapidly, unload the well and possibly induce a secondary kick.

As for the case considering a vertical well, the temperature gradient is set constant throughout the well. However, there will be heat transfer from the formation and the drillpipe into the annulus. This will give temperature variation for each time step, and John Emeka Udegbunam is currently working on such a temperature model. If this work is successfully implemented in the scheme, one can use this model in combination with mass transfer as mass transfer is heavily dependent on the heat transfer. The energy equation can then be bypassed, making the model less complex.

The liquid density in the scheme plays a large role when simulating the system. Currently in the scheme, it is dependent on the pressure and the temperature. One of the parameters used to calculate the density in the model is the thermal expansion coefficient, and this is set as a constant. It does, however, vary with increasing temperature. With an advanced temperature model, one can calculate the thermal expansion for each numerical cell, which gives a more exact density calculation.

Bibliography

Aadnøy, B. S. (2002). *Modern Well Design*. Boca Raton: CRC Press/Balkema.

Aadnøy, B. S. (2009). *Advanced Drilling and Well Technology*. Richardson, Texas: Society of Petroleum Engineers.

Adams, N. (1997). How to Control Differential Pipe Sticking. *Journal of Petroleum Technology, September*(3), 44-50.

Adams, N., & Kuhlman, L. (1994). *Kicks and Blowout Control*. Tulsa, Oklahoma: PennWell Books.

Affandi, M., Mamat, N., Kanafiah, S. N. A. M., & Khalid, N. S. (2013). Simplified Equations for Saturated Steam Properties for Simulation Purpose. *Procedia Engineering, 53*, 722-726. doi:http://dx.doi.org/10.1016/j.proeng.2013.02.095

Amani, M. (2012). The Rheological Properties of Oil-Based Mud Under High Pressure and High Temperature Conditions. *Advances in Petroleum Exploration and Development, 3*(2), 21-30. doi:10.3968/j.aped.1925543820120302.359

Amani, M., Al-Jubouri, M., & Arash, S. (2012). Comparative Study of Using Oil-Based Mud versus Water-Based Mud in HPHT Fields *Advances in Petroleum Exploration and Development, 4*(2), 18-27. doi:10.3968/j.aped.1925543820120402.987

American Petroleum Institute (2006). *Recommended practice for well control operation* (Second edition ed.). Washington, D.C.: American Petroleum Institute.

Atolini, T. M., & Ribeiro, P. R. (2007). Vapor-Liquid Mixture Behavior at High Temperatures and Pressures: A Review Directed to Drilling Engineering. *Brazilian Journal of Petroleum and Gas, 1*(2), 123-130.

Benzoni-Gavage, S. (1991). *Analyse Numerique des Modéles Hydrodynamiques d'Ecoulements Diphasique Instationnaires dans les Réseaux de Production Pétroliére.*, ENS de Lyon.

Bern, P. A., van Oort, E., Neusstadt, B., Ebeltoft, H., Zurdo, C., Zamora, M., & Slater, K. (1988). *Barite Sag: Measurement, Modelling and Management*. Paper presented at the IADC/SPE Asia Pacific Drilling Technology, Jakarta, Indonesia. SPE-47784-MS retrieved from http://dx.doi.org/10.2118/47784-MS

Bland, R. G., Mullen, G. A., Gonzalez, Y. N., Harvey, F. E., & Pless, M. L. (2006). *HPHT Drilling Fluid Challenges*. Paper presented at the IADC/SPE Asia Pacific Drilling Technology Conference and Exhibition, Bangkok, Thailand SPE-103731-MS retrieved from http://dx.doi.org/10.2118/103731-MS

Bradley, N. D., Low, E., Aas, B., Rommetveit, R., & Larsen, H. F. (2002). *Gas Diffusion - Its Impact on a Horizontal HPHT Well*. Paper presented at the SPE Annual Technical Conference and Exhibition, San Antonio, Texas. SPE-77474-MS retrieved from http://dx.doi.org/10.2118/77474-MS

Brunner, G. (1994). *Gas Extraction - An Introduction to Fundamentals of Supercritical Fluids and the Application to Separation Processes*. New York: Springer.

Bureau, N., de Hemptinne, J. C., Audibert, A., & Herzhaft, B. (2002). *Interactions Between Drilling Fluid and Reservoir Fluid*. Paper presented at the SPE Annual Technical Conference and Exhibition, San Antonio, Texas. SPE-77475-MS retrieved from http://dx.doi.org/10.2118/77475-MS

Caenn, R., Darley, H. C. H., & Gray, G. R. (2011). *Composition and properties of drilling and completion fluids* (6th edition ed.). Amsterdam: Elsevier.

Cockburn, A. (1987). The Driller's Problems With Gas Solution In Oil Based Muds *SPE-16995-MS*: Society of Petroleum Engineers.

Danielson, T. J., Brown, L. D., & Bansal, K. M. (2000). *Flow Management: Steady-State and Transient Multiphase Pipeline Simulation*. Paper presented at the Offshore Technology Conference, Houston, Texas. OTC-11965-MS retrieved from http://dx.doi.org/10.4043/11965-MS

Evje, S., & Fjelde, K. K. (2002). Hybrid flux-splitting schemes for a two-phase flow model. *J. Comput. Phys., 175*(2), 674-701. doi:10.1006/jcph.2001.6962

Evje, S., & Fjelde, K. K. (2003). On a rough AUSM scheme for a one-dimensional two-phase model. *Computers & Fluids, 32*(10), 1497-1530. doi:http://dx.doi.org/10.1016/S0045-7930(02)00113-5

Fjelde, K. K. (2011). *Well Flow Modeling Compendium*. University of Stavanger.

Fjelde, K. K., Frøyen, J., & Ghauri, A. A. (2016). *A Numerical Study of Gas Kick Migration Velocities and Uncertainty*. Paper presented at the SPE Bergen One Day Seminar, Grieghallen, Bergen, Norway. SPE-180053-MS retrieved from http://dx.doi.org/10.2118/180053-MS

Flatabø, G. Ø., Torsvik, A., Oltedal, V. M., Bjørkvik, B., Grimstad, A.-A., & Linga, H. (2015). *Experimental Gas Absorption in Petroleum Fluids at HPHT Conditions*. Paper presented at the SPE Bergen One Day Seminar, Bergen, Norway. SPE-173865-MS retrieved from http://dx.doi.org/10.2118/173865-MS

García-Cascales, J. R., & Paillère, H. (2006). Application of AUSM schemes to multi-dimensional compressible two-phase flow problems. *Nuclear Engineering and Design, 236*(12), 1225-1239. doi:http://dx.doi.org/10.1016/j.nucengdes.2005.11.013

Grace, R. D. (2003). *Advanced Blowout and Well Control*. Burlington: Elsevier Science.

Hall, J. E., Roche, J. R., & Boulet, C. G. (1986). *Means for Handling Gas Influx in a Marine Riser*. Paper presented at the SPE/IADC Drilling Conference, Dallas, Texas SPE-14739-MS retrieved from http://dx.doi.org/10.2118/14739-MS

Hirsch, C. (2007). *Numerical Computation of Internal and External Flows: The Fundamentals of Computational Fluid Dynamics, 2nd Edition*: Elsevier.

Hornung, M. R. (1990). *Kick Prevention, Detection, and Control: Planning and Training Guidelines for Drilling Deep High-Pressure Gas Wells*. Paper presented at the SPE/IADC Drilling Conference, Houston, Texas. SPE-19990-MS retrieved from http://dx.doi.org/10.2118/19990-MS

Johnson, A., Rezmer-Cooper, I., Bailey, T., & McCann, D. (1995). *Gas Migration: Fast, Slow or Stopped*. SPE-29342-MS retrieved from http://dx.doi.org/10.2118/29342-MS

Kenny, W. G. (2015). *Evaluation of Automated Well Safety and Early Kick Detection Technologies*. Retrieved from Houston, TX:

Kleppe, S., Michelsen, E., Handgraaf, P., Albriktsen, P., & Haugen, A. (2009). *Reusing Recovered Base Oil From OBM Cuttings*. SPE-123559-MS retrieved from http://dx.doi.org/10.2118/123559-MS

Kothandaraman, C. P. (2005). *Fundamentals of Heat and Mass Transfer*. Daryaganj: Daryaganj, Delhi, IND: New Age International.

Kozicz, J. R. (2012). *Development of a Marine Riser Gas Management System*. Paper presented at the IADC/SPE Asia Pacific Drilling Technology Conference and Exhibition, Tianjin, China. SPE-156399-MS retrieved from http://dx.doi.org/10.2118/156399-MS

LeVeque, R. J., & Yee, H. C. (1990). A study of numerical methods for hyperbolic conservation laws with stiff source terms. *J. Comput. Phys., 86*(1), 187-210. doi:10.1016/0021-9991(90)90097-k

Litlehamar, H. F. (2011). *Well Control Procedures and Simulations.* (Master), University of Stavanger, Stavanger.

Longeron, D. G., Alfenore, J., Salehi, N., & Saintpère, S. (2000). *Experimental Approach to Characterize Drilling Mud Invasion, Formation Damage and Cleanup Efficiency in Horizontal Wells with Openhole Completions*. Paper presented at the SPE International Symposium on Formation Damage Control, Lafayette, Louisiana. SPE-58737-MS retrieved from http://dx.doi.org/10.2118/58737-MS

Marteau, P., Obriot, J., Barreau, A., & Behar, E. (1997). Experimental Determination of the Phase Behavior of Binary Mixtures: Methane-Hexane and Methane-Benzene. *Fluid Phase Equilibria, 129*(1-2), 285-305. doi:10.1016/S0378-3812(96)03125-1

McMordie, W. C., Jr., Bland, R. G., & Hauser, J. M. (1982). *Effect of Temperature and Pressure on the Density of Drilling Fluids*. Paper presented at the SPE Annual Technical Conference and Exhibition, New Orleans, Louisiana. SPE-11114-MS retrieved from http://dx.doi.org/10.2118/11114-MS

Mosti, I., Anfinsen, B. T., & Flatebø, A. S. (2008). Impact of thermal expansion on kick tolerance should be part of pre-drilling risk assessment. *Drilling Contractor*(March/April), 104-106.

NORSOK. (2012). Drilling facilities, Rev 3.

NORSOK. (2013). Well integrity in drilling and well operations, Rev 4.

O'Brien, T. B. (1982). Handling Gas in Oil Based Mud Takes Special Precautions. *World Oil*, 83-86.

O'Bryan, P. L. (1985). *The Experimental and Theoretical Study of Methane Solubility in an Oil Base Drilling Fluid.* (Master), Louisiana State University, Baton Rouge, LA.

O'Bryan, P. L., & Bourgoyne, A. T. (1989). Methods for Handling Drilled Gas in Oil-Based Drilling Fluids. *SPE Drilling Engineering, 04*(03). doi:10.2118/16159-PA

O'Bryan, P. L., & Bourgoyne, A. T., Jr. (1987). *Swelling of Oil-Base Drilling Fluids Due to Dissolved Gas*. Paper presented at the SPE Annual Technical Conference and Exhibition, Dallas, Texas. SPE-16676-MS retrieved from http://dx.doi.org/10.2118/16676-MS

O'Bryan, P. L., Bourgoyne, A. T., Jr., Monger, T. G., & Kopcso, D. P. (1988). An Experimental Study of Gas Solubility in Oil-Based Drilling Fluids. *SPE Drilling Engineering, 03*(1). doi:10.2118/15414-PA

Peng, D.-Y., & Robinson, D. B. (1976). A New Two-Constant Equation of State. *Industrial & Engineering Chemistry Fundamentals, 15*, 59-64.

Petersen, J., & Carlsen, L. A. (2016). *Discussion on Potential Problems Due To Methane Invasion in OBM While Overbalanced*. Paper presented at the SPE Bergen One Day Seminar, Bergen, Norway. SPE-180035-MS retrieved from http://dx.doi.org/10.2118/180035-MS

Popiel, C. O., & Wojtkowiak, J. (1998). Simple Formulas for Thermophysical Properties of Liquid Water for Heat Transfer Calculations (from 0°C to 150°C). *Heat Transfer Engineering, 19*(3), 87-101. doi:10.1080/01457639808939929

Raymond, L. R. (1969). Temperature Distribution in a Circulating Drilling Fluid. *Journal of Petroleum Technology, 21*(03). doi:10.2118/2320-PA

Rehm, B. (2002). *Practical Underbalanced Drilling and Workover*. Austin, Texas: PETEX.

Rohsenow, W. M. (1951). *A Method of Correlating Heat Transfer Data for Surface Boiling of Liquids*: M.I.T. Division of Industrial Cooporation.

Rommetveit, R., & Bjorkevoll, K. S. (1997). *Temperature and Pressure Effects on Drilling Fluid Rheology and ECD in Very Deep Wells*. Paper presented at the SPE/IADC Middle East Drilling Technology Conference, Bahrain. SPE-39282-MS retrieved from http://dx.doi.org/10.2118/39282-MS

Rommetveit, R., Fjelde, K. K., Aas, B., Day, N. F., Low, E., & Schwartz, D. H. (2003). *HPHT Well Control; An Integrated Approach*. Paper presented at the Offshore Technology Conference, Houston, Texas. OTC-15322-MS retrieved from http://dx.doi.org/10.4043/15322-MS

Rommetveit, R., & Olsen, T. L. (1989). *Gas Kick Experiments in Oil-Based Drilling Muds in a Full-Scale, Inclined Research Well*. Paper presented at the SPE Annual Technical Conference and Exhibition, San Antonio, Texas. SPE-19561-MS retrieved from http://dx.doi.org/10.2118/19561-MS

Saasen, A., Jordal, O. H., Burkhead, D., Berg, P. C., Løklingholm, G., Pedersen, E. S., . . . Harris, M. J. (2002). *Drilling HT/HP Wells Using a Cesium Formate Based Drilling Fluid*. Paper presented at the IADC/SPE Drilling Conference, Dallas, Texas. SPE-74541-MS retrieved from http://dx.doi.org/10.2118/74541-MS

Santos, H. M., Catak, E., Kinder, J. I., & Sonnemann, P. (2007). *Kick Detection and Control in Oil-based Mud: Real Well Test Results Using Micro-Flux Control Equipment*. Paper presented at the SPE/IADC Drilling Conference, Amsterdam, The Netherlands SPE-105454-MS retrieved from http://dx.doi.org/10.2118/105454-MS

Santos, H. M., Catak, E., & Valluri, S. (2011). *Kick tolerance misconceptions and consequences to well design*. Paper presented at the SPE/IADC Drilling Conference and Exhibition, 1-3 March, Amsterdam, The Netherlands. SPE-140113-MS retrieved from http://dx.doi.org/10.2118/140113-MS

Silva, C. T., Mariolani, J. R. L., Bonet, E. J., Lomba, R. F. T., Santos, O. L. A., & Ribeiro, P. R. (2004). *Gas Solubility in Synthetic Fluids: A Well Control Issue*. Paper presented at the SPE Annual Technical Conference and Exhibition, Houston, Texas. SPE-91009-MS retrieved from http://dx.doi.org/10.2118/91009-MS

Skalle, P. (2013). *Drilling Fluid Engineering* (Third edition ed.): BookBoon.

Soave, G. (1972). Equilibrium constants from a modified Redlich-Kwong equation of state. *Chemical Engineering Science, 27*, 1197-1203.

Soliman, A. A. (1995). *Oil Base Mud in High Pressure, High Temperature Wells*. Paper presented at the Middle East Oil Show, Bahrain. SPE-29864-MS retrieved from http://dx.doi.org/10.2118/29864-MS

Stamnes, Ø. N. (2011). *Nonlinear Estimation with Application to Drilling.* (PhD), Norwegian University of Science and Technology (NTNU), Trondheim, Norway.

Standing, M. B. (1947). *A Pressure-Volume-Temperature Correlation For Mixtures Of California Oils And Gases*. Paper presented at the Drilling and Production Practice, New York, New York.

Thomas, D. C., Lea, J. F., Jr., & Turek, E. A. (1984). Gas Solubility in Oil-Based Drilling Fluids: Effects on Kick Detection. *Journal of Petroleum Technology, 36*(06). doi:10.2118/11115-PA

Torsvik, A., Skogestad, J. O., & Linga, H. (2016). *Impact on Oil-Based Drilling Fluid Properties from Gas Influx at HPHT Conditions*. Paper presented at the IADC/SPE Drilling Conference and Exhibition, Fort Worth, Texas. IADC/SPE-178860-MS retrieved from http://dx.doi.org/10.2118/178860-MS

Transocean. (2009). *Well Control Handbook* (Vol. 3rd edition).

Udegbunam, J. E., Fjelde, K. K., Evje, S., & Nygaard, G. (2015). On the Advection-Upstream-Splitting-Method Hybrid Scheme: A Simple Transient-Flow Model for Managed-Pressure-Drilling and Underbalanced-Drilling Applications. *SPE Drilling & Completion*. doi:10.2118/168960-PA

van Leer, B., Thomas, J. L., Roe, P., & Newsome, R. W. (1987). *A comparison of numerical flux formulas for the Euler and Navier-Stokes equations*. Paper presented at the 8th Computational Fluid Dynamics Conference. http://dx.doi.org/10.2514/6.1987-1104

Vargaftik, N. B., Volkov, B. N., & Voljak, L. D. (1983). International Tables of the Surface Tensions of Water. *Journal of Physical Chemistry, 12*(3), 817-820. doi:10.1063/1.555688

Wu, R., & Rosenegger, L. (2000). Comparison of PVT Properties From Equation of State Analysis and PVT Correlations for Reservoir Studies. *Journal of Canadian Petroleum Technology, 39*(07). doi:10.2118/00-07-03

Yeo, M., Macgregor, A. J., Pinkstone, H., & Piccolo, B. (2015). *Offshore Deepwater Managed Pressure Drilling and Riser Gas Handling Equipment Design*. Paper presented at the SPE/IADC Managed Pressure Drilling and Underbalanced Operations Conference & Exhibition, Dubai, UAE. SPE-173819-MS retrieved from http://dx.doi.org/10.2118/173819-MS

Appendix A Well pressure calculation and of phase velocities

Well pressure calcuation

Mass conservative variables (liquid and gas):

$$w_1 = \rho_l \alpha_l ; w_2 = \rho_g \alpha_g$$

$$w_1 = \rho_l \alpha_l = \rho_l (1 - \alpha_g) = \rho_l (1 - \frac{w_2}{\rho_g}) \tag{A-1}$$

Substituting Eq. 4 for gas density,

$$w_1 = \rho_l (1 - \frac{RTw_2}{p}) \Rightarrow pw_1 = \rho_l (p - w_2 RT) \tag{A-2}$$

Substituting Eq. 2 for liquid density,

$$pw_1 = (\rho_0 + \frac{\rho_0}{\beta}(p - p_0) - \rho_0 \alpha (T - T_0))(p - w_2 RT) \tag{A-3}$$

$$pw_1 = (\rho_0 - \frac{p_0 \rho_0}{\beta} + \frac{p \rho_0}{\beta} - \rho_0 \alpha (T - T_0))(p - w_2 RT)$$

$$pw_1 = (\rho_0 - \frac{p_0 \rho_0}{\beta} - \rho_0 \alpha (T - T_0) + \frac{p \rho_0}{\beta})(p - w_2 RT)$$

$$pw_1 = (x_1 + x_2 p)(p + x_3) \tag{A-4}$$

where:

$x_1 = \rho_0 - \frac{p_0 \rho_0}{\beta} - \rho_0 \alpha (T - T_0)$, $x_2 = \frac{\rho_0}{\beta}$, and $x_3 = -w_2 RT$

$$pw_1 = x_1 p + x_1 x_3 + x_2 p^2 + x_2 x_3 p$$

$$x_2 p^2 + (x_1 + x_2 x_3 - w_1) p + x_1 x_3 = 0$$

$$ap^2 + bp + c = 0 \tag{A-5}$$

$$p = \frac{-b + \sqrt{b^2 - 4ac}}{2a} \tag{A-6}$$

Where:

$a = x_2$, $b = x_1 + x_2 x_3 - w_1$, and $c = x_1 x_3$

Calcuation of phase velocities

We assume the two following slip relations:

$$v_g = k_0 v_{mix} + s_0$$

$$v_l = k_1 v_{mix} + s_1$$

The first relation is the one that we have originally while the second relation is defined artificially where we need to determine expressions for k_1 and s_1. This will be done at the end of Appendix B.

We also have:

$$q_{mix} = \rho_l \alpha_l v_l + \rho_g \alpha_g v_g$$

We now insert the two slip relations for the phase velocities:

$$q_{mix} = \rho_l \alpha_l (k_1 v_{mix} + s_1) + \rho_g \alpha_g (k_0 v_{mix} + s_o)$$

$$q_{mix} = (\rho_l \alpha_l k_1 + \rho_g \alpha_g k_0) v_{mix} + \rho_l \alpha_l s_1 + \rho_g \alpha_g s_0$$

We introduce help variables:

$$a = \rho_l \alpha_l k_1 + \rho_g \alpha_g k_0$$

$$b = \rho_l \alpha_l s_1 + \rho_g \alpha_g s_0$$

Using these, we have the following simple formula relating mixture velocity and mixture momentum.

$$v_{mix} = \frac{(q_{mix} - b)}{a}$$

The phase velocities can now be found from the corresponding slip relations.

But, we still need to find the coefficients k_1 and s_1.

We have

$$v_g = k_0 v_{mix} + s_0$$

Then multiply both sides with α_g and then add $\alpha_l v_l$ on both sides. This gives:

$$v_g \alpha_g + v_l \alpha_l = \alpha_g k_0 v_{mix} + \alpha_g s_0 + v_l \alpha_l$$

Left hand side is just an expression for v_{mix}. We then have

$v_l \alpha_l = v_{mix} - \alpha_g k_0 v_{mix} - \alpha_g s_0$ or

$$v_l = \frac{(1-\alpha_g k_0)}{\alpha_l} v_{mix} - \frac{\alpha_g s_0}{\alpha_l}$$

This gives:

$$k_1 = \frac{(1-\alpha_g k_0)}{\alpha_l}$$

$$s_1 = -\frac{\alpha_g s_0}{\alpha_l}$$

These are the main expression implemented in the code for gas volume fractions below 0.75. One should not that there is a singularity in the gas slip relation in general for higher gas volume fractions.

If we rewrite

$$v_g = k_0 v_{mix} + s_0$$

As

$$v_g = \frac{\alpha_l v_l k_0 + s_0}{1-\alpha_g k_0}$$

We will divide by zero if $\alpha_g = \frac{1}{k_0}$. If $k_0 = 1.2$, this will happen for a gas volume fraction of 0.83. It is natural to assume that when approaching one-phase gas flow, we will end up with no slip conditions, $v_g = v_l = v_{mix}$, which means that $k_0 = 1$, $s_0 = 0$. Hence a linear interpolation between these slip parameters have been used in the range of gas volume fractions from 0.75 to 1. It seems to work, but from a numerical point of view, one has to be careful in this transition and always ensure that one does not divide by zero anywhere.

Written by John Emeka Udegbunam.

Appendix B Matlab code for the horizontal cases with functions

Codes written in red are modified and diverge from the original code given to me.

The model also had to be made dependent on temperature. This has already been performed by Arne Kristoffer Torsdal, but I had to re-implement it to familiarize myself with the code. The system also had to be changed so that water/steam parameters is used.

```
% Transient two-phase code based on AUSMV scheme: Gas and Water
% The code assumes uniform geometry and the code is partially vectorized.

clear;
t = cputime
tic,

% Geometry data/ Must be specified
welllength = 2000;
nobox = 25; %Number of boxes in the well
nofluxes = nobox+1;
dx = welllength/nobox; % Boxlength
%dt = 0.005;

% Welldepth array
x(1)= 0.5*dx;
for i=1:nobox-1
 x(i+1)=x(i)+ dx;
end

dt= 0.01;  % Timestep
dtdx = dt/dx;
time = 0.0;
endtime = 3500; % Time for end of simulation
nosteps = endtime/dt;  %Number of total timesteps
timebetweensavingtimedata = 5;  % How often in s we save data vs time for plotting.
nostepsbeforesavingtimedata = timebetweensavingtimedata/dt;

% Slip parameters used in the gas slip relation. vg =Kvmix+S
k = 1.2;
s = 0.5;

% Variables
rho0 = 1000; %[kg/m3]
P0 = 10^5; % [Pa]
Bheta = 2.2*10^9;
Alpha = 0.000207;
tempstart = 273+20; % [K]
Rsteam = 461.5; % [J/(kg*K)] Steam

% Temperature distribution
temperature = 293; % [Kelvin]
dtemp = 90/nosteps;

% Viscosities (Pa*s)/Used in the frictional pressure loss model.
viscl = liqvisc(temperature); % Liquid phase
```

```
viscg = gasvisc(temperature); % Gas phase

% Density parameters. These parameters are used when finding the
% primitive variables pressure, densities in an analytical manner.
% Changing parameters here, you must also change parameters inside the
% density routines roliq and rogas.

% liquid density at stc and speed of sound in liquid
 dstc = 1000.0;   %Base density of liquid, See also roliq.
 pstc = 100000.0; % Pressure at standard conditions, 100000 Pascal
 al = 1500; % Speed of sound/compressibility of liquid phase.
 t1 = dstc-pstc/(al*al); % Help variable for calc primitive variables from
 % conservative variables
% Ideal gas law constant
 rt = 100000;

% Gravity constant

 g = 0.0; % Gravitational constant

% Well opening. opening = 1, fully open well, opening = 0 (<0.01), the well
% is fully closed. This variable will control what boundary conditions that
% will apply at the outlet (both physical and numerical): We must change
% this further below in the code if we want to change status on this.

 wellopening = 1.0;  % This variable determines if
%the well is closed or not, wellopening = 1.0 -> open. welllopening = 0
%-> Well is closed. This variable affects the boundary treatment.

 bullheading = 0.0; % This variable can be set to 1.0 if we want to simulate
% a bullheading operation. But the normal is to set this to zero.


% Specify if the primitive variables shall be found either by
% a numerical or analytical approach. If analytical = 1, analytical
% solution is used. If analytical = 0. The numerical approach is used.
% using the itsolver subroutine where the bisection numerical method
% is used.

 analytical = 1;


% Define and intilalize flow variables




% Here we specify the outer and inner diameter and the flow area

  for i = 1:nobox
 %  do(i) = 0.3112;
   do(i)=0.2159;
   di(i) = 0.0;
   area(i) = 3.14/4*(do(i)*do(i)- di(i)*di(i));
%   ang(i)=3.14/2;
  end
```

```
% Initialization of slope limiters.
 for i = 1:nobox
   sl1(i)=0;
   sl2(i)=0;
   sl3(i)=0;
   sl4(i)=0;
   sl5(i)=0;
   sl6(i)=0;
 end



% Now comes the intialization of the physical variables in the well.
% First primitive variables, then the conservative ones.




% Below we intialize pressure and fluid densities. We start from top of
% the well and calculated downwards. The calculation is done twice with
% updated values to get better approximation. Only hydrostatic
% considerations.

p(nobox)= 100000.0;   % Pressure
dl(nobox)=rholiq(p(nobox),temperature);  % Liquid density
dg(nobox)=rogas(p(nobox),temperature);   % Gas density

for i=nobox-1:-1:1
p(i)=100000.0;
dl(i)=rholiq(p(i),temperature);
dg(i)=rogas(p(i),temperature);
end

% Intitialize phase velocities, volume fractions, conservative variables
% The basic assumption is static fluid, one phase liquid.

for i = 1:nobox
  vl(i)=0; % Liquid velocity new time level.
  vg(i)=0; % Gas velocity at new time level
  eg(i)=0;  % Gas volume fraction
  ev(i)=1-eg(i); % Liquid volume fraction
  qv(i,1)=dl(i)*ev(i)*area(i);
  qv(i,2)=dg(i)*eg(i)*area(i);
  qv(i,3)=(dl(i)*ev(i)*vl(i)+dg(i)*eg(i)*vg(i))*area(i);
  fricgrad(i)=0;
  hydgrad(i)=g* qv(i,1);
end

source = zeros(nobox,3);
```

```
% Section where we also initialize values at old time level


for i=1:nobox
  dlo(i)=dl(i);
  dgo(i)=dg(i);
  po(i)=p(i);
  ego(i)=eg(i);
  evo(i)=ev(i);
  vlo(i)=vl(i);
  vgo(i)=vg(i);
  qvo(i,1)=qv(i,1);
  qvo(i,2)=qv(i,2);
  qvo(i,3)=qv(i,3);
end


% Intialize fluxes between the cells/boxes

for i = 1:nofluxes
  for j =1:3
   flc(i,j)=0.0; % Flux of liquid over box boundary
   fgc(i,j)=0.0; % Flux of gas over box boundary
   fp(i,j)= 0.0; % Pressure flux over box boundary
  end
end


%  Main program. Here we will progress in time. First som intializations
% and definitions to take out results. The for loop below runs until the
% simulation is finished.

countsteps = 0;
counter=0;
printcounter = 1;
pbot(printcounter) = p(1);
pchoke(printcounter)= p(nobox);
liquidmassrateout(printcounter) = 0;
gasmassrateout(printcounter)=0;
tempin(printcounter)=0;
timeplot(printcounter)=time;
kickvolume=0;
bullvolume=0;
tempplot(printcounter)=tempstart;
sourceplot(printcounter)=0;
vlplot(printcounter)=0;

for i = 1:nosteps
   countsteps=countsteps+1;
   counter=counter+1;
   time = time+dt;

  temperature = temperature+dtemp;

       % Viscosities (Pa*s)/Used in the frictional pressure loss model.
      viscl = liqvisc(temperature); % Liquid phase
```

```
    viscg = gasvisc(temperature); % Gas phase

% Then a section where specify the boundary conditions.
% Here we specify the inlet rates of the different phases at the
% bottom of the pipe in kg/s. We interpolate to make things smooth.
% It is also possible to change the outlet boundary status of the well
% here. First we specify rates at the bottom and the pressure at the outlet
% in case we have an open well. This is a place where we can change the
% code to control simulations.

% In the example below, we take a gas kick and then circulate this
% out of the well without closing the well. (how you not should perform
% well control)

XX = 0;
% XX (kg/s) is a variable for introducing a kick in the well.
YY = 0; % Liquid flowrate (kg/s) (1 kg/s = 1 l/s approx)
if (time < 10)

  inletligmassrate=0.0;
  inletgasmassrate=0.0;

elseif ((time>=10) & (time < 20))
  inletligmassrate = 0*(time-10)/10;
  inletgasmassrate = XX*(time-10)/10;

elseif ((time >=20) & (time<110))
  inletligmassrate = 0;
  inletgasmassrate = XX;

elseif ((time>=110)& (time<120))
  inletligmassrate = 0;
  inletgasmassrate = XX-XX*(time-110)/10;
elseif ((time>=120&time<130))
  inletligmassrate =0;
  inletgasmassrate =0;
elseif ((time>=130)&(time<300))
  inletligmassrate =0;
  inletgasmassrate =0;
elseif ((time>=300)&(time<310))
  inletligmassrate= YY*(time-300)/10;
  inletgasmassrate =0;
elseif((time>=310))
  inletligmassrate= YY;
  inletgasmassrate =0;
end

kickvolume = kickvolume+inletgasmassrate/dgo(1)*dt;




% specify the outlet pressure /Physical. Here we have given the pressure as
% constant. It would be possible to adjust it during openwell conditions
```

```
% either by giving the wanted pressure directly (in the command lines
% above) or by finding it indirectly through a chokemodel where the wellopening
% would be an input parameter. The wellopening variable would equally had
% to be adjusted inside the command line structure given right above.

 pressureoutlet = 100000.0;

% Based on these boundary values combined with use of extrapolations techniques
% for the remaining unknowns at the boundaries, we will define the mass and
% momentum fluxes at the boundaries (inlet and outlet of pipe).

% inlet/bottom fluxes first.
  if (bullheading<=0)

    flc(1,1)= inletligmassrate/area(1);
    flc(1,2)= 0.0;
    flc(1,3)= flc(1,1)*vlo(1);



    fgc(1,1)= 0.0;
    fgc(1,2)= inletgasmassrate/area(1);
    fgc(1,3)= fgc(1,2)*vgo(1);

    fp(1,1)= 0.0;
    fp(1,2)= 0.0;

% Old way of treating the boundary
%     fp(1,3)= po(1)+0.5*(po(1)-po(2)); %Interpolation used to find the
% pressure at the inlet/bottom of the well.

% New way of treating the boundary
     fp(1,3)= po(1)...
          +0.5*dx*(dlo(1)*evo(1)+dgo(1)*ego(1))*g...
          +0.5*dx*fricgrad(1);



  else
    flc(1,1)=dlo(1)*evo(1)*vlo(1);
    flc(1,2)=0.0;
    flc(1,3)=flc(1,1)*vlo(1);

    fgc(1,1)=0.0;
    fgc(1,2)=dgo(1)*ego(1)*vgo(1);
    fgc(1,3)=fgc(1,2)*vgo(1);

    fp(1,1)=0.0;
    fp(1,2)=0.0;
    fp(1,3)=20000000; % This was a fixed pressure set at bottom when bullheading
  end



% Outlet fluxes (open & closed conditions)

   if (wellopening>0.01)
```

```
% Here open end condtions are given. We distinguish between bullheading
% & normal circulation.

      if (bullheading<=0)

         flc(nofluxes,1)= dlo(nobox)*evo(nobox)*vlo(nobox);
         flc(nofluxes,2)= 0.0;
         flc(nofluxes,3)= flc(nofluxes,1)*vlo(nobox);


         fgc(nofluxes,1)= 0.0;
         fgc(nofluxes,2)= dgo(nobox)*ego(nobox)*vgo(nobox);
         fgc(nofluxes,3)= fgc(nofluxes,2)*vgo(nobox);

         fp(nofluxes,1)= 0.0;
         fp(nofluxes,2)= 0.0;
         fp(nofluxes,3)= pressureoutlet;
      else
         flc(nofluxes,1)= inletligmassrate/area(nobox);
         flc(nofluxes,2)= 0.0;
         flc(nofluxes,3)= flc(nofluxes,1)*vlo(nobox);

         fgc(nofluxes,1)=0.0;
         fgc(nofluxes,2)=0.0;
         fgc(nofluxes,3)=0.0;

         fp(nofluxes,1)=0.0;
         fp(nofluxes,2)=0.0;
         fp(nofluxes,3)= po(nobox)...
         -0.5*dx*(dlo(nobox)*evo(nobox)+dgo(nobox)*ego(nobox))*g...
         +0.5*dx*fricgrad(nobox);
      end
   else

% Here closed end conditions are given

       flc(nofluxes,1)= 0.0;
       flc(nofluxes,2)= 0.0;
       flc(nofluxes,3)= 0.0;

       fgc(nofluxes,1)= 0.0;
       fgc(nofluxes,2)= 0.0;
       fgc(nofluxes,3)= 0.0;

       fp(nofluxes,1)=0.0;
       fp(nofluxes,2)=0.0;

   %   Old way of treating the boundary
   %    fp(nofluxes,3)= po(nobox)-0.5*(po(nobox-1)-po(nobox));

   %   New way of treating the boundary
       fp(nofluxes,3)= po(nobox)...
       -0.5*dx*(dlo(nobox)*evo(nobox)+dgo(nobox)*ego(nobox))*g;
   %    -0.5*dx*fricgrad(nobox); % Neglect friction since well is closed.
      end
```

```
% Implementation of slopelimiters. They are applied on the physical
% variables like phase densities, phase velocities and pressure.



    for i=2:nobox-1
     sl1(i)=minmod(dlo(i-1),dlo(i),dlo(i+1),dx);
     sl2(i)=minmod(po(i-1),po(i),po(i+1),dx);
     sl3(i)=minmod(vlo(i-1),vlo(i),vlo(i+1),dx);
     sl4(i)=minmod(vgo(i-1),vgo(i),vgo(i+1),dx);
     sl5(i)=minmod(ego(i-1),ego(i),ego(i+1),dx);
     sl6(i)=minmod(dgo(i-1),dgo(i),dgo(i+1),dx);
    end

% Slopelimiters in boundary cells are set to zero!
    sl1(nobox)=0;
    sl2(nobox)=0;
    sl3(nobox)=0;
    sl4(nobox)=0;
    sl5(nobox)=0;
    sl6(nobox)=0;

 % Ny Kode 11/11-15
    sl1(1)=0;
    sl2(1)=0;
    sl3(1)=0;
    sl4(1)=0;
    sl5(1)=0;
    sl6(1)=0;



% Now we will find the fluxes between the different cells.
% NB - IMPORTANE -  Note that if we change the compressibilities/sound velocities of
% the fluids involved, we need to do changes inside the csound function.

    for j = 2:nofluxes-1

%%%%%%%%%%%%%%%%%%%%%%%%%%%%%%%%%%%%%%%%%%%%%%%%%%%%%%%%%%%%%%%%%%%%%%%%
%%%%%%%%%%%%%%%%%%%%%%%%%%%%%%%%%%%%%%%%%%%%%%%%%%%%%%%%%%%%%%%%%%%%%%%%
% First order method is from here:
%       cl = csound(ego(j-1),po(j-1),dlo(j-1),k);
%       cr = csound(ego(j),po(j),dlo(j),k);
%       c = max(cl,cr);
%       pll = psip(vlo(j-1),c,evo(j));
%       plr = psim(vlo(j),c,evo(j-1));
%       pgl = psip(vgo(j-1),c,ego(j));
%       pgr = psim(vgo(j),c,ego(j-1));
%       vmixr = vlo(j)*evo(j)+vgo(j)*ego(j);
%       vmixl = vlo(j-1)*evo(j-1)+vgo(j-1)*ego(j-1);
%
%       pl = pp(vmixl,c);
%       pr = pm(vmixr,c);
%       mll= evo(j-1)*dlo(j-1);
%       mlr= evo(j)*dlo(j);
%       mgl= ego(j-1)*dgo(j-1);
%       mgr= ego(j)*dgo(j);
%
```

```
%       flc(j,1)= mll*pll+mlr*plr;
%       flc(j,2)= 0.0;
%       flc(j,3)= mll*pll*vlo(j-1)+mlr*plr*vlo(j);
%
%       fgc(j,1)=0.0;
%       fgc(j,2)= mgl*pgl+mgr*pgr;
%       fgc(j,3)= mgl*pgl*vgo(j-1)+mgr*pgr*vgo(j);
%
%       fp(j,1)= 0.0;
%       fp(j,2)= 0.0;
%       fp(j,3)= pl*po(j-1)+pr*po(j);

 %  First order methods ends here
 %%%%%%%%%%%%%%%%%%%%%%%%%%%%%%%%%%%%%%%%%%%%%%%%%%%%%%%%%%%%%%

%%%%%%%%%%%%%%%%%%%%%%%%%%%%%%%%%%%%%%%%%%%%%%%%%%%%%%%%%%%%%%
%%




%%%%%%%%%%%%%%%%%%%%%%%%%%%%%%%%%%%%%%%%%%%%%%%%%%%%%%%%%%%%%%
%%%%
%%%%%%%%%%%%%%%%%%%%%%%%%%%%%%%%%%%%%%%%%%%%%%%%%%%%%%%%%%%%%%
%%%%
% Second order method starts here:
% Here slopelimiter is used on all variables except phase velocoties

    psll = po(j-1)+dx/2*sl2(j-1);
    pslr = po(j)-dx/2*sl2(j);
    dsll = dlo(j-1)+dx/2*sl1(j-1);
    dslr = dlo(j)-dx/2*sl1(j);
    dgll = dgo(j-1)+dx/2*sl6(j-1);
    dglr = dgo(j)-dx/2*sl6(j);

    vlv = vlo(j-1)+dx/2*sl3(j-1);
    vlh = vlo(j)-dx/2*sl3(j);
    vgv = vgo(j-1)+dx/2*sl4(j-1);
    vgh = vgo(j)-dx/2*sl4(j);

    gvv = ego(j-1)+dx/2*sl5(j-1);
    gvh = ego(j)-dx/2*sl5(j);
    lvv = 1-gvv;
    lvh = 1-gvh;

    cl = csound(gvv,psll,dsll,k);
    cr = csound(gvh,pslr,dslr,k);
    c = max(cl,cr);

    pll = psip(vlo(j-1),c,lvh);
    plr = psim(vlo(j),c,lvv);
    pgl = psip(vgo(j-1),c,gvh);
    pgr = psim(vgo(j),c,gvv);
    vmixr = vlo(j)*lvh+vgo(j)*gvh;
    vmixl = vlo(j-1)*lvv+vgo(j-1)*gvv;

    pl = pp(vmixl,c);
    pr = pm(vmixr,c);
```

```
    mll= lvv*dsll;
    mlr= lvh*dslr;
    mgl= gvv*dgll;
    mgr= gvh*dglr;

    flc(j,1)= mll*pll+mlr*plr;
    flc(j,2)= 0.0;
    flc(j,3)= mll*pll*vlo(j-1)+mlr*plr*vlo(j);



    fgc(j,1)=0.0;
    fgc(j,2)= mgl*pgl+mgr*pgr;
    fgc(j,3)= mgl*pgl*vgo(j-1)+mgr*pgr*vgo(j);

    fp(j,1)= 0.0;
    fp(j,2)= 0.0;
    fp(j,3)= pl*psll+pr*pslr;


%%% Second order method ends here
%%%%%%%%%%%%%%%%%%%%%%%%%%%%%%%%%%%%%%%%%%%%%%%%%%%%%%%%%%%%%%%%%%
%%%%%%
%%%%%%%%%%%%%%%%%%%%%%%%%%%%%%%%%%%%%%%%%%%%%%%%%%%%%%%%%%%%%%%%%%
%%%%%%

% Here sloplimiters is used on all variables. This
% has not worked so well yet.

%       psll = po(j-1)+dx/2*sl2(j-1);
%       pslr = po(j)-dx/2*sl2(j);
%       dsll = dlo(j-1)+dx/2*sl1(j-1);
%       dslr = dlo(j)-dx/2*sl1(j);
%       dgll = dgo(j-1)+dx/2*sl6(j-1);
%       dglr = dgo(j)-dx/2*sl6(j);
%
%       vlv = vlo(j-1)+dx/2*sl3(j-1);
%       vlh = vlo(j)-dx/2*sl3(j);
%       vgv = vgo(j-1)+dx/2*sl4(j-1);
%       vgh = vgo(j)-dx/2*sl4(j);
%
%       gvv = ego(j-1)+dx/2*sl5(j-1);
%       gvh = ego(j)-dx/2*sl5(j);
%       lvv = 1-gvv;
%       lvh = 1-gvh;
%
%       cl = csound(gvv,psll,dsll,k);
%       cr = csound(gvh,pslr,dslr,k);
%       c = max(cl,cr);
%
%       pll = psip(vlv,c,lvh);
%       plr = psim(vlh,c,lvv);
%       pgl = psip(vgv,c,gvh);
%       pgr = psim(vgh,c,gvv);
%       vmixr = vlh*lvh+vgh*gvh;
%       vmixl = vlv*lvv+vgv*gvv;
%
```

```
%       pl = pp(vmixl,c);
%       pr = pm(vmixr,c);
%       mll= lvv*dsll;
%       mlr= lvh*dslr;
%       mgl= gvv*dgll;
%       mgr= gvh*dglr;
%
%       flc(j,1)= mll*pll+mlr*plr;
%       flc(j,2)= 0.0;
%       flc(j,3)= mll*pll*vlv+mlr*plr*vlh;
%
%
%       fgc(j,1)=0.0;
%       fgc(j,2)= mgl*pgl+mgr*pgr;
%       fgc(j,3)= mgl*pgl*vgv+mgr*pgr*vgh;
%
%       fp(j,1)= 0.0;
%       fp(j,2)= 0.0;
%       fp(j,3)= pl*psll+pr*pslr;


    end

% Fluxes have now been calculated. We will now update the conservative
% variables in each of the numerical cells.

%     hydgrad = g*(dlo.*evo+dgo.*ego);
%     fricgrad = dpfric1(vlo,vgo,evo,ego,dlo,dgo,po,do,di,viscl,viscg);

% Alternatively the source terms can be calculated by using a
% for loop instead of the vectorized form above.
% Note that the model is sensitive to how we treat the model
% for low Reynolds numbers (possible discontinuty in the model
      for j=1:nobox
       fricgrad(j)=dpfric(vlo(j),vgo(j),evo(j),ego(j),dlo(j),dgo(j), ...
         po(j),do(j),di(j),viscl,viscg);
       hydgrad(j)=g*(dlo(j)*evo(j)+dgo(j)*ego(j));
      end

     sumfric = 0;
     sumhyd= 0;

% Mass Transfer Equation

  if temperature>373
        for j=1:nobox
           boiltemp(j)=(1/373-(8.314*log(p(j)/100000))/(specenthalpy(373)*18))^(-1);
           if temperature>=boiltemp(j)
              hfg(j) = specenthalpy(temperature)*10^3;
              q(j)=viscl*hfg(j)*((9.81*(dlo(j)-dgo(j))/interfacetension(temperature))^0.5)*(4190*(temperature-
373)/(0.013*hfg(j)*1.75))^3;
              source(j,1) = -q(j)/hfg(j);
              source(j,2) = -source(j,1);
           else
              source(j,1)=0;
              source(j,2)=0;
           end

        end
```

```
  end




    % Constant numerical value for mass transfer
  value =1.0;
       if temperature > 373
          for j=1:nobox
               source(j,1)=-(temperature-373)/10*value;
               source(j,2)=-source(j,1);
          end
       end

     for j=1:nobox
                  ar = area(j);



     qv(j,1)=qvo(j,1)-dtdx*((ar*flc(j+1,1)-ar*flc(j,1))...
                       +(ar*fgc(j+1,1)-ar*fgc(j,1))...
                       +(ar*fp(j+1,1)-ar*fp(j,1)))+dtdx*ar*source(j,1);

     qv(j,2)=qvo(j,2)-dtdx*((ar*flc(j+1,2)-ar*flc(j,2))...
                       +(ar*fgc(j+1,2)-ar*fgc(j,2))...
                       +(ar*fp(j+1,2)-ar*fp(j,2)))+dtdx*ar*source(j,2);

     qv(j,3)=qvo(j,3)-dtdx*((ar*flc(j+1,3)-ar*flc(j,3))...
                       +(ar*fgc(j+1,3)-ar*fgc(j,3))...
                       +(ar*fp(j+1,3)-ar*fp(j,3)))...
               -dt*ar*(fricgrad(j)+hydgrad(j));

%
     sumfric=sumfric+fricgrad(j)*dx;
     sumhyd=sumhyd+hydgrad(j)*dx;

     end




% Section where we find the physical variables (pressures, densities etc)
% from the conservative variables. Some trickes to ensure stability. These
% are induced to avoid negative masses.

     qv(:,1)=qv(:,1)./area';
     qv(:,2)=qv(:,2)./area';

     gasmass=0;
     liqmass=0;

     for j=1:nobox
```

```
% Remove the area from the conservative variables to find the
% the primitive variables from the conservative ones.

%      qv(j,1)= qv(j,1)/area(j);
%      qv(j,2)= qv(j,2)/area(j);

     if (qv(j,1)<0.00000001)
       qv(j,1)=0.00000001;
     end

     if (qv(j,2)< 0.00000001)
       qv(j,2)=0.00000001;
     end


     gasmass = gasmass+qv(j,2)*area(j)*dx;
     liqmass = liqmass+qv(j,1)*area(j)*dx;


    end  % end of fix loop



% Below, we find the primitive variables pressure and densities based on
% the conservative variables q1,q2. One can choose between getting them by
% analytical or numerical solution approach specified in the beginning of
% the program.
   if (analytical == 1)
     % Coefficients:
%       a = 1/(al*al);
%       b = t1-qv(:,1)'-rt*qv(:,2)'/(al*al);
%       c = -1.0*t1*rt*qv(:,2)';
          x1 = rho0-(P0*rho0/Bheta)-(rho0*Alpha*(temperature-tempstart));
          x2 = rho0/Bheta;
          x3 = -1.0*qv(:,2)'*Rsteam*temperature;

          a = x2;
          b = x1+x2*x3-qv(:,1)';
          c = x1*x3;

        % Analytical solution:
         p=(-b+sqrt(b.*b-4*a.*c))/(2*a);  % Pressure
        dl=rholiq(p,temperature); % Density of liquid
        dg=rogas(p,temperature); % Density of gas
   else
      for j=1:nobox
     %Numerical Solution:
     [p(j),error]=itsolver(po(j),qv(j,1),qv(j,2),temperature); % Pressure
     dl(j)=rholiq(p(j),temperature); % Density of liquid
     dg(j)=rogas(p(j),temperature); % Density of gas

     % Incase a numerical solution is not found, the program will write out "error":
     if error > 0
       error
     end
      end
   end
```

```
%     if (analytical == 1)
%       % Coefficients:
%       a = 1/(al*al);
%       b = t1-qv(j,1)-rt*qv(j,2)/(al*al);
%       c = -1.0*t1*rt*qv(j,2);
%
%       % Analytical solution:
%        p(j)=(-b+sqrt(b*b-4p*a*c))/(2*a);  % Pressure
%        dl(j)= dstc + (p(j)-pstc)/(al*al); % Density of liquid
%        dg(j) = p(j)/rt;                   % Density of gas
%     else
%       %Numerical Solution:
%       [p(j),error]=itsolver(po(j),qv(j,1),qv(j,2)); % Pressure
%       dl(j)=rholiq(p(j)); % Density of liquid
%       dg(j)=rogas(p(j)); % Density of gas
%
%       % Incase a numerical solution is not found, the program will write out "error":
%       if error > 0
%          error
%       end
%     end


 % Find the phase volume fractions based on new conservative variables and
 % updated densities.

 %     eg(j)= qv(j,2)/dg(j);
 %     ev(j)=1-eg(j);

       eg=qv(:,2)'./dg;
       ev=1-eg;

 %     Reset average conservative varibles in cells with area changes inside.

 %       qv(j,1)=qv(j,1)*area(j);
 %       qv(j,2)=qv(j,2)*area(j);

      qv(:,1)=qv(:,1).*area';
      qv(:,2)=qv(:,2).*area';


 %     The section below is used to find the primitive variables vg,vl
 %    (phase velocities) based on the updated conservative variable q3 and
 %     the slip relation.


 % Part where we interpolate in the slip parameters to avoid a
 % singularities when approaching one phase gas flow.
 % In the transition to one-phase gas flow, we need to
 % have a smooth transition to no-slip conditions.

   gasvol=0;

   for j=1:nobox
```

```
% The  interpolations introduced below are included
% to omit a singularity in the slip relation when the gas volume
% fraction becomes equal to 1/K. In additon, S is interpolated to
% zero when approaching one phase gas flow. In the transition to
% one phase gas flow, we have no slip condtions (K=1, S=0)

  ktemp=k;
  stemp=s;

  k0(j) = ktemp;
  s0(j) = stemp;
  if ((eg(j)>=0.7) & (eg(j)<=0.8))
    xint = (eg(j)-0.7)/0.1;
    k0(j) =1.0*xint+k*(1-xint);
  elseif(eg(j)>0.8)
    k0(j)=1.0;
  end

  if ((eg(j)>=0.9) & (eg(j)<=1.0))
    xint = (eg(j)-0.9)/0.1;
    s0(j) = 0.0*xint+s*(1-xint);
  end

  if (eg(j)>=0.999999)
    k1(j) = 1.0;
    s1(j) = 0.0;
  else
    k1(j) = (1-k0(j)*eg(j))/(1-eg(j));
    s1(j) = -1.0*s0(j)*eg(j)/(1-eg(j));
  end


  % Variable for summarizing the gas volume content in the well.
  gasvol=gasvol+eg(j)*area(j)*dx;


end


%   Below we find the phase velcoties by combining the
%   conservative variable defined by the mixture momentum equation
%   with the gas slip relation. The code commented away was before
%   vectorization.

%     help1 = dl(j)*ev(j)*k1+dg(j)*eg(j)*k0;
%     help2 = dl(j)*ev(j)*s1+dg(j)*eg(j)*s0;
%
%     vmixhelpl = (qv(j,3)/area(j)-help2)/help1;
%     vg(j)=k0*vmixhelpl+s0;
%     vl(j)=k1*vmixhelpl+s1;

  help1 = dl.*ev.*k1+dg.*eg.*k0;
  help2 = dl.*ev.*s1+dg.*eg.*s0;

  vmixhelpl = (qv(:,3)'./area-help2)./help1;
  vg=k0.*vmixhelpl+s0;
  vl=k1.*vmixhelpl+s1;
```

```
% Old values are now set equal to new values in order to prepare
% computation of next time level.


  po=p;
  dlo=dl;
  dgo=dg;
  vlo=vl;
  vgo=vg;
  ego=eg;
  evo=ev;
  qvo=qv;




% Section where we save some timedependent variables in arrays.
% e.g. the bottomhole pressure. They will be saved for certain
% timeintervalls defined in the start of the program in order to ensure
% that the arrays do not get to long!

 if (counter>=nostepsbeforesavingtimedata)
   printcounter=printcounter+1;
   time

   % Outlet massrates vs time
   liquidmassrateout(printcounter)=dl(nobox)*ev(nobox)*vl(nobox)*area(nobox);
   gasmassrateout(printcounter)=dg(nobox)*eg(nobox)*vg(nobox)*area(nobox);

   % Hydrostatic and friction pressure in well vs time
   hyd(printcounter)=sumhyd/100000;
   fric(printcounter)=sumfric/100000;

   % Volume of gas in well vs time

   volgas(printcounter)=gasvol;

   % Total phase masses in the well vs time
   massgas(printcounter)=gasmass;
   massliq(printcounter)=liqmass;
   % pout defines the exact pressure at the outletboundary!
   pout(printcounter)=p(nobox)-0.5*dx*...
   (dlo(nobox)*evo(nobox)+dgo(nobox)*ego(nobox))*g-dx*0.5*fricgrad(nobox);
   % pin defines the exact pressure at the bottom boundary
   pin(printcounter)= p(1)+0.5*dx*(dlo(1)*evo(1)+dgo(1)*ego(1))*g+0.5*dx*fricgrad(1);

   % Time variable
   timeplot(printcounter)=time;

   % Temperature variable
   tempplot(printcounter)=temperature;
```

```
    % Mass transfer
    for j=1:nobox
    sourceplot(j,printcounter)=source(j,2);
    end

    % Gas fraction overall
    for j=1:nobox
       fracplot(j,printcounter)=eg(j);
    end

    % Velocity variable
    vlplot(printcounter)=vl(nobox);
    counter = 0;


  end
end

% end of stepping forward in time.




% Printing of resultssection


countsteps % Marks number of simulation steps.


% Plot commands for variables vs time. The commands can also
% be copied to command screen where program is run for plotting other
% variables.

toc,
e = cputime-t

% Plot bottomhole pressure
plot(timeplot,pin/100000)

% Show cfl number used.
disp('cfl')
cfl = al*dt/dx


%plot(timeplot,liquidmassrateout)
%plot(timeplot,gasmassrateout)

%Plot commands for variables vs depth/Only the last simulated
%values at endtime is visualised

%plot(vl,x);
%plot(vg,x);
%plot(eg,x);
%plot(p,x);
%plot(dl,x);
```

```
%plot(dg,x);
```

Function for gas density

```
function rhog = rogas(pressure,temperature)

%Simple gas density model. Temperature is neglected.
% rhogas = pressure / (velocity of sound in the gas phase)^2 = pressure /
% rT --> gas sound velcoity = SQRT(rT)
 r = 461.5; % [J/(kg*K)] Steam
 %r = 296.8; % [J/(kg*K)] Air
 rhog = pressure/(r*temperature);

end
```

Function for liquid density

```
function [rhol] = rholiq(pressure,temperature)
%Simple model for liquid density
p0 = 100000.0; % Assumed
t0 = 273.15+20; % Assumed

beta = 2.2*10^9; % [Pa] Bulk modulus of liquid.
alpha = 0.000207; % [K^(-1)] Volumetric thermal expansion of liquid.
rho0 = 1000;

rhol = rho0 + (rho0/beta)*(pressure-p0)-(rho0*alpha*(temperature-t0));
end
```

Function for mixed sound velocity

```
function mixsoundvelocity = csound(gvo,po,dlo,k)
% Note that at this time k is set to 1.0 (should maybe be
% included below

temp= gvo*dlo*(1.0-gvo);
a=1;
if (temp < 0.01)
  temp = 0.01;
end

cexpr = sqrt(po/temp);

if (gvo <= 0.5)
 mixsoundvelocity = min(cexpr,1500);
else
 mixsoundvelocity = min(cexpr,477.5);
end
```

Function for interfacial tension between water and steam

```
function [sigma] = interfacetension(temperature)
% An equation developed by the international association for the properties
% of Water and Steam.
% Constants
Tcrit = 647; %[Kelvin] Critical temperature of water
B = 235.8; %[mN/m]
b = -0.625;
my = 1.256;

%Variable
tau = (1-temperature/Tcrit);

% Equation
sigma = B*tau^(my)*(1+b*tau)*10^-3; %[N/m]
```

Function for evaporation energy of liquid

```
function [hfg] = specenthalpy(temperature)

a=2500.304;
b=-2.2521025;
c= -0.021465847;
d = 3.1750136*10^(-4);
e = -2.8607959*10^(-5);
T = temperature-273;

hfg = a+b*T+c*T^(1.5)+d*T^(2.5)+e*T^3; % [kJ/kg]
```

Function for gas viscosity

```
function [gasviscosity] = gasvisc(temperature)
% Model for gas viscosity

%ref_gas_visc = 1.827*10^(-5); % air
%ref_temp = 291.15; % air
%C = 120; % air

ref_gas_visc = 1.2*10^(-5); % steam
ref_temp = 373.15; % steam
C = 961; % steam

gasviscosity = ref_gas_visc*(temperature/ref_temp)^(3/2)*((ref_temp+C)/temperature+C);

end
```

Function for liquid viscosity

```
function [liqviscosity] = liqvisc(temperature)
% Model for liquid viscosity

ref_water_visc = 2.414*10^(-5); % [Pa*s]

liqviscosity = ref_water_visc*10^(247.8/(temperature-140));
end
```

Appendix C Matlab code for the vertical case

```
% Transient two-phase code based on AUSMV scheme: Gas and Water
% The code assumes uniform geometry and the code is partially vectorized.

clear;
t = cputime
tic,

% Geometry data/ Must be specified
welldepth = 2000;
nobox = 25; %Number of boxes in the well
nofluxes = nobox+1;
dx = welldepth/nobox; % Boxlength
%dt = 0.005;

% Welldepth array
x(1)= -1.0*welldepth+0.5*dx;
for i=1:nobox-1
 x(i+1)=x(i)+ dx;
end

dt= 0.01;  % Timestep
dtdx = dt/dx;
time = 0.0;
endtime = 2000; % Time for end of simulation
nosteps = endtime/dt;  %Number of total timesteps
timebetweensavingtimedata = 5;  % How often in s we save data vs time for plotting.
nostepsbeforesavingtimedata = timebetweensavingtimedata/dt;

% Slip parameters used in the gas slip relation. vg =Kvmix+S
k = 1.2;
s = 0.5;

% Variables
rho0 = 1000; %[kg/m3]
P0 = 10^5; % [Pa]
Bheta = 2.2*10^9;
Alpha = 0.000207;
tempstart = 273+20; % [K]
Rsteam = 461.5; % [J/(kg*K)] Steam

% Temperature distribution
tempbot = 150+273; % [Kelvin]
temptop = 40+273;
tempdist = (tempbot-temptop)/nobox;
tempstart = 20+273;
for i=1:nobox
   temperature(i)=tempbot-tempdist*i;
end

% Viscosities (Pa*s)/Used in the frictional pressure loss model.
for i=1:nobox
viscl(i) = liqvisc(temperature(i)); % Liquid phase
viscg(i) = gasvisc(temperature(i)); % Gas phase
end
% Density parameters. These parameters are used when finding the
% primitive variables pressure, densities in an analytical manner.
```

```
% Changing parameters here, you must also change parameters inside the
% density routines roliq and rogas.

% liquid density at stc and speed of sound in liquid
 dstc = 1000.0;   %Base density of liquid, See also roliq.
 pstc = 100000.0; % Pressure at standard conditions, 100000 Pascal
 al = 1500; % Speed of sound/compressibility of liquid phase.
 t1 = dstc-pstc/(al*al); % Help variable for calc primitive variables from
 % conservative variables
% Ideal gas law constant
 rt = 100000;

% Gravity constant

 g = 9.81; % Gravitational constant

% Well opening. opening = 1, fully open well, opening = 0 (<0.01), the well
% is fully closed. This variable will control what boundary conditions that
% will apply at the outlet (both physical and numerical): We must change
% this further below in the code if we want to change status on this.

 wellopening = 1.0;  % This variable determines if
%the well is closed or not, wellopening = 1.0 -> open. welllopening = 0
%-> Well is closed. This variable affects the boundary treatment.

 bullheading = 0.0; % This variable can be set to 1.0 if we want to simulate
% a bullheading operation. But the normal is to set this to zero.


% Specify if the primitive variables shall be found either by
% a numerical or analytical approach. If analytical = 1, analytical
% solution is used. If analytical = 0. The numerical approach is used.
% using the itsolver subroutine where the bisection numerical method
% is used.

 analytical = 1;


% Define and intilalize flow variables




% Here we specify the outer and inner diameter and the flow area

  for i = 1:nobox
 %  do(i) = 0.3112;
   do(i)=0.2159;
   di(i) = 0.0;
   area(i) = 3.14/4*(do(i)*do(i)- di(i)*di(i));
%   ang(i)=3.14/2;
  end
```

```
% Initialization of slope limiters.
 for i = 1:nobox
   sl1(i)=0;
   sl2(i)=0;
   sl3(i)=0;
   sl4(i)=0;
   sl5(i)=0;
   sl6(i)=0;
 end



% Now comes the intialization of the physical variables in the well.
% First primitive variables, then the conservative ones.




% Below we intialize pressure and fluid densities. We start from top of
% the well and calculated downwards. The calculation is done twice with
% updated values to get better approximation. Only hydrostatic
% considerations.

p(nobox)= 100000.0+0.5*dx*9.81*dstc;   % Pressure
dl(nobox)=rholiq(p(nobox),temperature(nobox));  % Liquid density
dg(nobox)=rogas(p(nobox),temperature(nobox));   % Gas density

for i=nobox-1:-1:1
p(i)=p(i+1)+dx*9.81*dl(i+1);
dl(i)=rholiq(p(i),temperature(i));
dg(i)=rogas(p(i),temperature(i));
end

for i=nobox-1:-1:1
p(i)=p(i+1)+dx*9.81*(dl(i+1)+dl(i))*0.5;
dl(i)=rholiq(p(i),temperature(i));
dg(i)=rogas(p(i),temperature(i));
end

% Intitialize phase velocities, volume fractions, conservative variables
% The basic assumption is static fluid, one phase liquid.

for i = 1:nobox
  vl(i)=0; % Liquid velocity new time level.
  vg(i)=0; % Gas velocity at new time level
  eg(i)=0;  % Gas volume fraction
  ev(i)=1-eg(i); % Liquid volume fraction
  qv(i,1)=dl(i)*ev(i)*area(i);
  qv(i,2)=dg(i)*eg(i)*area(i);
  qv(i,3)=(dl(i)*ev(i)*vl(i)+dg(i)*eg(i)*vg(i))*area(i);
  fricgrad(i)=0;
  hydgrad(i)=g* qv(i,1);
end
```

```
source = zeros(nobox,3);


% Section where we also initialize values at old time level


for i=1:nobox
  dlo(i)=dl(i);
  dgo(i)=dg(i);
  po(i)=p(i);
  ego(i)=eg(i);
  evo(i)=ev(i);
  vlo(i)=vl(i);
  vgo(i)=vg(i);
  qvo(i,1)=qv(i,1);
  qvo(i,2)=qv(i,2);
  qvo(i,3)=qv(i,3);
end


% Intialize fluxes between the cells/boxes

for i = 1:nofluxes
  for j =1:3
    flc(i,j)=0.0; % Flux of liquid over box boundary
    fgc(i,j)=0.0; % Flux of gas over box boundary
    fp(i,j)= 0.0; % Pressure flux over box boundary
  end
end


%  Main program. Here we will progress in time. First som intializations
% and definitions to take out results. The for loop below runs until the
% simulation is finished.

countsteps = 0;
counter=0;
printcounter = 1;
pbot(printcounter) = p(1);
pchoke(printcounter)= p(nobox);
liquidmassrateout(printcounter) = 0;
gasmassrateout(printcounter)=0;
tempin(printcounter)=0;
timeplot(printcounter)=time;
kickvolume=0;
bullvolume=0;
sourceplot(printcounter)=0;
vlplot(printcounter)=0;

for i = 1:nosteps
   countsteps=countsteps+1;
   counter=counter+1;
   time = time+dt;

% Then a section where specify the boundary conditions.
% Here we specify the inlet rates of the different phases at the
% bottom of the pipe in kg/s. We interpolate to make things smooth.
```

```
% It is also possible to change the outlet boundary status of the well
% here. First we specify rates at the bottom and the pressure at the outlet
% in case we have an open well. This is a place where we can change the
% code to control simulations.

% In the example below, we take a gas kick and then circulate this
% out of the well without closing the well. (how you not should perform
% well control)

XX = 0;
% XX (kg/s) is a variable for introducing a kick in the well.
YY = 0; % Liquid flowrate (kg/s) (1 kg/s = 1 l/s approx)
if (time < 10)

  inletligmassrate=0.0;
  inletgasmassrate=0.0;

elseif ((time>=10) & (time < 20))
  inletligmassrate = 0*(time-10)/10;
  inletgasmassrate = XX*(time-10)/10;

elseif ((time >=20) & (time<110))
  inletligmassrate = 0;
  inletgasmassrate = XX;

elseif ((time>=110)& (time<120))
  inletligmassrate = 0;
  inletgasmassrate = XX-XX*(time-110)/10;
elseif ((time>=120&time<130))
  inletligmassrate =0;
  inletgasmassrate =0;
elseif ((time>=130)&(time<300))
  inletligmassrate =0;
  inletgasmassrate =0;
elseif ((time>=300)&(time<310))
  inletligmassrate= YY*(time-300)/10;
  inletgasmassrate =0;
elseif((time>=310))
  inletligmassrate= YY;
  inletgasmassrate =0;
end

kickvolume = kickvolume+inletgasmassrate/dgo(1)*dt;

% specify the outlet pressure /Physical. Here we have given the pressure as
% constant. It would be possible to adjust it during openwell conditions
% either by giving the wanted pressure directly (in the command lines
% above) or by finding it indirectly through a chokemodel where the wellopening
% would be an input parameter. The wellopening variable would equally had
% to be adjusted inside the command line structure given right above.
```

```
 pressureoutlet = 100000.0;

% Based on these boundary values combined with use of extrapolations techniques
% for the remaining unknowns at the boundaries, we will define the mass and
% momentum fluxes at the boundaries (inlet and outlet of pipe).

% inlet/bottom fluxes first.
  if (bullheading<=0)

    flc(1,1)= inletligmassrate/area(1);
    flc(1,2)= 0.0;
    flc(1,3)= flc(1,1)*vlo(1);



    fgc(1,1)= 0.0;
    fgc(1,2)= inletgasmassrate/area(1);
    fgc(1,3)= fgc(1,2)*vgo(1);

    fp(1,1)= 0.0;
    fp(1,2)= 0.0;

% Old way of treating the boundary
%     fp(1,3)= po(1)+0.5*(po(1)-po(2)); %Interpolation used to find the
% pressure at the inlet/bottom of the well.

% New way of treating the boundary
     fp(1,3)= po(1)...
          +0.5*dx*(dlo(1)*evo(1)+dgo(1)*ego(1))*g...
          +0.5*dx*fricgrad(1);



  else
    flc(1,1)=dlo(1)*evo(1)*vlo(1);
    flc(1,2)=0.0;
    flc(1,3)=flc(1,1)*vlo(1);

    fgc(1,1)=0.0;
    fgc(1,2)=dgo(1)*ego(1)*vgo(1);
    fgc(1,3)=fgc(1,2)*vgo(1);

    fp(1,1)=0.0;
    fp(1,2)=0.0;
    fp(1,3)=20000000; % This was a fixed pressure set at bottom when bullheading
  end



% Outlet fluxes (open & closed conditions)

   if (wellopening>0.01)

% Here open end condtions are given. We distinguish between bullheading
% & normal circulation.
```

```
      if (bullheading<=0)

         flc(nofluxes,1)= dlo(nobox)*evo(nobox)*vlo(nobox);
         flc(nofluxes,2)= 0.0;
         flc(nofluxes,3)= flc(nofluxes,1)*vlo(nobox);


         fgc(nofluxes,1)= 0.0;
         fgc(nofluxes,2)= dgo(nobox)*ego(nobox)*vgo(nobox);
         fgc(nofluxes,3)= fgc(nofluxes,2)*vgo(nobox);

         fp(nofluxes,1)= 0.0;
         fp(nofluxes,2)= 0.0;
         fp(nofluxes,3)= pressureoutlet;
      else
         flc(nofluxes,1)= inletligmassrate/area(nobox);
         flc(nofluxes,2)= 0.0;
         flc(nofluxes,3)= flc(nofluxes,1)*vlo(nobox);

         fgc(nofluxes,1)=0.0;
         fgc(nofluxes,2)=0.0;
         fgc(nofluxes,3)=0.0;

         fp(nofluxes,1)=0.0;
         fp(nofluxes,2)=0.0;
         fp(nofluxes,3)= po(nobox)...
         -0.5*dx*(dlo(nobox)*evo(nobox)+dgo(nobox)*ego(nobox))*g...
         +0.5*dx*fricgrad(nobox);
      end
   else

% Here closed end conditions are given

      flc(nofluxes,1)= 0.0;
      flc(nofluxes,2)= 0.0;
      flc(nofluxes,3)= 0.0;

      fgc(nofluxes,1)= 0.0;
      fgc(nofluxes,2)= 0.0;
      fgc(nofluxes,3)= 0.0;

      fp(nofluxes,1)=0.0;
      fp(nofluxes,2)=0.0;

   %   Old way of treating the boundary
   %    fp(nofluxes,3)= po(nobox)-0.5*(po(nobox-1)-po(nobox));

   %   New way of treating the boundary
      fp(nofluxes,3)= po(nobox)...
      -0.5*dx*(dlo(nobox)*evo(nobox)+dgo(nobox)*ego(nobox))*g;
   %    -0.5*dx*fricgrad(nobox); % Neglect friction since well is closed.
      end


% Implementation of slopelimiters. They are applied on the physical
% variables like phase densities, phase velocities and pressure.
```

```
    for i=2:nobox-1
     sl1(i)=minmod(dlo(i-1),dlo(i),dlo(i+1),dx);
     sl2(i)=minmod(po(i-1),po(i),po(i+1),dx);
     sl3(i)=minmod(vlo(i-1),vlo(i),vlo(i+1),dx);
     sl4(i)=minmod(vgo(i-1),vgo(i),vgo(i+1),dx);
     sl5(i)=minmod(ego(i-1),ego(i),ego(i+1),dx);
     sl6(i)=minmod(dgo(i-1),dgo(i),dgo(i+1),dx);
    end

 % Slopelimiters in boundary cells are set to zero!
    sl1(nobox)=0;
    sl2(nobox)=0;
    sl3(nobox)=0;
    sl4(nobox)=0;
    sl5(nobox)=0;
    sl6(nobox)=0;

  % Ny Kode 11/11-15
    sl1(1)=0;
    sl2(1)=0;
    sl3(1)=0;
    sl4(1)=0;
    sl5(1)=0;
    sl6(1)=0;


% Now we will find the fluxes between the different cells.
% NB - IMPORTANE -  Note that if we change the compressibilities/sound velocities of
% the fluids involved, we need to do changes inside the csound function.

    for j = 2:nofluxes-1

 %%%%%%%%%%%%%%%%%%%%%%%%%%%%%%%%%%%%%%%%%%%%%%%%%%%%%%%%%%%%%%%%%%%%%%%
 %%%%%%%%%%%%%%%%%%%%%%%%%%%%%%%%%%%%%%%%%%%%%%%%%%%%%%%%%%%%%%%%%%%%%%%
 % First order method is from here:
%       cl = csound(ego(j-1),po(j-1),dlo(j-1),k);
%       cr = csound(ego(j),po(j),dlo(j),k);
%       c = max(cl,cr);
%       pll = psip(vlo(j-1),c,evo(j));
%       plr = psim(vlo(j),c,evo(j-1));
%       pgl = psip(vgo(j-1),c,ego(j));
%       pgr = psim(vgo(j),c,ego(j-1));
%       vmixr = vlo(j)*evo(j)+vgo(j)*ego(j);
%       vmixl = vlo(j-1)*evo(j-1)+vgo(j-1)*ego(j-1);
%
%       pl = pp(vmixl,c);
%       pr = pm(vmixr,c);
%       mll= evo(j-1)*dlo(j-1);
%       mlr= evo(j)*dlo(j);
%       mgl= ego(j-1)*dgo(j-1);
%       mgr= ego(j)*dgo(j);
%
%       flc(j,1)= mll*pll+mlr*plr;
%       flc(j,2)= 0.0;
%       flc(j,3)= mll*pll*vlo(j-1)+mlr*plr*vlo(j);
%
%       fgc(j,1)=0.0;
```

```
%       fgc(j,2)= mgl*pgl+mgr*pgr;
%       fgc(j,3)= mgl*pgl*vgo(j-1)+mgr*pgr*vgo(j);
%
%       fp(j,1)= 0.0;
%       fp(j,2)= 0.0;
%       fp(j,3)= pl*po(j-1)+pr*po(j);

 %  First order methods ends here
 %%%%%%%%%%%%%%%%%%%%%%%%%%%%%%%%%%%%%%%%%%%%%%%%%%%%%%%

%%%%%%%%%%%%%%%%%%%%%%%%%%%%%%%%%%%%%%%%%%%%%%%%%%%%%%%
%%




%%%%%%%%%%%%%%%%%%%%%%%%%%%%%%%%%%%%%%%%%%%%%%%%%%%%%%%
%%%%
%%%%%%%%%%%%%%%%%%%%%%%%%%%%%%%%%%%%%%%%%%%%%%%%%%%%%%%
%%%%
% Second order method starts here:
% Here slopelimiter is used on all variables except phase velocoties

    psll = po(j-1)+dx/2*sl2(j-1);
    pslr = po(j)-dx/2*sl2(j);
    dsll = dlo(j-1)+dx/2*sl1(j-1);
    dslr = dlo(j)-dx/2*sl1(j);
    dgll = dgo(j-1)+dx/2*sl6(j-1);
    dglr = dgo(j)-dx/2*sl6(j);

    vlv = vlo(j-1)+dx/2*sl3(j-1);
    vlh = vlo(j)-dx/2*sl3(j);
    vgv = vgo(j-1)+dx/2*sl4(j-1);
    vgh = vgo(j)-dx/2*sl4(j);

    gvv = ego(j-1)+dx/2*sl5(j-1);
    gvh = ego(j)-dx/2*sl5(j);
    lvv = 1-gvv;
    lvh = 1-gvh;

    cl = csound(gvv,psll,dsll,k);
    cr = csound(gvh,pslr,dslr,k);
    c = max(cl,cr);

    pll = psip(vlo(j-1),c,lvh);
    plr = psim(vlo(j),c,lvv);
    pgl = psip(vgo(j-1),c,gvh);
    pgr = psim(vgo(j),c,gvv);
    vmixr = vlo(j)*lvh+vgo(j)*gvh;
    vmixl = vlo(j-1)*lvv+vgo(j-1)*gvv;

    pl = pp(vmixl,c);
    pr = pm(vmixr,c);


   mll= lvv*dsll;
   mlr= lvh*dslr;
   mgl= gvv*dgll;
```

```
mgr= gvh*dglr;

flc(j,1)= mll*pll+mlr*plr;
flc(j,2)= 0.0;
flc(j,3)= mll*pll*vlo(j-1)+mlr*plr*vlo(j);



fgc(j,1)=0.0;
fgc(j,2)= mgl*pgl+mgr*pgr;
fgc(j,3)= mgl*pgl*vgo(j-1)+mgr*pgr*vgo(j);

fp(j,1)= 0.0;
fp(j,2)= 0.0;
fp(j,3)= pl*psll+pr*pslr;


%%% Second order method ends here
%%%%%%%%%%%%%%%%%%%%%%%%%%%%%%%%%%%%%%%%%%%%%%%%%%%%%%%%%%%%%
%%%%%%
%%%%%%%%%%%%%%%%%%%%%%%%%%%%%%%%%%%%%%%%%%%%%%%%%%%%%%%%%%%%%
%%%%%%

% Here sloplimiters is used on all variables. This
% has not worked so well yet.

%     psll = po(j-1)+dx/2*sl2(j-1);
%     pslr = po(j)-dx/2*sl2(j);
%     dsll = dlo(j-1)+dx/2*sl1(j-1);
%     dslr = dlo(j)-dx/2*sl1(j);
%     dgll = dgo(j-1)+dx/2*sl6(j-1);
%     dglr = dgo(j)-dx/2*sl6(j);
%
%     vlv = vlo(j-1)+dx/2*sl3(j-1);
%     vlh = vlo(j)-dx/2*sl3(j);
%     vgv = vgo(j-1)+dx/2*sl4(j-1);
%     vgh = vgo(j)-dx/2*sl4(j);
%
%     gvv = ego(j-1)+dx/2*sl5(j-1);
%     gvh = ego(j)-dx/2*sl5(j);
%     lvv = 1-gvv;
%     lvh = 1-gvh;
%
%     cl = csound(gvv,psll,dsll,k);
%     cr = csound(gvh,pslr,dslr,k);
%     c = max(cl,cr);
%
%     pll = psip(vlv,c,lvh);
%     plr = psim(vlh,c,lvv);
%     pgl = psip(vgv,c,gvh);
%     pgr = psim(vgh,c,gvv);
%     vmixr = vlh*lvh+vgh*gvh;
%     vmixl = vlv*lvv+vgv*gvv;
%
%     pl = pp(vmixl,c);
%     pr = pm(vmixr,c);
%     mll= lvv*dsll;
%     mlr= lvh*dslr;
%     mgl= gvv*dgll;
%     mgr= gvh*dglr;
```

```
%
%       flc(j,1)= mll*pll+mlr*plr;
%       flc(j,2)= 0.0;
%       flc(j,3)= mll*pll*vlv+mlr*plr*vlh;
%
%
%       fgc(j,1)=0.0;
%       fgc(j,2)= mgl*pgl+mgr*pgr;
%       fgc(j,3)= mgl*pgl*vgv+mgr*pgr*vgh;
%
%       fp(j,1)= 0.0;
%       fp(j,2)= 0.0;
%       fp(j,3)= pl*psll+pr*pslr;


    end

% Fluxes have now been calculated. We will now update the conservative
% variables in each of the numerical cells.

%     hydgrad = g*(dlo.*evo+dgo.*ego);
%     fricgrad = dpfric1(vlo,vgo,evo,ego,dlo,dgo,po,do,di,viscl,viscg);

% Alternatively the source terms can be calculated by using a
% for loop instead of the vectorized form above.
% Note that the model is sensitive to how we treat the model
% for low Reynolds numbers (possible discontinuty in the model
      for j=1:nobox
       fricgrad(j)=dpfric(vlo(j),vgo(j),evo(j),ego(j),dlo(j),dgo(j), ...
         po(j),do(j),di(j),viscl(j),viscg(j));
       hydgrad(j)=g*(dlo(j)*evo(j)+dgo(j)*ego(j));
      end

     sumfric = 0;
     sumhyd= 0;
     value=1;
        for j=1:nobox
           if p(j)<=5000000
                source(j,1)=-(5000000-p(j))/5000000*value;
                source(j,2)=-source(j,1);
           else
              source(j,1)=0;
              source(j,2)=0;
           end

        end



     for j=1:nobox
                  ar = area(j);


%
%                 source(j,1)=0;
%                 source(j,2)=0;
```

```
    qv(j,1)=qvo(j,1)-dtdx*((ar*flc(j+1,1)-ar*flc(j,1))...
                    +(ar*fgc(j+1,1)-ar*fgc(j,1))...
                    +(ar*fp(j+1,1)-ar*fp(j,1)))+dtdx*ar*source(j,1);

    qv(j,2)=qvo(j,2)-dtdx*((ar*flc(j+1,2)-ar*flc(j,2))...
                    +(ar*fgc(j+1,2)-ar*fgc(j,2))...
                    +(ar*fp(j+1,2)-ar*fp(j,2)))+dtdx*ar*source(j,2);

    qv(j,3)=qvo(j,3)-dtdx*((ar*flc(j+1,3)-ar*flc(j,3))...
                    +(ar*fgc(j+1,3)-ar*fgc(j,3))...
                    +(ar*fp(j+1,3)-ar*fp(j,3)))...
              -dt*ar*(fricgrad(j)+hydgrad(j));

%
    sumfric=sumfric+fricgrad(j)*dx;
    sumhyd=sumhyd+hydgrad(j)*dx;

    end




% Section where we find the physical variables (pressures, densities etc)
% from the conservative variables. Some trickes to ensure stability. These
% are induced to avoid negative masses.

    qv(:,1)=qv(:,1)./area';
    qv(:,2)=qv(:,2)./area';

    gasmass=0;
    liqmass=0;

    for j=1:nobox


% Remove the area from the conservative variables to find the
% the primitive variables from the conservative ones.

%     qv(j,1)= qv(j,1)/area(j);
%     qv(j,2)= qv(j,2)/area(j);

    if (qv(j,1)<0.00000001)
      qv(j,1)=0.00000001;
    end

    if (qv(j,2)< 0.00000001)
      qv(j,2)=0.00000001;
    end


    gasmass = gasmass+qv(j,2)*area(j)*dx;
    liqmass = liqmass+qv(j,1)*area(j)*dx;


   end  % end of fix loop
```

```
% Below, we find the primitive variables pressure and densities based on
% the conservative variables q1,q2. One can choose between getting them by
% analytical or numerical solution approach specified in the beginning of
% the program.
for j=1:nobox
   if (analytical == 1)
     % Coefficients:
%       a = 1/(al*al);
%       b = t1-qv(:,1)'-rt*qv(:,2)'/(al*al);
%       c = -1.0*t1*rt*qv(:,2)';
         x1 = rho0-(P0*rho0/Bheta)-(rho0*Alpha*(temperature(j)-tempstart));
         x2 = rho0/Bheta;
         x3 = -1.0*qv(j,2)'*Rsteam*temperature(j);

         a = x2;
         b = x1+x2*x3-qv(j,1)';
         c = x1*x3;

        % Analytical solution:
         p(j)=(-b+sqrt(b.*b-4*a.*c))/(2*a);  % Pressure
        dl(j)=rholiq(p(j),temperature(j)); % Density of liquid
        dg(j)=rogas(p(j),temperature(j)); % Density of gas
   else
      for j=1:nobox
     %Numerical Solution:
     [p(j),error]=itsolver(po(j),qv(j,1),qv(j,2),temperature(j)); % Pressure
     dl(j)=rholiq(p(j),temperature(j)); % Density of liquid
     dg(j)=rogas(p(j),temperature(j)); % Density of gas

     % Incase a numerical solution is not found, the program will write out "error":
     if error > 0
       error
     end
      end
   end
end

%    if (analytical == 1)
%      % Coefficients:
%      a = 1/(al*al);
%      b = t1-qv(j,1)-rt*qv(j,2)/(al*al);
%      c = -1.0*t1*rt*qv(j,2);
%
%      % Analytical solution:
%       p(j)=(-b+sqrt(b*b-4p*a*c))/(2*a);  % Pressure
%       dl(j)= dstc + (p(j)-pstc)/(al*al); % Density of liquid
%       dg(j) = p(j)/rt;                   % Density of gas
%    else
%      %Numerical Solution:
%      [p(j),error]=itsolver(po(j),qv(j,1),qv(j,2)); % Pressure
%      dl(j)=rholiq(p(j)); % Density of liquid
%      dg(j)=rogas(p(j)); % Density of gas
%
%      % Incase a numerical solution is not found, the program will write out "error":
%      if error > 0
%        error
%      end
```

```
%     end


 % Find the phase volume fractions based on new conservative variables and
 % updated densities.

 %     eg(j)= qv(j,2)/dg(j);
 %     ev(j)=1-eg(j);

       eg=qv(:,2)'./dg;
       ev=1-eg;

 %     Reset average conservative varibles in cells with area changes inside.

 %      qv(j,1)=qv(j,1)*area(j);
 %      qv(j,2)=qv(j,2)*area(j);

      qv(:,1)=qv(:,1).*area';
      qv(:,2)=qv(:,2).*area';


 %     The section below is used to find the primitive variables vg,vl
 %    (phase velocities) based on the updated conservative variable q3 and
 %     the slip relation.


 % Part where we interpolate in the slip parameters to avoid a
 % singularities when approaching one phase gas flow.
 % In the transition to one-phase gas flow, we need to
 % have a smooth transition to no-slip conditions.

   gasvol=0;

   for j=1:nobox


   % The  interpolations introduced below are included
   % to omit a singularity in the slip relation when the gas volume
   % fraction becomes equal to 1/K. In additon, S is interpolated to
   % zero when approaching one phase gas flow. In the transition to
   % one phase gas flow, we have no slip condtions (K=1, S=0)

      ktemp=k;
      stemp=s;

      k0(j) = ktemp;
      s0(j) = stemp;
      if ((eg(j)>=0.7) & (eg(j)<=0.8))
        xint = (eg(j)-0.7)/0.1;
        k0(j) =1.0*xint+k*(1-xint);
      elseif(eg(j)>0.8)
        k0(j)=1.0;
      end

      if ((eg(j)>=0.9) & (eg(j)<=1.0))
        xint = (eg(j)-0.9)/0.1;
        s0(j) = 0.0*xint+s*(1-xint);
```

```
    end

    if (eg(j)>=0.999999)
      k1(j) = 1.0;
      s1(j) = 0.0;
    else
      k1(j) = (1-k0(j)*eg(j))/(1-eg(j));
      s1(j) = -1.0*s0(j)*eg(j)/(1-eg(j));
    end


    % Variable for summarizing the gas volume content in the well.
    gasvol=gasvol+eg(j)*area(j)*dx;




%   Below we find the phase velcoties by combining the
%   conservative variable defined by the mixture momentum equation
%   with the gas slip relation. The code commented away was before
%   vectorization.

    help1(j) = dl(j)*ev(j)*k1(j)+dg(j)*eg(j)*k0(j);
    help2(j) = dl(j)*ev(j)*s1(j)+dg(j)*eg(j)*s0(j);

    vmixhelpl(j) = (qv(j,3)/area(j)-help2(j))/help1(j);
    vg(j)=k0(j)*vmixhelpl(j)+s0(j);
    vl(j)=k1(j)*vmixhelpl(j)+s1(j);

%     help1 = dl.*ev.*k1+dg.*eg.*k0;
%     help2 = dl.*ev.*s1+dg.*eg.*s0;
%
%     vmixhelpl = (qv(:,3)'./area-help2)./help1;
%     vg=k0.*vmixhelpl+s0;
%     vl=k1.*vmixhelpl+s1;




% Old values are now set equal to new values in order to prepare
% computation of next time level.


  po(j)=p(j);
  dlo(j)=dl(j);
  dgo(j)=dg(j);
  vlo(j)=vl(j);
  vgo(j)=vg(j);
  ego(j)=eg(j);
  evo(j)=ev(j);
  for m=1:3
  qvo(j,m)=qv(j,m);
  end
  end
```

```
% Section where we save some timedependent variables in arrays.
% e.g. the bottomhole pressure. They will be saved for certain
% timeintervalls defined in the start of the program in order to ensure
% that the arrays do not get to long!

 if (counter>=nostepsbeforesavingtimedata)
   printcounter=printcounter+1;
   time

   % Outlet massrates vs time
   liquidmassrateout(printcounter)=dl(nobox)*ev(nobox)*vl(nobox)*area(nobox);
   gasmassrateout(printcounter)=dg(nobox)*eg(nobox)*vg(nobox)*area(nobox);

   % Hydrostatic and friction pressure in well vs time
   hyd(printcounter)=sumhyd/100000;
   fric(printcounter)=sumfric/100000;

   % Volume of gas in well vs time

   volgas(printcounter)=gasvol;

   % Total phase masses in the well vs time
   massgas(printcounter)=gasmass;
   massliq(printcounter)=liqmass;
   % pout defines the exact pressure at the outletboundary!
   pout(printcounter)=p(nobox)-0.5*dx*...
   (dlo(nobox)*evo(nobox)+dgo(nobox)*ego(nobox))*g-dx*0.5*fricgrad(nobox);
   % pin defines the exact pressure at the bottom boundary
   pin(printcounter)= p(1)+0.5*dx*(dlo(1)*evo(1)+dgo(1)*ego(1))*g+0.5*dx*fricgrad(1);
   % Time variable
   timeplot(printcounter)=time;

   % Mass transfer
   for j=1:nobox
   sourceplot(j,printcounter)=source(j,2);
   end

   % Gas fraction
   for j=1:nobox
      fracplot(j,printcounter)=eg(j);
   end
   % Pressure
   for j=1:nobox
      pressureplot(j,printcounter)=p(j);
   end

   % Velocity variable
   vlplot(printcounter)=vl(nobox);
   counter = 0;


 end
end
```

```
% end of stepping forward in time.



% Printing of resultssection


countsteps % Marks number of simulation steps.


% Plot commands for variables vs time. The commands can also
% be copied to command screen where program is run for plotting other
% variables.

toc,
e = cputime-t

% Plot bottomhole pressure
plot(timeplot,pin/100000)

% Show cfl number used.
disp('cfl')
cfl = al*dt/dx


%plot(timeplot,liquidmassrateout)
%plot(timeplot,gasmassrateout)

%Plot commands for variables vs depth/Only the last simulated
%values at endtime is visualised

%plot(vl,x);
%plot(vg,x);
%plot(eg,x);
%plot(p,x);
%plot(dl,x);
%plot(dg,x);
```